

Aus dem Berliner Institut für Gesundheitsforschung
– Zentrum für Regenerative Therapien
der Medizinischen Fakultät Charité – Universitätsmedizin Berlin

DISSERTATION

**Scalable differentiation of human pluripotent stem cells into in two
and three - dimensional proximal tubule cells**
**(Skalierbare Differenzierung humaner pluripotenter Stammzellen in
zwei- und dreidimensionale proximale Tubuluszellen)**

zur Erlangung des akademischen Grades
Doctor rerum medicinalium (Dr. rer. medic.)

vorgelegt der Medizinischen Fakultät
Charité – Universitätsmedizin Berlin

von

Ngo, Thi Thanh Thao

Datum der Promotion: 30th November 2023

TABLE OF CONTENT

LIST OF TABLE	4
LIST OF ABBREVIATIONS	5
ABSTRACT	6
1. INTRODUCTION	10
1.1. KIDNEYS AND FILTERING SYSTEM.....	10
1.2. PTEC SOURCES FOR NEPHROTOXICITY SCREENING, TISSUE MODELLING AND REGENERATIVE THERAPIES.....	14
1.3. GENERATION AND CHARACTERIZATION OF HPSC-DERIVED PTEC IN TWO DIMENSIONAL STATIC AND MICROFLUIDIC CULTURE	20
1.4. MICROCARRIERS FOR ANCHORAGE-DEPENDENT CELL GROWTH IN FLUIDIC SYSTEMS	21
1.5. HYPOTHESIS, AIMS AND THE PRESENT STUDY.....	25
2. METHODS	26
2.1. MEDIUM SCREENING FOR PTEC DIFFERENTIATION OF HPSC IN 2D CULTURE.....	27
2.2. EXPANSION AND DIFFERENTIATION OF CELLS ON MATRIGEL-COATED ALGINATE BEADS WITH BIOLEVITATION.....	30
2.3. CULTURE PARAMETERS OF HPSC ON MATRIGEL-COATED ALGINATE BEADS WITH BIOLEVITATION	31
2.4. PROCESSING MATRIGEL-COATED ALGINATE BEADS FOR CHARACTERIZATION.....	32
2.5. FLOW CYTOMETRY.....	32
2.6. IMMUNOFLUORESCENCE.....	33
2.7. TRANSMISSION ELECTRON MICROSCOPY.....	33
2.8. CYTOTOXICITY ASSAY.....	34
2.9. TRANSPORT ASSAYS	34
2.9.1. <i>Glucose assay on Matrigel-coated alginate beads</i>	35
2.9.2. <i>Albumin assay on Matrigel-coated alginate beads</i>	35
2.9.3. <i>Organic anion uptake assay on Matrigel-coated alginate beads</i>	35
2.9.4. <i>Organic cation uptake assays Matrigel-coated alginate beads</i>	36
2.9.5. <i>Transport assay of renal efflux P-Glycoprotein Matrigel-coated alginate beads</i>	37
2.10. TRANSEPITHELIAL ELECTRICAL RESISTANCE.....	37
3. RESULTS	38
3.1. DIFFERENTIATION OF RENAL PROGENITOR CELLS AND PTEC ON GELTREX-COATED POLYSTYRENE IN 2D AND ON MATRIGEL-COATED ALGINATE BEADS WITH BIOLEVITATION	38
3.2. EXPANSION EFFICACY OF CELLS ON MATRIGEL-COATED BEADS WITH BIOLEVITATION	40
4. DISCUSSION	42
4.1. SHORT SUMMARY OF RESULTS.....	42
4.2. EMBEDDING THE RESULTS INTO THE CURRENT STATE OF RESEARCH	42
4.3. LIMITATIONS AND FURTHER OPTIMIZATION APPROACHES	43
4.4. IMPLICATIONS FOR PRACTICE AND/OR FUTURE RESEARCH	45
4.4.1. <i>Good Manufacturing practice product for reliable PTEC source</i>	45
4.4.2. <i>Clinical applications</i>	45
5. CONCLUSION	47
REFERENCE LIST	48
STATUTORY DECLARATION	60
DECLARATION OF YOUR OWN CONTRIBUTIONS TO THE PUBLICATIONS	61
EXCERPT FROM JOURNAL SUMMARY LIST	63
PRINTING COPY OF THE PUBLICATION	66
CURRICULUM VITAE	80
PUBLICATION LIST	84

List of Table

Table 1. List of transporters in PTEC	12
Table 2. PTEC lines used for establishment of PT models	17
Table 3. Animal models of kidney diseases	18
Table 4. Human PSC-lines used in this study	26
Table 5. List of antibodies used for immunofluorescence and flow cytometry	26
Table 6. Equipments used in this study	27
Table 7. Composition of medium used to differentiate renal vesicle cells into PTEC in this study	28
Table 8. The flow cytometry showed percentage of d16 hPSC-derived PTEC on MABB uptake substrates in presence and absence of inhibitors	39
Table 9. Cell yield on 40cm² Matrigel-coated alginate beads with biolevitation	41

List of abbreviations

2D	Two dimensional	P-gp	Permeability glycoprotein
3D	Three dimensional	RAS	Renin-angiotensin system
AKI	Acute kidney injury	ROS	Reactive oxidant species
AQP1	Aquaporin 1	RET	Receptor Tyrosine Kinase
BCRP	Breast cancer resistance protein	SGLT2	Sodium-glucose linked transporter-2
CKD	Chronic kidney disease	SIX2	SIX Homebox 2
ESRD	end-stage renal disease		
GLUT	Glucose transporters		
hPSC	Human pluripotent stem cells		
hiPSC	Human induced pluripotent stem cells		
KIM-1	Kidney injury marker-1		
LRP2	Low-density lipoprotein-related protein 2		
MAB	Matrigel coated alginate beads		
MABB	Matrigel coated alginate beads in a fluidic biolevitation environment		
MRP	Multidrug resistance associated protein		
MATE	Multidrug and toxic compound extrusion		
Na ⁺ /K ⁺ -ATPase	Sodium-Potassium ATPase		
OAT	Organic anion transporter		
OCT	Organic cation transporter		
PTEC	Proximal tubular epithelial cells		
PT	Proximal tubule		
pH	Potentia hydrogenii		

Abstract

There is an increasing need for a highly standardized, scalable source of proximal tubular epithelial cells (PTEC) for pre-clinical models of the kidney, for large-scale substance-induced nephrotoxicity and drug screening, or for application in cell therapies. Major problems of classical resources of primary and immortalized PTEC are frequent dedifferentiation, lack of personalization, and non-availability of functional equivalence. These limitations can be solved by PTEC derived from human pluripotent stem cell (hPSC) which offers an endless cell source, specificity with each donor, capability of genetic modifications. For these reasons, research using hPSC is widespread, but adequate technologies for mass production of hPSC and derived products are lacking. My goal was to develop an approach for hPSC-derived PTEC.

The first aim was to identify media composition which support the efficient generation of hPSC-derived PTEC in two dimensional (2D) culture. The second aim was to determine culture parameters for large scale generation of hPSC-derived PTEC in a bioreactor environment based on the identified media composition in 2D culture. In order to mass-produce hPSC-derived PTEC in an automated and reproducible way, the complete process of expansion and directed differentiation of hPSC was performed on matrix-coated alginate beads in a dynamic fluidics system, called biolevitation. Three dimensional (3D) culture in biolevitation showed significant improvements in both cell expansion and differentiation efficacy compared 2D culture. After 24 days, overall expansion of cells on matrix-coated alginate beads in biolevitation was 9-10 times. This yield was around 4 times higher than those in 2D culture. Besides expressing Aquaporin 1 (AQP1), Sodium-Potassium ATPase (Na^+/K^+ -ATPase), Low-density lipoprotein-related protein 2 (LRP2/Megalin) and Sodium-glucose linked transporter-2 (SGLT2) like hPSC-derived PTEC in 2D culture. PTEC on beads showed expression of functional proteins for detoxification including organic anion transporters (OAT) and organic cation transporters (OCT). PTEC on beads were functional with respect to the reabsorption of glucose and albumin as well as in uptaking organic ions from peritubular capillaries. After treatment with the common chemotherapy agent cisplatin, PTEC on beads expressed Kidney injury marker-1 (KIM-1) indicating suitability for nephrotoxicity applications. Moreover, PTEC harvested from beads could form a monolayer and stably expressed functional solute transporters. My study was the first

research of mass production of human PTEC using biolevitation and matrix-coated alginate beads.

Zusammenfassung

Es besteht ein zunehmender Bedarf für eine hoch standardisierte, skalierbare Quelle proximaler tubulärer Epithelzellen (PTEC) für präklinische Modelle der Niere, für substanzinduzierte Hochdurchsatz Nephrotoxizitäts- und Arzneimittelscreenings oder für die Anwendung in Zelltherapien. Hauptprobleme bei klassischen Ressourcen von primären und immortalisierten PTEC sind häufige Dedifferenzierung, fehlende Personalisierung und nicht-Verfügbarkeit von funktionaler Äquivalenz. Diese Einschränkungen können durch PTEC aus humanen pluripotenten Stammzellen (hPSC) überwunden werden, die eine unlimitierte Zellquelle, Spenderspezifität und die Fähigkeit genetischer Modifikationen bieten. Aus diesen Gründen ist die Forschungsverwendung von hPSC weit verbreitet, es fehlen jedoch adäquate Technologien für die Massenproduktion humaner PSC und abgeleiteter Produkte. Mein Ziel war es, hierfür einen Ansatz für hPSC – abgeleitete PTEC zu entwickeln.

Das erste Ziel bestand darin, Medienzusammensetzungen zu identifizieren, die die effiziente Erzeugung von hPSC-abgeleiteten PTEC in zweidimensionaler (2D) Kultur unterstützen. Das zweite Ziel war die Bestimmung von Kulturparametern für die Generierung von hPSC-abgeleiteten PTEC im großen Maßstab in einer Bioreaktorumgebung basierend auf der identifizierten Medienzusammensetzung in 2D-Kultur. Um hPSC-abgeleitete PTEC auf automatisierte und reproduzierbare Weise in Massenproduktion herzustellen, wurde der vollständige Prozess der hPSC-Expansion und gerichteten Differenzierung an neuartigen matrixbeschichteten Alginatekügelchen in einem dynamischen Fluidiksystem namens Biolevitation durchgeführt. Die 3D-Kultur in Biolevitation zeigte signifikante Verbesserungen sowohl der Zellexpansion als auch der Differenzierungseffizienz im Vergleich zur 2D-Kultur. Nach 24 Tagen betrug die Gesamtexpansion der Zellen auf matrixbeschichteten Alginatekügelchen in Biolevitation das 9- bis 10-fache. Diese Ausbeute aus der Biolevitation war etwa 4-mal höher als bei der 2D-Kultur. Neben der Expression von Aquaporin 1 (AQP1), Natrium-Kalium-ATPase (Na^+/K^+ -ATPase), Megalin und Natrium-Glucose-linked Transporter-2 (SGLT2) wie hPSC-abgeleitete PTEC in 2D-Kultur, PTEC auf Kügelchen zeigte die Expression funktioneller Proteine für die Entgiftung, einschließlich Transporter für organische Anionen (OAT) und Transporter für organische Kationen (OCT). PTEC waren funktionell in Bezug auf die Reabsorption von Glucose und Albumin sowie bei der

Aufnahme organischer Ionen aus peritubulären Kapillaren. Nach der Behandlung mit dem gängigen Chemotherapeutikum Cisplatin exprimierten PTEC den Kidney Injury Marker-1 (KIM-1), was auf die Eignung für Nephrotoxizitätsanwendungen hinweist. Darüber hinaus eine effiziente Zellernte möglich; die geernteten PTEC bildeten mit funktionellen Transportern ausgestattete Epithelteppiche. Meine Studie war die erste Forschung für die reproduzierbare Massenproduktion von humanen hPSC – abgeleiteten PTEC geeignete Technologie.

1. Introduction

1.1. KIDNEYS AND FILTERING SYSTEM

Vertebrates, including humans have two kidneys, which play a crucial role in blood filtration, liquid homeostasis and blood pressure regulation. Regarding anatomy from outermost part into innermost part, kidney is composed of cortex, medulla, and pelvis. The functional unit of the kidney, the nephron, is mainly located in the cortex (Figure 1). In humans, each kidney contains approximately one million nephrons. Nephrons are composed of a blood filtration system, called renal corpuscle, and a long tubular system responsible for absorption of substances and fluid as well as secretion of toxic compounds. The glomerulus is a blood filtering unit of the renal corpuscle allowing water and small molecules such as glucose, electrolytes, creatinine to pass through its filtration barrier while keeping blood cells and large molecules in circulation. Filtrate from glomerulus called pre-urine passes directly into a tubular system beginning with proximal tubule, followed by the Henle loop, distal tubule and ending at the collecting duct. The proximal tubule is responsible for reabsorption of water, essential substances as well as detoxification.

The nephron is composed of more than 20 cell types ¹. The scope of this study was restricted to proximal tubular epithelial cells (PTEC) forming the proximal tubule (PT). PTEC are cuboidal polarized cells with apical side facing the filtrate from glomerulus and basolateral side facing vascular capillaries (Figure 2). PTEC selectively reabsorb the majority of essential compounds from the pre-urine like water, glucose, albumin. Additionally, abundant organic solute transporters enable PTEC to secrete organic acids including creatinine and bases into the urine, regulating the *potentia hydrogenii* (pH) of the filtrate. The transporter system of PTEC is presented in Table 1.

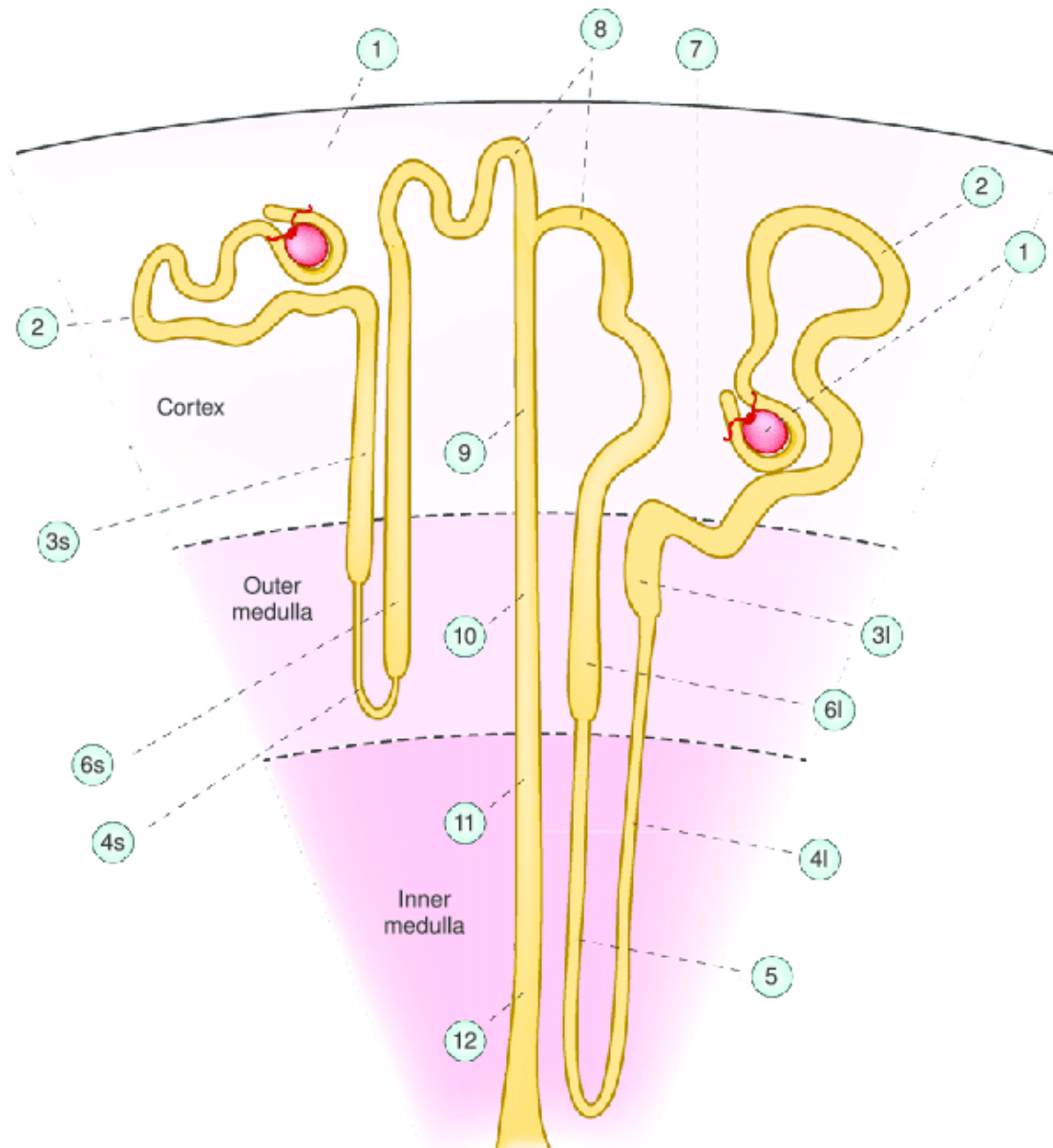


Figure 1. Nephron structure. 1. glomerulus; 2, proximal convoluted tubule; 3s and 3l, proximal straight tubule in the shortlooped nephron (3s) and long looped nephron (3l); 4s and 4l, thin descending limb; 5, thin ascending limb; 6s and 6l, medullary thick ascending limb; 7, macula densa; 8, distal convoluted tubule; 9, cortical collecting duct; 10, outer medullary collecting duct; 11, initial inner medullary collecting duct; and 12, terminal inner medullary collecting duct (Figure and legend from Weiner ID, 2015)².

Table 1. List of transporters in PTEC

SOLUTE AND SUBSTANCES TRANSPORTERS FOR REABSORPTION					
Transporter	Location	Substrate	Function	Mechanism	Ref
AQP1	A,B	Water	Transport water from filtrate into PTEC then into blood stream	Mainly by transcellular osmosis; partialy by paracellular route	Baum M,2005 ³
Na⁺/K⁺-ATPase	B	Na ⁺ , K ⁺	Transport actively Na ⁺ from PTEC into blood, resulting secondary reabsorption of water, glucose and other solutes; Transport K ⁺ from blood into PTEC	Primary active transport (uniport)	Jorgensen PL, 1986 ⁴
SGLT2	A	Na ⁺ , Glucose	Transport glucose from filtrate into PTEC	Secondary active transport (Cotransport/ symport)	Malhotra A, 2015 ⁵
GLUT	B	Glucose	Transport glucose from PTEC into blood stream	Diffusion	Lu IT, 2019 ⁶
Megalin	A	Albumin	Transport albumin from filtrate into PTEC	Receptor mediated endocytosis	Ferrell N, 2012 ⁷
Cubilin	A	Albumin	Transport albumin from filtrate into PTEC	Receptor mediated endocytosis	Ferrell N, 2012 ⁷
ORGANIC TRANSPORTERS FOR DETOXIFICATION					
OAT1	B	OA	Transport OA from blood into PTEC	Tetiary active transport (exchange/antiport OA/dicarboxylate)	Sandoval P, 2021, Faucher Q, 2020 ^{8,9}
OAT3	B	OA, OC (creatinine)	transport OA from blood into PTEC	Tetiary active transport (exchange/antiport OA/dicarboxylate)	Sandoval P, 2021, Faucher Q, 2020, Nishijima T, 2019 ⁸⁻¹⁰

MRP2	A	OA	Transport OA from PTEC into filtrate	Secondary active transport (uniport)	Faucher Q, 2020 ^{9,11}
MRP4	A	OA	Transport OA from PTEC into filtrate	Secondary active transport (uniport)	Faucher Q, 2020 ^{9,11}
BCRP	A	OA	Transport OA from PTEC into filtrate	Secondary active transport (uniport)	Faucher Q, 2020 ⁹ , Schaub TP, 1999 ¹¹
OCT2	B	OC (Creatinine, cisplatin)	Transport OC from blood into PTEC	Passive transport (Electrogenic facilitated diffusion/uniport)	Faucher Q, 2020 ⁹ , Wright SH, 2019 ¹² , Ciarimboli G, 2012 ¹³
OCT3	B	OC	Transport OC from blood into PTEC	Passive transport (Electrogenic facilitated diffusion/uniport)	Nishijima T, 2019 ¹⁰
MATE	A	OC (cisplatin)	Transport OC from PTEC into filtrate	Secondary active transport (exchange/antiport OC/H ⁺)	Faucher Q, 2020 ⁹ , Wright SH, 2019 ¹²
P-gp	A	OC	Transport OC from PTEC into filtrate	Secondary Active transport (uniport)	Faucher Q, 2020 ^{9,14}

Aquaporin 1 (AQP1), Sodium-Potassium ATPase (Na⁺/K⁺-ATPase), Sodium-Glucose linked transporter-2 (SGLT2), Organic anion transporter 1 (OAT1), Organic anion transporter 3 (OAT3), Multidrug resistance associated protein 2 (MRP2), Multidrug resistance associated protein 4 (MRP4), Breast cancer resistance protein (BCRP), organic cation transporter 2 (OCT2), organic cation transporter 3 (OCT3), Multidrug and toxic compound extrusion (MATE), Permeability glycoprotein (P-gp); A: apical side, B:

basolateral side; OA: organic anions, OC: organic cations; Ref: reference. Transporters used for characterization in my study were highlighted in bold type. (Table 1: own representation: Ngo,Thi Thanh Thao)

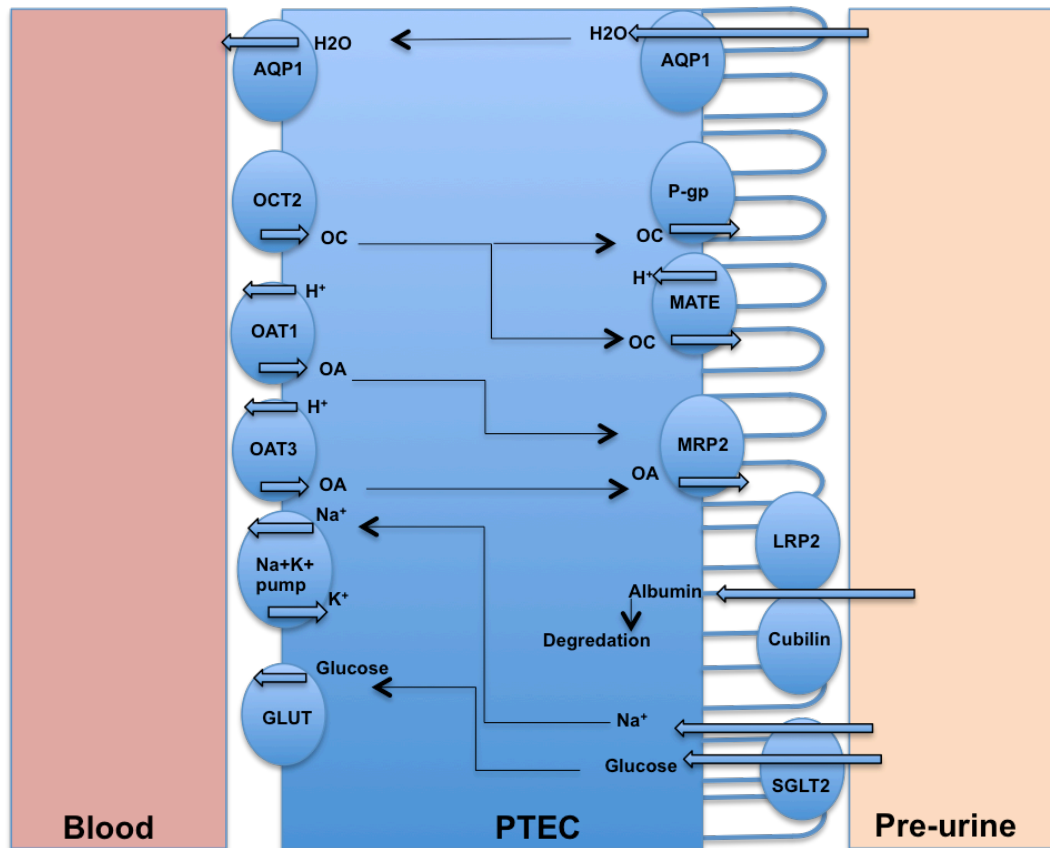


Figure 2. Transport system in PTEC. Aquaporin 1 (AQP1), organic cation transporter 2 (OCT2), Organic anion transporter 1 (OAT1), Organic anion transporter 3 (OAT3), Sodium-Potassium ATPase (Na^+/K^+ pump), Glucose transporters (GLUT), Sodium-Glucose linked transporter-2 (SGLT2), low-density lipoprotein-related protein 2 (Megalin/LRP2), Multidrug resistance associated protein 2 (MRP2), Multidrug and toxic compound extrusion (MATE), Permeability glycoprotein (P-gp). (Figure 2: own photograph: Ngo, Thi Thanh Thao).

1.2. PTEC SOURCES FOR NEPHROTOXICITY SCREENING, TISSUE MODELLING AND REGENERATIVE THERAPIES

The proximal tubule (PT) is a primary target organ for acute tissue injury (AKI) because of its steady exposure to metabolites and substances in the filtrate and blood. Clinical observation shows that repeated AKI accompanied by inflammation often results in a chronic stage and eventually in renal dysfunction (end-stage renal disease-ESRD);

however, how AKI progress to chronic kidney disease (CKD) in some patients as well as role of PT in this progression are still under investigated.^{15,16}

Patients are able to completely recover from tubular injury in general, and injured PT in particular. PTEC dedifferentiate, proliferate and differentiate to repair the injury¹⁶. However, severe or repeated injury may cause cell cycle arrest, mitochondrial dysfunction, epigenetic changes, metabolic changes, activation of the renin-angiotensin system (RAS), overproduction of reactive oxidant species (ROS) resulting in the loss or reduced regenerative potency and progression to CKD¹⁷. Some mechanism were suggested to explain the role of injured PT for progression of renal pathology from AKI to CKD. Firstly, injured PTEC promote tubular inflammation through secretion of pro-inflammatory cytokines and chemokines¹⁶, which is exacerbated by overproduction of ROS due to oxidative stress in injured PT^{16,18}. Prominent inflammation markers for CKD produced by injured PT include interleukin-6 (IL-6), interleukin-1 (IL-1), C-reactive protein and tumor necrosis factor-alpha (TNF-alpha)^{16,18}. Secondly, injured PT induce tubulointerstitial fibrosis, a typical feature of CKD¹⁶. Injured PTEC arrest at G2/M phase of cell cycle and secrete pro-fibrotic factors such as transforming growth factor- β (TGF- β), platelet-derived growth factor (PDGF) and connective tissue growth factor (CTGF) that promote transition of PTEC to fibroblasts and myofibroblasts¹⁶. Moreover, AKI associated activation of the RAS may cause tubulointerstitial fibrosis through action of Angiotensin II, a cleavage product of angiotensinogen^{16,19}. Angiotensin II activates pro-fibrosis mechanisms of TGF- β , and promotes proliferation of renal fibroblasts. Angiotensin II also promotes inflammation in glomerulus and tubular interstitium through recruiting inflammatory cells^{16,17}. Another contributor for tubulointestitial fibrosis is Canonical Wnt pathway^{16,20}. Last but not least, an *in-vitro* model investigating exposure of PTEC to high concentration of proteins like albumin, or transferrin suggested that injured PTEC with proteinuria can cause tubulointerstitial fibrosis through secretion of Endothelin-1, a pro-fibrosis and pro-inflammation factor¹⁶. Finally, some reports implied metabolic aberrations such as fatty acid oxidation resulting in accumulation of lipids in PTEC, and epigenetic changes in PTEC after injury to induce CKD progression¹⁶.

Disorders, and diseases relating or originating from PT are various; hence, there is a high need for kidney models mimicking the human disease at different stages, which are suitable for drug- and toxicity screening (Table 2, Table 3).

Existing *in vitro* PT models use a number of conventional PTEC sources. The use of primary PTEC isolated from human nephrectomies or urine ²¹ increased because they possess intrinsic characteristics of the *in vivo* system. However, laborious isolation, limited growth capacity, differential gene expression and phenotype in *in vitro* culture conditions limit reproducibility and utility of this source²². For example, only after a few days of culture, primary cells lose OCT2 transporter expression, which represents the most abundant organic cation transporter in PTEC ²³.

Several PTEC lines like HK-2, the human telomerase reverse transcriptase (hTERT) transgene immortalized human RPTEC/TERT1-line and the conditionally inactivated ciPTEC-hTERT line with a proliferation capacity of at least 90 population doublings ²⁴ are available for PT modeling. The HK-2 cell line was obtained by transduction of human papilloma virus 16 (HPV-16) E6/E7 genes ²². The RPTEC/TERT1 was made by transduction of a construct containing hTERT - a catalytic unit of telomerase enzyme. ciPTEC-hTERT was obtained by transfection using hTERT and a temperature-sensitive mutant of SV40T, allowing to switch between proliferating and differentiating stages of the PTEC ²⁵. Despite their high proliferation capacity, important characteristics of the original cells are not seen in these cell lines over time in culture ²⁶. Transporters for detoxification including organic ion transporters such as OAT1, OAT3, OCT2 and efflux transporters like MRP2, BCRP are absent in the HK-2 cells. Compared with HK-2 cells, RPTEC/TERT1 and ciPTEC lines possess more similar characteristics to primary cells such as high polarization, dome formation, expression of functional transporters including OCT2 and efflux transporters; However, transgene transduction was required to force expression of the OAT1 and OAT3 in these cells ²⁷.

Animal models have been largely used to mimic kidney diseases *in vivo* (Table 3); however, there are genetic, physiological and pathological differences between animal and human kidneys, which hamper interpretation of results from these models for their applicability to humans.

Table 2. PTEC lines used for establishment of PT models

Model	Used cell lines	Establishment	Characteristic of model	Ref
3D bioprinted and perfusion vascularised PT model	RPTEC/TERT1	Model includes separating PT channel and EC channel locating on high permeable ECM.	PT expressed transporters, uptaked glucose and vascularised by endothelial cells	Lin NYC, 2019 ²⁸
3D bioprinted and perfusion PT on chips	RPTEC/TERT1	Model is a PT with an open lumen. PTEC were embeded into ECM on a perfusable tissue chip, where physiological shear stress can be applied.	2 months stable, expressed key transporters, uptaked anbumin, and reacted to nephrotoxic.	Homan KA, 2016 ²⁹
3D Microfluidic PT	Primary hPTEC	Model includes separating PT channel and EC channel locating on membrane.	PT expressed transporters, uptaked glucose.	Vedula EM, 2017 ³⁰
3D PT model on hollow fibers	ciPTEC	ciPTEC were seeded into hollow fibers membranes	Form of an epithelial monolayer with expression of ZO1 and activity of OCT2	Prange JA, 2016 ³¹
AKI-induced hyperglycemia	HK2; RPTEC/TERT1; ciPTEC; LLC-PK1	Cells were treated by 20-25mM glucose	2D models used to study SGLT2 inhibitors, injuries caused by high glucose concentration in PTEC	Faria J, 2021 ³² , Harwood, 2007 ³³
AKI-induced nephrotoxic drugs	RPTEC/TERT1; ciPTEC	Cells were treated with different concentration of cisplatin, tenofovir, tobramycin, cyclosporin	3D model investigated nephrotoxicity through cell viability, LDH, miRNA analysis, toxicity markers.	Vormann MK, 2021 ³⁴
AKI-induced hypoxia	Primary PTEC; LLC-PK1	Cells were cultured in condition without oxygen and glucose supply for 18 hours.	Injury of cells were evaluated via LDH assay as well as generation of arachidonic acid metabolites	Turman MA, 1997 ³⁵

EC: endothelial cells, Conditionally immortalized PTEC from kidney tissue or from urine (Jansen J, 2014³⁶), LLC-PK1: Porcine tubular epithelial cell line, OCT: organic cation transporters, LDH: lactate dehydrogenase. (Table 2: own representation: Ngo,Thi Thanh Thao).

Table 3. Animal models of kidney diseases

Model	Species	Protocol/dosage	Advantages	Disadvantages	Ref
AKI-induced cisplatin	Mice/rat	6-20mg/kg cisplatin	Simple, highly reproducible	Utility of cisplatin in clinical is declined	Bao YW, 2018 ³⁷
CKD-induced cisplatin	Mice	Repeatedly inject cisplatin (15mg/kg)	Simple, highly reproducible	Utility of cisplatin in clinical is declined	Torres R, 2016 ³⁸
AKI-induced DT	Mice	0.25ng/g DT	DT only target to PTEC		Takaori K, 2016 ¹⁵
CKD-induced DT	Mice	Repeated injection of 0.25ng/g DT	DT only target to PTEC		Takaori K, 2016 ¹⁵
AKI-induced ischemia-reperfusion	Mice/rat	30-45 minutes for ischemia; 24-48h for reperfusion	Low cost, Closed to clinical pathology condition	Requirement of surgery after inducing.	Bao YW, 2018 ³⁷
CKD-induced diabetes	Mice/rat	Activation of RAS and YAP/TAZ by hybridization; Streptozotocin; diet	Genetic modification, commercial availability	Lack of a ideal model to mimic	Bao YW, 2018 ³⁷ , He X, 2019 ³⁹ , Nagao S, 2020 ⁴⁰
PKD in transgenic mice	Mice	Genetic modifications of pkd1 or pkd2	Easy to mimic PKD with single mutation, widely used		Bao YW, 2018 ³⁷ , Nagao S, 2012 ⁴¹
Alport syndrome (AS)	Mice	COL4A3 gene knockout mouse	Main model to investigate pathogenesis of AS		Bao YW, 2018 ³⁷ , Korstanje R, 2014 ⁴²
CKD-induced hypertension	Mice	Spontaneous hypertension plus unilateral nephrectomy; injection of angiotensin II	Compatible with hypertension nephropathy	Requirement of surgery after inducing.	Bao YW, 2018 ^{37,43}
Renal mass reduction	Rat	5/6 nephrectomy	Mimic well progression of renal failure	requirement of surgery after inducing	Bao YW, 2018 ³⁷ , Leelahav anichkul A, 2010 ⁴⁴

Amyloid A amyloidosis	Mice	Injection of casein, lipopolysaccharide	Widely used	Not often progress renal failure	Bao YW, 2018 ³⁷ , Simons JP, 2013 ⁴⁵
Systemic lupus erythematosus	Mice	Genetic modifications of murine models: MRL, CD95 mutants	Widely used due to development of proteinuria, lymphoproliferation, mimic well human lupus nephritis	Features of the disease are not fully mimiced	Bao YW, 2018 ³⁷ , Nickerson KM, 2013 ⁴⁶
Focal segmental glomerulosclerosis (FSGS)	Mice	Injection of adriamycin and puromycin	Common model to study FSGS	Dosage of toxins are different from species and strain.	Cao Q, 2010 ⁴⁷

DT: diphtheria toxin, RAS: renal angiotensin system, YAP: Yes-Associated Protein, TAZ: Transcriptional coactivator with PDZ-binding motif, STZ: streptozotocin, PKD: Polycystic kidney disease. (Table 3: own representation: Ngo,Thi Thanh Thao).

An emerging advanced *in vitro* model, offering extensive utilization for regenerative medicine and disease modelling are human kidney organoids. While mouse kidney organoids have been established since the 1960th from mouse embryonic kidneys^{48,49} the generation of human kidney organoids has not been possible for lack of source materials. However, human kidney epithelial cells obtained from biopsies have been used to build kidney spheroids⁵⁰. More recently, human kidney organoids were established from hPSC. Till today, the highest complexity of kidney organoids can be reached due to self-organization of PSC-derived kidney organoids, a structure including different cell types of kidney⁵¹. Kidney organoid models are excellent to study developmental processes, morphogenesis and genetic effects. However, for nephrotoxicity and drug screening, renal organoids are at the current stage of limited utility. Due to a mixture of renal and non-renal cell types, the immature state and lack of vascularization, as well 3D structural complexity, kidney organoids are confronted with translational and technological challenges: which compound concentrations have effects on which cell type, exposure to apical side or basolateral side for analyzing function of specific transporters and mode of delivery due to lack of vascularization⁵².

Moreover, high- and medium throughput imaging is highly demanding and other non-visual assays yet to be resolved technologically.

To overcome above mentioned shortcomings in terms of high functionality, robustness, unlimited source, homogeneity and reproducibility of PTEC, hPSC may provide an excellent source material. In addition, induced PSC technology offers the possibility of personalized kidney modeling and genetic stratification of models. To date, there have been several protocols describing the differentiation of hPSC into PTEC^{52–56}.

1.3. GENERATION AND CHARACTERIZATION OF hPSC-DERIVED PTEC IN TWO DIMENSIONAL STATIC AND MICROFLUIDIC CULTURE

For the first time, hPSC were reported to differentiate into PTEC in 2013 using a 20 days-protocol in 2D culture⁵³. This heterogenous mixture expressed different metanephric kidney markers, not only AQP1 and *Lotus tetragonolobus lectin* (LTL) characteristic for PT, but also podocalyxin and peanut agglutinin, typical for cells in the glomerulus and α SMA for smooth muscle cells. One year later, also in 2D culture, Lam et al published an 11-days protocol that differentiated hPSC specifically into a tubule-like structure. At protein level, more typical markers for PTEC including LTL, N-cadherin, AQP1 and Megalin were detected. However, cells comprising a tubular structure also expressed Nephhrin (NPHS1) and Synaptopodin (SYNPO) characteristic for podocytes, Uromodulin (UMOD) for loop of Henle, and AQP2 for collecting duct⁵⁴. Similarly to previous publications, Hariharan et al. (2017) described the directed generation of PTEC within 14 days with an efficiency of around 57%, based on AQP1 expression⁵⁵. In order to use PTEC from these protocols, a further enrichment step is required. There are some complications to do this step because of poor recovery of PTEC after cell sorting by flow cytometry or magnetic-activated cell sorting (MACS).

Kandasamy et al, successfully developed in 2015 a rapid one-step protocol for the differentiation of human induced pluripotent stem cells (hiPSC) on Matrigel-coated plates into PTEC within 8 days with more than 90% purity. On day 8, cells expressed PTEC-specific markers at protein level including AQP1, SGLT1, Glucose transporter 1 (GLUT1), OAT3, Peptidtransporter 1 (PEPT1), Na^+/K^+ ATPase and Zonula occluden-1 (ZO-1). OAT and OCT2 activity were confirmed by functional assays. However, these markers were stable for only 2 days⁵⁶. Recently, Chandrasekaran et al. (2021)

developed a step-wise protocol by using small molecules and growth factors to generate PTEC within 14 days that showed expression and function of Megalin and ATP-binding cassette transporter protein (ABCB1). These markers were stable for up to 7 days⁵². Despite the generation of PTEC with high purity, similar to previous 2D protocols, PTEC from these both protocols highly expressed the injury marker KIM-1 without any drug treatment and did not show correct apical-basolateral polarization of functional transporters²⁴. Moreover, only few solute transporters for detoxification were reported in these publications.

Maintaining transporters and metabolic function of hPSC-derived PTEC as well as achieving maturity and competence of hPSC-derived PTEC to recapitulate *in vivo* cell characteristics and polarization seems to be impossible in static 2D culture, likely because of a lack of shear stimulation/fluid flow across the cell surface⁵⁷. This led to the development of different 2.5 dimensional (2.5D) formats⁵⁸⁻⁶⁰, microfluidic and three dimensional (3D) culture systems. Improvement was shown in the maintenance of primary PTEC and immortalised cell lines cultivated on 2D microfluidic chips^{24,57}, or on fabricated 3D perfusable chips²⁹, where fluidic flow can be applied across the apical pole of the cells and PTEC were maintained in culture up to 2 months²⁹. However, to our knowledge, there has not been any system used to differentiate hPSC into PTEC and maintain these cells in a fluidic environment in continuous cultivation in a scalable system.

1.4. MICROCARRIERS FOR ANCHORAGE-DEPENDENT CELL GROWTH IN FLUIDIC SYSTEMS

Microcarrier technology has been developed for a long time. Anchorage-dependent cell growth as monolayers on the surface of microcarriers or small beads was reported for the first time in 1967⁶¹. These beads possessed a positively charged surface and were used for cultivation of human embryonic lung cells. The increasing surface area/volume ratio, approximately 20cm²/ml versus 4cm²/ml in comparison to Petri dishes, resulted in a significantly increased yield of cells from small culture volume (10-fold or more)⁶¹. Thus, by applying continuous propagation techniques, cultivation of anchorage-dependent cells on beads in suspension cultures like stirred bioreactors does not require elaborate sub-culturing steps and is only dependent on the available surface area and bioreactor volume.

A microcarrier is composed of a base that is often a cross-linked polysaccharide with or without a polypeptide conjugated to the base component^{62,63}. Microcarrier bases can be formed by cross-linked polysaccharide such as agarose, starch, dextran, cellulose or polyglucose beads, or alginate. Conjugation of a polypeptide to the base requires a free carboxylic acid group. A carboxylic acid group needs to be introduced in most microcarrier-bases while they are naturally available in microcarrier bases generated from alginate. Furthermore, alginate is readily available in clinical grade and has been used in for multiple clinical applications, for example to encapsulate beta cells^{63,64}. These features make using alginate to produce beads highly advantageous. Many commercial microcarriers are available for the expansion of anchorage-dependent cell types, typically as dextran microcarriers – like Cytodex, and cellulose microcarriers – like Cytopore. Among Cytodex microcarriers, Cytodex 3, additionally, covered by a denatured type 1 collagen layer is the most suitable one for the cultivation of several different primary cell types and established cell lines⁶¹. However, due to the inert xeno-free characteristics, natural availability and abundant resources, easy modification of physical properties such as stiffness and reversible gelation and possible biodegradability, alginate beads offer a variety of application advantages for tissue modelling. Importantly, clinical grade alginates are already used as vehicles for drug delivery, immunoisolated transplantation via microcapsules with a proven safety record^{64–68}; however, reports for the cultivation of adherent cells on alginate beads are very limited. Rowley et al, 1998 reported an enhanced attachment of mouse skeletal myoblasts on surfaces of alginate hydrogel coupled with a sequence arginine-glycine-aspartic acid (RGD) used as adhesion ligands⁶². RGD-modified alginate hydrogels also allow cultivation of chondrocytes, ovarian follicle cells, and bone marrow stromal cells⁶⁵. Additionally, modifications with YIGSR peptides enhance the adhesion of neuronal cells⁶⁹. Few publications reported expansion and differentiation of hPSC on alginate hydrogel⁶⁶. Expansion and differentiation of hPSC on alginate beads was reported by Gepp et al⁷⁰. Gepp showed a high attachment of hiPSC on Matrigel-coated alginate beads. Moreover, Gepp showed a better attachment of human mesenchymal stem cells on these alginate beads compared to collagen 1-precoated dextran microcarriers. Since hPSC need a specific matrix to attach and grow, Matrigel-coated alginate beads offer a promising condition for the cultivation and expansion of hPSC. Before coated by Matrigel, alginate beads need to be modified with a amide-containing linker that increases coating efficacy by enhancing absorption of Matrigel proteins on alginate

surface, resulting in high attachment of hPSC on the beads⁷⁰. Therefore, Gepp reported a protocol for the modification of alginate beads, which finally allows a standard surface coating of the beads⁷⁰. Additionally, Gepp successfully showed the attachment and contraction of hiPSC-derived cardiomyocytes on these alginate beads.

hPSC can be expanded as adherent monolayer colonies in 2D cultures, as single cell suspensions^{71,72}, encapsulated in thermoresponsive hydrogels⁷² or on surface of microcarriers like alginate beads⁷⁰ in bioreactors. There are many kinds of bioreactors used for cell expansion including shaking flasks and spinner flask systems with capacities ranging from 100ml to several liters^{71,72}. Compared to static cultures, bioreactor-based processes reduces the laboratory work, generates a homogenous medium for cell development due to presence of rotating or stirring systems; however, most systems mentioned above require large medium consumption and are most suitable for applications where a large number of cells is needed in one batch. Furthermore, most bioreactor systems submit significant shear stress to cells. Generating cells for biobanking or preclinical applications require highly flexible systems, which are suitable to produce smaller cell numbers with minimal medium consumption and high flexibility of culture condition adjustments, and scalability to produce high cell numbers under optimized cultivation conditions. Biolevitation furthermore offers the possibility to provide fluidic flow under very low shear stress conditions. Midi-scalable bioreactors based on biolevitation principles appear to be highly suitable for cultivation of hPSC and their differentiation into a diverse array of cell types and subsequent upscaling. Furthermore, alginate beads can easily be adopted for biolevitation-based cell cultivation due to their flexible mechanic-physical properties. However, there has not been any publication using alginate beads in combination with biolevitation for the expansion and differentiation of hPSC in a single step.

BiolevitatorTM from Cero offers a system suitable for setting standard procedures for expansion and differentiation of hPSC at affordable cost. In addition, the number of reactor vessels is scalable unlimitedly and thus providing flexibility to produce a wide range of cell numbers. One Cero system operates four separated 50ml-Cerotubes that have small fins and flat bottom to reduce shear stress to cultured cells but providing adjustable flow stimulation. To the best of our knowledge, Cero was used for the first time in 2015 by Elanzew⁷² for the cultivation of hPSC as aggregates, which led to a 5-

fold expansion after 4 days. Additionally, Fischer et al, 2018 reported a successful induction of single hiPSC into cardiospheres using the Cero system⁷³.

1.5. HYPOTHESIS, AIMS AND THE PRESENT STUDY

In summary, there is a high need for a continuous supply of PTEC for human PT modelling, reproducible and reliable large scale drug – and toxicity screening. Human PSC-derived PTEC provide a personalized cell source material, with multiple established protocols for their differentiation into PTEC. I hypothesized that fluidic environments may provide favourable conditions to generate high numbers of reproducibly functional PTEC and better maintenance of typical PTEC characteristics upon differentiation. Matrigel-coated alginate beads have been shown to promote hPSC expansion. Using a controllable fluidics environment in a biolevitation bioreactor we furthermore hypothesized that differentiation of hPSC on Matrigel-coated alginate beads may facilitate an adjustable surface for tubular formations for maturation of PTEC in a reproducible way.

Aim of the study was to develop a reliable, high efficient technique to direct hPSC towards the renal lineage and into functional PTEC.

2. Methods

This section explains the principles of the methods used for the study. Materials used for this study were presented in Table 4, Table 5 and Table 6.

Table 4. Human PSC-lines used in this study

Cell line	Source	Vector	Factors
WAe001-A	Human embryo		
WISCI004-A	Lung fibroblasts	Lentivirus	Oct4, Sox2, Nanog, Lin28
BCRTi005-A	Urinary cells	Sendai virus	Oct4, Sox2, Klf4, cMyc

(Table 4: own representation: Ngo,Thi Thanh Thao)

Table 5. List of antibodies used for immunofluorescence and flow cytometry

Name	Species	Description	Company	Cat.Nr
AQP1	Rabbitpolyclonal	Apical/Basolateral side of PTEC	Proteintech	20333-1-AP
Na ⁺ /K ⁺ -ATPase	Rabbitpolyclonal	Basolateral side of PTEC	Abcam	ab76020
SGLT2	Mousepolyclonal	Basolateral side of PTEC	Abcam	ab58298
LRP2	Rabbitpolyclonal	Apical side of PTEC	Abcam	ab76969
E-cadherin	Mousepolyclonal	Basolateral side of PTEC	BD Biosciences	610181
KIM-1	Mousepolyclonal	Apical side	ThermoFisher	
OCT2	Mousemonoclonal	Basolateral side of PTEC	Abcam	ab242317
OAT1	Rabbitpolyclonal	Basolateral side of PTEC	LSBio	LS-B10034
OAT3	Rabbitpolyclonal	Basolateral side of PTEC	Abcam	ab247055
P-gp	Mousemonoclonal	Apical side of PTEC	Abcam	ab253265
MRP2	Mousemonoclonal	Apical side of PTEC	ThermoFisher	MA1-26535
Six2	Mousemonoclonal	Embryonic cap mesenchyme	Abnova	H00010736-M01
RET	Rabbitpolyclonal	Ureteric buds	LSBio	53164
JAG1	Rabbitpolyclonal	Renal vesicle	Abcam	ab7771
WT1	Mousemonoclonal	Renal vesicle	SCBT	sc192

(Table 5: own representation: Ngo,Thi Thanh Thao)

Table 6. Equipments used in this study

Equipment	Manufacturer/Supplier
Cero	OLS
Cerotube™	OLS
Operetta High Content Screener	Perkin Elmer, Waltham
MACSQuant Analyzer Cytometer	Miltenyi Biotec
Microtome	Leica RM2255
Zeiss EM 906 electron microscope	Carl Zeiss, Oberkochen, Germany
Microplate reader	Spectra max 384 WPI
EVOM3 Ohmmeter	
Incubator 11-13625	BINDER GmbH, Tuttlingen
Cell scraper	TPP® Techno Plastic Products AG, Trasadingen

(Table 6: own representation: Ngo,Thi Thanh Thao)

2.1. MEDIUM SCREENING FOR PTEC DIFFERENTIATION OF HPSC IN 2D CULTURE

Two human induced pluripotent stem cell (hiPSC) lines (BCRTi005-A, WISCi004-A) and one human embryonic stem cell (hESC) line (WAe001-A) were cultured in defined serum-free Essential 8 (E8) medium on 2D plates coated by Geltrex that is the same Matrigel but from different company. When hPSC reached 70-80% confluence, they were differentiated into renal progenitor cells (day 8 cells) using an 8-day protocol developed by Hariharan et al⁵⁵. Specifically, by using a combination of Activin A, Retinoic Acid, and recombinant human bone morphogenetic protein 4 (BMP4) for the first 4 days hPSC were induced into intermediate mesoderm. For further 4 days, cells were induced into renal vesicle cells (day 8 cells) using Glial derived neurotrophic factor (GDNF). Day 8 (d8) cells were further differentiated into PTEC using 6 different media compositions (Table 7).

Table 7. Composition of medium used to differentiate renal vesicle cells into PTEC in this study

	Medium 1	Medium 2	Medium 3	Medium 4	Medium 5	Medium 6
Basal medium	DMEM-Ham'sF12 (1:1)	DMEM-Ham'sF12 (1:1)	DMEM/F12 (1:1)	Low glucose DMEM/F12 (1:1)	Low DMEM-Ham'sF12 plus KSFM (1:1)	DMEM/F12 plus KSFM (1:1)
Supplement						
ITS	x	x	x	x	x	x
EGF	x	x	x	x	x	x
Hydrocortisone	x	x	x	x	x	x
T3	x	x				
Prostaglandin E1	x	x				
Ascorbic acid		x				
DMSO					x	x
Bovine pituitary extract						x
Cholera toxin						x
Retinoic acid	x					
Ethanolamine	x					
Phosphorylethanolamine	x					
Dexamethasone	x					
Trace elements	x					
Cell line cultured	Porcine PTEC	RPTEC/TE RT1	RPTEC/TE RT1	RPTEC/TE RT1	hPSC-induced PTEC	Rat-PTEC
Reference	Humes, 1999 ⁷⁴	Wieser, 2008 ²⁵	Ellis, 2011 ⁷⁵	Radford, 2012 ⁷⁶	Home-made	Chang, 2013 ⁷⁷

Dulbecco's modified Eagle's medium (DMEM); Keratinocyte serum-free medium (KSFM), Insulin-Transferrin-Selenium (ITS), Recombinant human epidermal growth factor (EGF), Triiodothyronine (T₃), Dimethyl sulfoxide (DMSO). (Table 7: own representation: Ngo,Thi Thanh Thao).

To differentiate renal vesicle cells (d8 cells) into PTEC, different previously published PTEC medium compositions for the cultivation of primary PTEC and immortal cell line were tested. Additionally, the home-made media, media 5, was enrolled in the screening. The composition of medium 5 was defined as followed: It was reported

previously, that PTEC require a low glucose medium for growth⁷⁸, therefore we switched from high-glucose basal media to low-glucose media. We modified basal media using low glucose DMEM/Ham'sF12 instead of high glucose DMEM/F12 (17mM). Glucose concentration of this home-made medium was around 7.6mM that was quite similar to those of commercial renal epithelial growth medium (REGM, Lonza) 6.6mM. For medium 4 it was reported, that RPTEC/TERT1 was also cultured in a low glucose medium⁷⁶. Additionally, we eliminated the xeno-components and replaced them by chemically-defined Insulin-Transferin-Selelium (ITS) supplement. Regarding the choice of growth factors for the home-made medium, we chose and picked commonly used growth factors that were co-present in REGM and others including Recombinant human epidermal growth factor (EGF) and hydrocortisol. Dimethyl sulfoxide (DMSO) was only present in medium 6 but also included into the formulation of medium 5. Beside being a drug solvent, a cryoprotectant, DMSO was also a potent inducer in studies of cardiac differentiation⁷⁹⁻⁸². I think that DMSO might have a certain effect on our PTEC differentiation. This was confirmed via our experiment. In medium with presence of DMSO, cells exhibited a cobblestone appearance with dome formation while without DMSO supplement, these events were not seen (Figure 3). Additionally, hydrocortisone concentration in our home-made medium was reduced 1000 times to 1 μ M compared to 1mM in medium 6 since hydrocortisone induces high sensitivity to EGF resulting in an increased proliferation rate while under normal circumstances, PTEC divides at a low rate *in vivo*⁸³.

In conclusion: The medium screening on 2D culture plates revealed the home-made medium 5 generated highest differentiation efficiency for PTEC with 70% AQP1, and 80% SGLT2. From this result, this medium was called PTEC medium.

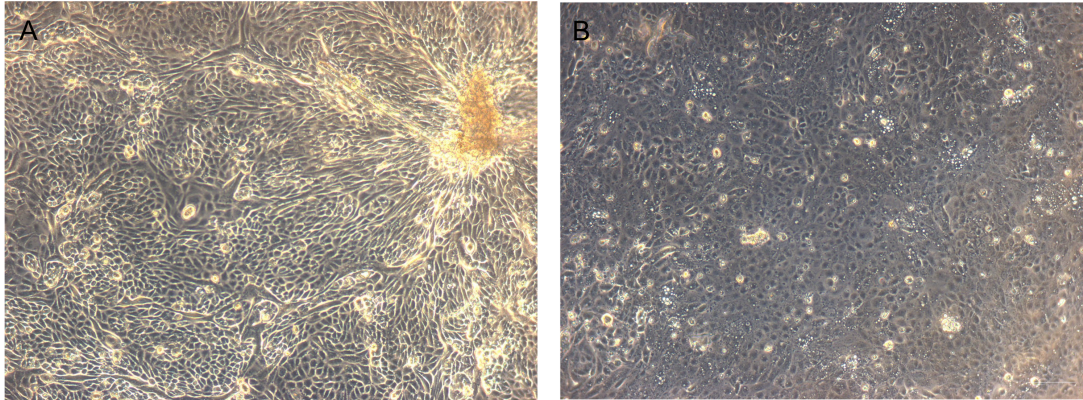
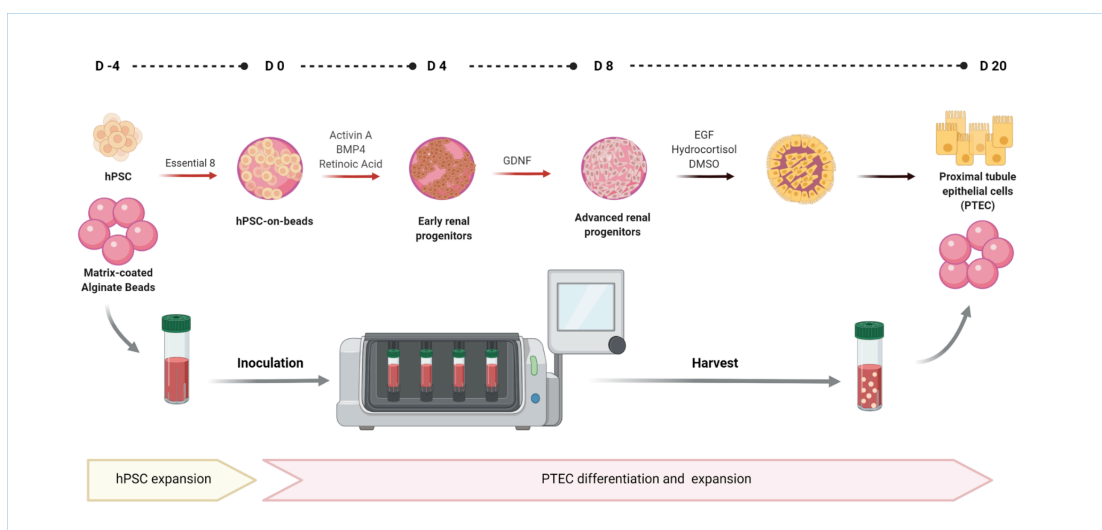


Figure 3. Phase contrast pictures of d16 cells on 6 well-plates in presence (A) and absence (B) of DMSO. (Figure 3: own representation: Ngo, Thi Thanh Thao).

2.2. EXPANSION AND DIFFERENTIATION OF CELLS ON MATRIGEL-COATED ALGINATE BEADS WITH BIOLEVITATION

The 2D differentiation protocol presented above was directly applied to the 3D hPSC-differentiation performed on Matrigel-coated alginate beads (MAB) in a fluidic biolevitation environment (MABB), called Cero. In particular, hPSC were seeded on MAB on day -4 (d-4). After 4 days, when cells covered almost surface of beads, on day 0 (d0) cells were differentiated into progenitor cells for 8 days⁵⁵ and further differentiated into PTEC until day 20 (d20). Schematic diagram of differentiation protocol is shown in Figure 4.



“Figure 4. Protocol of expansion and differentiation of hPSC on Matrigel-coated alginate beads in Cero (Figure 4 has been published in Ngo et al, 2022⁸⁴)”

2.3. CULTURE PARAMETERS OF HPSC ON MATRIGEL-COATED ALGINATE BEADS WITH BIOLEVITATION

For a homogenous distribution of hPSC on MAB, generation of small hPSC-colonies were required. 70-80% confluent hPSC on the culture plates were incubated with 0.5mM ethylenediaminetetraacetic acid (EDTA) for 3 minutes, dislodged by a scrapper and gently transferred to MAB. To prevent MAB from floating in medium that effects on attachment efficiency of hPSC on beads as well as minimize rotation speed causing shear stress for cells, MAB density of 40cm² in 10ml medium was used for each Cerotube. Additionally, to prevent the form of complex agglomerates from small beads⁷⁰ as well as a reduction in the final cell yield/g bead from using large beads, MAB with medium size from 300-400µM were used in my study⁶¹.

The culture process of cells in MABB is composed of three stages: inoculation, culture and harvest. The most important stage is the initial stage in which cells start to attach and proliferate on the beads. In this stage, inoculation density need to be optimised to get a maximum cell yield for the expansion stage⁶¹. A minimum inoculation density is required whereby the cells can attach homogenously all beads, since afterwards cells are not going to migrate from one bead to others. Additionally, cell number should not be too high to prevent multilayer formation on the beads. Minimum inoculation density alters for each cell type⁶¹. We tested different inoculation densities of hPSC on 40cm² of MAB, and 6.5x10⁴ cells/cm² was my optimised minimum inoculation density for all three hPSC lines used. With this inoculation density, cells covered more than 90% of the beads after 4 days.

To enhance exposure of cells with MAB, low medium volume and intermittent stirring method of Clark were applied for the inoculation step⁸⁵. Specifically, hPSC were inoculated in 3-4ml E8 for 5 hours with 2 minutes agitation at 40rpm in alternating direction (4s/direction) and 15 minutes agitation pause. After the inoculation step, in the further culture step, cells were cultivated in 10ml medium at 37°C and 5% CO₂ under continuous rotation at 40rpm in alternating directions (4s/direction).

2.4. PROCESSING MATRIGEL-COATED ALGINATE BEADS FOR CHARACTERIZATION

For cell characterization of hPSC-derived PTEC on MAB, PTEC were directly fixed on beads and encapsulated into 4% low-melting agarose. The melting temperature of this agarose is at 65.5°C and still remains liquid at 37°C. Low gelling point at 24-28°C is considered as a huge advantage of low-melting agarose compared to standard agarose with a gelling point at 34-38°C. Beside the protection of the cells on the beads from destruction by high temperature, it is also easier to handle low-melting agarose. Afterward, the agarose blocks containing the cell-bead structures were dehydrated, samples were passed through a series of different alcohol solutions with increasing alcoholic concentration to remove all fixating solution and sample fluid which were finally replaced by the organic solvent xylol due to its miscible property with both paraffin as well as the alcohol used to dehydrate samples. After dehydration, samples were embedded in paraffin to become solid for the cutting procedure and to preserve sample structures.

2.5. FLOW CYTOMETRY

Cell characterization, including renal progenitor subsets, analysis of PTEC-markers, populations conducting transport assays from differentiated cells was performed by flow cytometry. Flow cytometry bases on light scattering and fluorescent emission of single cells labelled by fluorescent molecules. This technique is used to measure and analyse physical characteristics of single cells such as internal complexity, size or cell surface area, fluorescently labelled-antibodies positive cells within heterogeneous suspensions when cells pass through one or multiple laser beams. Specifically, the laser beam excites cells from ground state at lowest energy level to excited singlet states; when cells return to vibrational relaxation and finally to ground state, cells scatter light and emit fluorescence that are captured, filtered spectrally, and converted to electronic signals (voltage) through photodetectors. The voltage data is transferred to an external cytometer computer for storage and further analysis.

It is very important to use viability dyes to exclude dead cells from flow cytometry analysis, because dead cells have high level of autofluorescence and increased non-specific antibody binding resulting false positive results. In this study, I used LIVE/DEAD™ Fixable Dead Cell Stain Kit for this purpose. These are protein binding

dyes binding to free primary amine on proteins on the surface of cells. In dead cells, the dyes enter into the cells and bind to intracellular primary amines; therefore, dead cells have greater fluorescence and easily distinguished from live cells. Additionally, unstained control, and controls with only secondary antibodies to set gating regions and separate positive from negative cells were used.

2.6. IMMUNOFLUORESCENCE

This assay is based on the specificity of antibodies to detect proteins in cellular contexts via antigen – antibody reaction. In comparison with flow cytometry, this method is more useful in analysing the precise localization of the protein of interest within the cultured cells and in tissue sections. There are two different immunofluorescence assays including indirect and direct immunofluorescence. Because of high sensitivity, easy to change signal color, I used the indirect method to detect proteins including Aquaporin 1 (AQP1), Sodium-Potassium ATPase (Na^+/K^+ -ATPase), Sodium-Glucose co-transporter-2 (SGLT2), Megalin/LRP2, E-Cadherin, Laminin, and Kidney injury molecular-1 (KIM-1). For indirect immunofluorescence method, cells are incubated first with an unlabeled primary antibody. Afterwards, a secondary fluorophore-coupled antibody is added which is recognizing and binding to the primary antibody. Fluorescent antibodies allow to visualize the protein of interest using fluorescent microscopy.

2.7. TRANSMISSION ELECTRON MICROSCOPY

I used this technique to visualize small morphological structures of PTEC like microvilli and organelles in PTEC cytoplasm. The working principle of transmission electron microscope (TEM) is comparable to the light microscope. Microscopes create a magnified image through the use of a series of lenses, glass lenses for light microscope and electromagnets for TEM. However, a basic difference is the illuminating source they use to focus and to produce the image. While light microscope uses a beam of light, of an approximal wavelength of 400-700 nanometers (nm), TEM uses a beam of electrons, approximally equivalent wavelength of 1nm to focus on the specimen. Therefore, principally the image is formed by the absorption of light waves for light microscopy, and by transmission of electrons for TEM. The wavelength is closely related to resolution of an image. Shorter wavelengths have greater resolution than longer wavelengths. Regarding this mechanism, to increase image resolution, light microscope has to decrease the wavelength of the light, while transmission electron

microscope increase the wavelength of electron transmission. Because electrons have 100.000 times shorter wavelength than light, resolution of TEM is 1000 times, and magnification is over 2 million times higher than light microscope.

2.8. CYTOTOXICITY ASSAY

To investigate whether generated PTEC can be used to model nephrotoxicity, a MTT cytotoxicity assay with Cisplatin was performed. This is a non-radioactive, colorimetric assay, measuring cell viability after Cisplatin treatment using MTT compound (3-(4,5-dimethylthiazol-2-yl)-2,5-diphenyltetrazolium bromide). This is a yellow tetrazolium salt, which is soluble in culture medium and cell permeable. Once inside the cells, MTT is reduced to purple formazan crystals due to activity of NAD(P)H-dependent oxidoreductase enzymes in viable cells. Reduction level of enzymes with MTT correlates with the number of viable, metabolically active cells. Resulting purple formazan crystals accumulate inside the cells. Finally, after the addition of a solubilization solution, the formazan becomes solubilized, forming a coloured solution. The coloured solution is quantified by measuring absorbance or optical density (OD) at 570nm and 650 nm for background using a multi-well spectrophotometer. Cisplatin untreated cells were used as negative controls.

Cell viability was calculated by formula:

$$\frac{\text{OD}(570) - \text{OD}(650) \text{ of treated sample}}{\text{OD}(570) - \text{OD}(650) \text{ of untreated sample}} \times 100$$

Besides cell viability, I also checked Cisplatin cytotoxicity on cell through KIM-1 expression.

2.9. TRANSPORT ASSAYS

Radioactivity is the most popular method used to investigate membrane transporter characterization. However, there are many disadvantages of this approach such as high cost and health risks for users. Unlike radioactivity, assays based on fluorescence are much cheaper and safer⁸⁶. Therefore, in this study, I used fluorescent-based assays for

the analysis of membrane transport functionality. The uptake of substrates was characterised by flow cytometry or fluorescence microscopy.

2.9.1. Glucose assay on Matrigel-coated alginate beads

To investigate glucose uptake of SGLT2 transporter, 2-NBDG (2-(N-(7-Nitrobenz-2-oxa-1,3-diazol-4-yl) Amino)-2-Deoxyglucose) was used. *In vivo*, in PTEC, 90% glucose is reabsorbed from glomerular filtrate through SGLT2 located on apical side of PTEC of the proximal tubule (S1/S2 segments)⁸⁷. 2-NBDG is a fluorescent derivative of D-glucose used to investigate direct glucose uptake in living cells. Cells, which take up this fluorescent tracer will fluoresce green. Transport rate of 2-NBDG is generally slower than glucose. Once taken up, cellular metabolism turns this compound into a non-fluorescent derivative. Therefore, quantification of 2-NBDG take-up has to be conducted quickly after incubating cells with this compound.

Dapagliflozin was used to block glucose uptake through inhibiting SGLT2. Action mechanism of this inhibitor was reported is independent of pancreatic β cell function and modulation of insulin sensitivity but not displayed in detail⁸⁸. In my study, cells were incubated with this inhibitor 30 minutes before an incubation with 2-NBDG for a specific uptake. Also, cells needed to be washed several time with medium without glucose to prevent glucose in medium from impeding 2-NBDG uptake.

2.9.2. Albumin assay on Matrigel-coated alginate beads

FITC-albumin (fluorescein isothiocyanate-tagged albumin) was used to investigate cellular endocytosis of albumin mediated by apical transporter LRP2/Megalin in PTEC. Before albumin uptake assay was conducted, cells needed to be cultured in medium without serum for at least some hours; however, PTEC medium is defined medium without serum, thus FITC-albumin was directly added to cultured cells. Because there is no way to effectively inhibit Megalin we could find, we tested albumin uptake with different concentrations and saw an uptake dependent on used concentration.

2.9.3. Organic anion uptake assay on Matrigel-coated alginate beads

OAT family is responsible for the excretion of many substrates such as drugs, toxins, metabolites, endogenous hormones, nutrients from the blood to urine. Due to binding

albumin, drugs and substrates mediated by OAT family do not pass glomerular filtrate, resulting continue into petri-tubular capillaries and get inside into PTEC through basolateral transporters OAT1 and/or OAT3. Fluorescent anion 6-CF (6-Carboxyfluorescein) is a tracer used to investigate anion uptake by OAT1⁸⁹; however, there is an overlap in substrate specificity for OAT3 and OAT1. Therefore, 6-CF was used to investigate organic anion uptake by OAT1 and OAT3 in parallel, as described by Lawrence et al.³⁶. This substrate is not membrane-permeable and only loaded into PTEC through OAT1 and OAT3. Probenecid, a specific inhibitor of OAT1 and OAT3, blocks anion transport by OAT1 and OAT3, and was used to demonstrate specificity of fluorescent anion uptake.

2.9.4. Organic cation uptake assays Matrigel-coated alginate beads

Cation uptake in human PTEC is mainly conducted by the most abundant basolateral transporter OCT2, and only slightly by OCT3 and OCT1⁹⁰. In mice DAPI can be transported by both OCT1 and OCT2^{91,92}. It was also reported that, the two substrates DAPI and Metformine (anti-diabetes drug) are transported by OCT, while Cimetidine is inhibiting the uptake⁹³⁻⁹⁵.

DAPI is not permeable in live cells and only actively transported into intact PTEC through OCT2 and OCT1 into the lumen. Also, DAPI only emits fluorescence after intercalating with double-stranded DNA⁹¹. Therefore, we used DAPI to investigate cation uptake of OCT2 in our PTEC in presence or absence of the cationic drug Metformin and Cimetidine as described by Lawrence et al⁹². This combination can be explained that Metformin shares substrate recognition site with DAPI, resulting competing DAPI uptake while Cimetidine can be recognized as an inhibitor of OCT2⁹¹.

The activity of renal OCT2 influx protein was also examined using fluorescent OCT substrate 4-Di-2-ASP (Sigma-Aldrich). 15mM OCT inhibitor Tetrapentylammonium chloride (TPA) (Santa Cruz) was used as an inhibitor. 4-Di-2-ASP is the preferable fluorescent probe used currently because of strong fluorescence, temperature and pH stability⁸⁶.

In my study, PTEC on MAB were incubated for 30 minutes with TPA inhibitor before incubating with 4-Di-2-ASP for only 15 minutes in continued presence of TPA, one of inhibitor of OCT2⁹⁵.

2.9.5. Transport assay of renal efflux P-Glycoprotein Matrigel-coated alginate beads

Calcein-AM (Calcein acetoxymethyl ester) is a non-fluorescent acetomethoxy derivate of the fluorescein complex Calcein. Due to protection of carboxylic acid groups by hydrophobic acetomethoxy groups (AM) from the phospholipid bilayer cellular membrane, highly lipid soluble Calcein-AM dye can passively diffuse into viable cells. Once inside, endogenous esterase remove/cleave ester bond/the AM groups/moiety from Calcein-AM to produce the impermeable, fluorescent Calcein that is well retained in the cytosol and can be detected by flow cytometry⁹⁶.

P-glycoprotein (P-gp) actively pumps endogenous and exogenous toxic compounds out of PTEC. We used nonfluorescent Calcein-AM to check P-gp function through retention of Calcein in PTEC in presence of P-gp inhibitor PSC833 as described by Foll et al⁹⁷. In absence of the inhibitor, P-gp pumps Calcein-AM out of PTEC resulting a decrease in fluorescence of Calcein in the cytosol.

2.10. TRANSEPIHELIAL ELECCTRICAL RESISTANCE

Transepithelial electrical resistance (TEER) is a reliable, non-invasive method to evaluate integrity and permeability of a cellular monolayer via measurement of electrical resistance across the cellular monolayer. In order to measure TEER values, PTEC were first seeded on Transwell insert where cells can form a monolayer on a porous membrane, and medium can be added and changed separately on the apical and basolateral side of the cells. TEER ($\Omega \cdot \text{cm}^2$) is measured by placing two electrodes on each side of the monolayer along with applying a low frequency current. TEER value ($\Omega \cdot \text{cm}^2$), An insert with media only was used to measure blank resistance. TEER of monolayer was calculated by subtracting blank resistance, then multiplied by the surface area.

3. Results

My PhD project focused on experiments with the goal to efficiently and reproducibly obtain large amounts of hPSC-derived PTEC. I used Matrigel-coated alginate beads (MAB) in a fluidic biolevitation environment (MABB) to achieve maturation and function of the cells. My results confirmed the hypothesis that the fluidic, homogenous condition is suitable to produce a reproducible source of mature PTEC with functional transporters as well as significant expansion rates.

3.1. DIFFERENTIATION OF RENAL PROGENITOR CELLS AND PTEC ON GELTREX-COATED POLYSTYRENE IN 2D AND ON MATRIGEL-COATED ALGINATE BEADS WITH BIOLEVITATION

Differentiation of hPSC into renal cells was measured by expression of typical markers for different stages of maturation. Expression of SIX Homebox 2 (SIX2) and Receptor Tyrosine Kinase (RET) was determined, two key transcription factors for formation of intermediate mesoderm and ureteric bud, respectively. In cells differentiated in a conventional 2D system, and in MABB 70-80% of cells expressed SIX2 and 50-60% cells expressed RET after 4 days of differentiation with Activin A, Retinoic Acid and BMP4. Two indicators of renal vesicle stage differentiation, Wilms' tumor protein 1 (WT1) and Jagged 1 (JAG1) were also detected in cells of both culture conditions in similar proportions. The JAG1 cell population increased on d8 upon treatment of d4 cells with GDNF, an inducer of ureteric bud formation.

However, differentiation efficacy of renal progenitor cells (d8) into PTEC (d16) showed clear differences between MABB and 2D culture. In 2D culture, 70% and 80% of cells were labelled with AQP1, and SGLT2 respectively. However, only 30% of cells were detected with Na⁺/K⁺-ATPase. Expression levels decreased to 50% on d20. Additionally, these PTEC were not viable after passaging and thus harvesting for subsequent experiments was not possible.

In MABB, expression of PTEC markers AQP1, SGLT2 and Megalin was already detectable at d12. On d16, AQP1, SGLT2, Megalin, Na⁺/K⁺-ATPase were detected in more than 80% of the cells. Transporter proteins for detoxification such as OCT2, OAT1, OAT3, P-gp and MRP2 were also detected in around 40-60% of the cells. Moreover, these PTEC-markers were stably detectable until d20 with the same

proportions. Furthermore, results of transmission electron microscopy (TEM) and immunofluorescent staining showed polarization of PTEC via detection of microvilli, organelles and proper localization of SGLT2 on apical side and Laminin on baselateral side of MAB. Importantly, functional assays confirmed transporter activities. Functional test results of transporter proteins are presented in Table 8.

Table 8. The flow cytometry showed percentage of d16 hPSC-derived PTEC on MABB uptake substrates in presence and absence of inhibitors

Functional test	Transporter	Substrate	Percentage of d16 cells uptake substrate	Inhibitor	Percentage of d16 cells uptake substrate in presence of inhibitor
<i>Glucose uptake</i>	SGLT2	2-NBDG	50%	Dapagliflozin	25%
<i>Albumin uptake</i>	LRP2	FITC-albumin	20-40%	Gentamicine	20-40%
<i>Organic anion uptake</i>	OAT1/OAT3	6-CF	50%	Probenecid	8%
<i>Organic cation uptake</i>	OCT2	4-Di-2-ASP	45%	TPA	3%
<i>Organic cation uptake</i>	OCT2	DAPI	25%	Metformin, Cimetidine	11%
<i>Renal efflux</i>	P-gp	Calcein-AM	59%	PSC833	51%

ND: Data is presented as Mean with $p \leq 0.05$. (Table 8: own representation: Ngo, Thi Thanh Thao).

Solute transporters were not only functional on MABB – expanded PTEC but also stable and functional even after PTEC were harvested from the beads. Specifically, passaged and harvested PTEC formed a tight monolayer when seeded on Transwell inserts as well as showed expression of KIM-1 when cells were treated with Cisplatin. The drug induced nephrotoxicity in these cells indicates their utility for drugs testing.

In conclusion, by using MABB, we generated a homogenous, functional hPSC-derived PTEC population that can be directly used for preclinical applications such as drug screening, disease modelling or kidney organ engineering. Differentiation efficacy was enhanced significantly to above 80%.

3.2. EXPANSION EFFICACY OF CELLS ON MATRIGEL-COATED BEADS WITH BIOLEVITATION

A comparison in terms of cell numbers of the stages hPSC expansion, renal progenitor differentiation, PTEC differentiation and PTEC expansion showed significant expansion of cells in MABB compared to 2D. It is known that hPSC-lines show diverse proliferation and differentiation behaviours. Therefore, one hESC-line, WAe001-A, and two hiPSC-lines, BCRTi005-A and WISCi004-A were used to assess reproducibility of expansion rates.

Starting with 2.6×10^6 hPSC, fold expansion was measured on 4d after hPSC seeding. On MAB, fold expansion was around 6 for two hiPSC-lines and around 10 for hESC-line used. These expansion rates were around 2 times higher than those observed in 2D culture. Subsequently, the number of renal vesicle cells harvested from MAB on d8 was 4-5 times higher compared to 2D condition.

With only 2.6×10^6 hPSC at the beginning, around $2.4-2.6 \times 10^7$ cells in total were harvested after 24 days from MAB while in 2D culture, only around 12×10^6 cells were harvested. Compared to 2D culture, cell yield in MABB was 2-2.2 times higher than in 2D. However, differentiation efficacy for PTEC in 2D culture was only around 50% on d20. Thus around 6×10^6 hPSC-derived PTEC were generated in this condition. Considering both elements, final cell yield and differentiation efficacy, hPSC-derived PTEC yield from MABB was around 4 times higher than those in 2D culture. Comparing to starter seeding (2.6×10^6 hPSC), overall expansion of cells on MABB was 9-10 times.

In conclusion, expansion efficacy of cells was significantly enhanced in MABB compared to 2D culture starting with the same initial material. The remarkable expansion of cells on MABB is summarized in Table 9.

Table 9. Cell yield on 40cm² Matrigel-coated alginate beads with biolevitation

Cell line	Day (-4)	Day 0	Day 8	Day 20
	hPSC	hPSC	Progenitor cells	PTEC
BCRTi005-A	2.6x10 ⁶	16x10 ⁶	17.2x10 ⁶	24 x10 ⁶
WISCi004-A	2.6x10 ⁶	17.6x10 ⁶	15.2 x10 ⁶	24 x10 ⁶
WAe001-A	2.6x10 ⁶	25.2x10 ⁶	21.6 x10 ⁶	26.4 x10 ⁶

Data is presented as Mean with $p \leq 0.05$. “Table 9 modified from Table 1 Ngo et al, 2022⁸⁴”

4. Discussion

4.1. SHORT SUMMARY OF RESULTS

I successfully developed a defined medium and optimised differentiation protocol of hPSC into PTEC. Using a novel and scalable cultivation system on Matrigel-coated alginate beads in a biolevitation environment, I generated a homogenous, functional PTEC population that can be directly used for preclinical applications without further enrichment steps. A fluidic environment with homogenous distribution of supplements to cells and adjustable mechanical shear and flow offered by biolevitation was a key factor that enhanced differentiation efficacy compared to conventional static 2D culture. Matrigel-coated alginate beads (MAB) provided optimal surfaces for cell adhesion and subsequent expansion. With an inoculation density of 6.5×10^4 hPSC/cm², after 24 days we generated $2.4-2.6 \times 10^7$ cells. More than 80% of the expanded cells showed PTEC phenotypes. PTEC highly and stably expressed AQP1, Na⁺/K⁺-ATPase, protein transporters SGLT2 for glucose uptake, Megalin/LRP2 for albumin endocytosis, organic ion transporters for detoxification such as OCT2, OAT1, OAT3 and P-gp and MRP2 for disposal of toxic compounds from PTEC to pre-urine. Functional activity of these transporters confirmed phenotypic conformity of the generated PTECs.

4.2. EMBEDDING THE RESULTS INTO THE CURRENT STATE OF RESEARCH

Although biolevitation by the Cero reactor system was used before for expansion as well as differentiation of hPSC^{30,31}, my study was the first report that cultured and differentiated hPSC on the surface of microcarriers.

Regarding quantity, our differentiation efficacy for PTEC was comparable to those of Kandasamy et al⁵⁶ and Chandrasekaran et al⁵² with above 80% differentiation efficacy. However, regarding quality, generated PTEC were showed broader marker expression profiles, expression stability and functionality. Comparing to existing immortalized human proximal tubule cell lines like HK2, RPTEC-hTERT and ciPTEC-hTERT, the MABB-generated PTEC possess organic transporters while these immortalized cell lines do not express these, requiring genetic engineering for expression of transporters.

Common inoculation density of hPSC for expansion in bioreactors ranged from 2×10^5 to 1×10^6 cells/ml. Although inoculation densities were quite high, the expansion of hPSC in these studies were moderate⁷¹. Expansion of hPSC using MABB in my study was significant, around 6-fold for two hiPSC lines and 10-fold for hESC line in 4 days, with an average inoculation density $6,5 \times 10^5$ cells/ml. Kallos et al, 2019 reported a low inoculation density, 2×10^4 cells/ml but high expansion of hPSC, 32-fold in 6 days⁷¹. For our MABB, with a low inoculation density, there was increased number of MAB not covered by cells.

After expansion and differentiation of hPSC, we harvested $2,4 \times 10^7$ PTEC for each Cerotube. This number is not only enough for bioprinting but also for setting up toxicity tests using different drugs and controls^{98,99}. For scaling potency of PTEC, it can be conducted via an increase of Cerotube number.

4.3. LIMITATIONS AND FURTHER OPTIMIZATION APPROACHES

Although we showed the generation of a reproducible PTEC source, some optimization can be conducted.

At first, further optimization of coating surface on alginate beads to allow clinical applications. Specifically, xeno-free extracellular matrix (ECM) to replace mouse-derived Matrigel should be used. One option would be human kidney derived decellularized ECM (dECM) or ECM-components that specifically enhance maturation of cells¹⁰⁰. Similarly, alginate allows functionalization via chemical linkage of organic molecules, which may have properties to enhance attachment, proliferation, differentiation and harvesting of cells.

Second, polarization of PTEC on MAB was shown with the basolateral pole side resting on beads and functional transporters are present on the cells. This arrangement could be further utilized for new approaches to monitor movement of substrates through the PTEC cell monolayer. Since each monolayer is covering one bead, each bead is assumed as a proximal tubule comprising the external side contacting the glomerular filtrate and the internal side connecting to the blood stream. Upscaling of assays targeting the proximal tubulus may therefore be possible. A potential method to detect

how substrates are transported into the bead volume may be based on high throughput fluorescence microscopy in combination with fluorescent substrates at optimized incubation times and substrate concentrations. The use of patient – derived or genetically characterized hPSC as source material, would allow to personalize these assays (Figure 5).

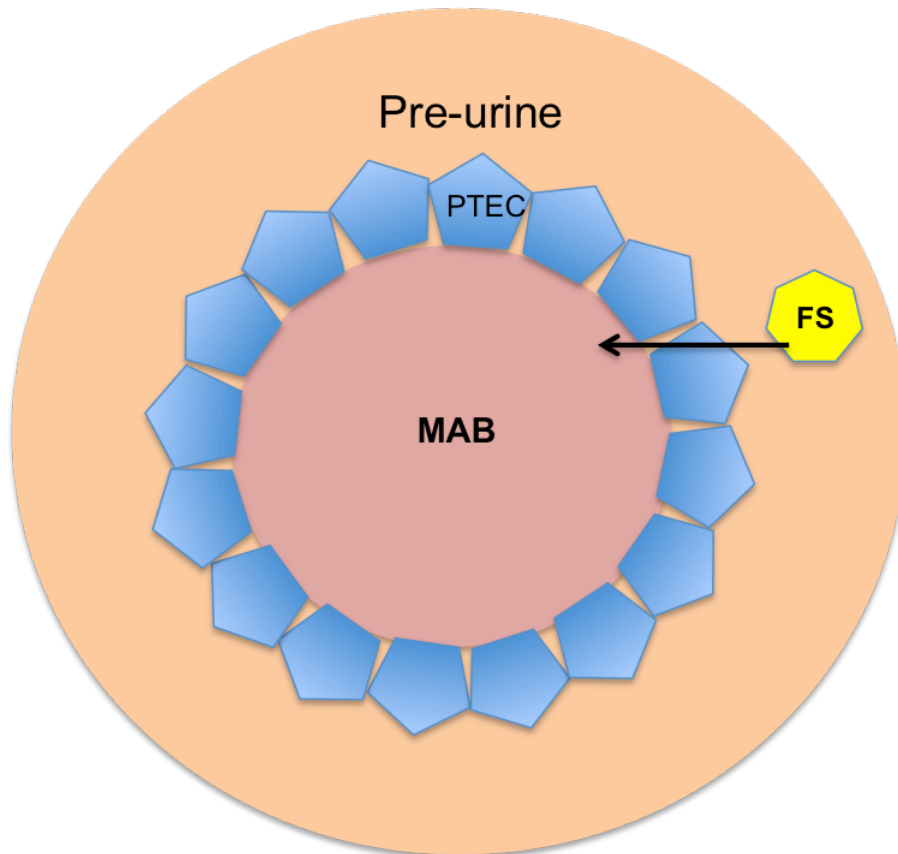


Figure 5. An assumed proximal tubule with a monolayer of PTEC on the surface of a Matrigel-coated alginate bead (MAB). Internal side of MAB is considered as tubular lumen where blood stream flow. External side of MAB contact the glomerular filtrate (pre-urine). This model could be used to detect movement of fluorescent substrates (FS). (Figure 5: own representation: Ngo,Thi Thanh Thao).

Third, establishing disease models using patient-specific hiPSC like polycystic kidney disease ¹⁰¹ requires cell sources of reproducible quality and at sufficient quantities to perform high throughput assays. Disease models directly employing patient-specific hiPSC allow studying pathogenesis on a personalized level. Moreover, models using patient-specific hiPSC-derived PTEC are directly clinically relevant, for example, for diagnosis, prognosis and to identify optimal treatment options.

4.4. IMPLICATIONS FOR PRACTICE AND/OR FUTURE RESEARCH

4.4.1. Good Manufacturing practice product for reliable PTEC source

The applied bioreactor system (Cero®) provides the option for a closed production process and a pipeline for the production of PTEC with a high standard. Its conversion to a good manufacturing practice (GMP) procedure is thus in principle feasible for commercial and validated production process implementation. Beside Matrigel-coated alginate beads, other alginate-matrix combinations are already available. For example, Laminin-coated alginate constitute a defined humanized matrix for cell growth and differentiation. In preliminary experiments, I confirmed a good quality of hPSC-derived PTEC differentiated on Laminin in 2D cultures.

4.4.2. Clinical applications

The renal proximal tubule is extremely vulnerable to injuries, which can lead to acute kidney injury (AKI) and chronic kidney disease (CKD). For both cases, it was shown that they constitute two cell populations, one undergoing regeneration while another becoming atrophied and nonfunctional¹⁰². PTEC have some capacity for regeneration that exceed the regenerative potency of cells of the glomerulus and distal tubule¹⁰². It was demonstrated that CD24-positive PTEC scattered in the proximal tubule are in the G1 phase of the cell cycle and in order to respond to injuries, they are ready to dedifferentiate and proliferate¹⁰³. Directly injecting MABB-derived PTEC into kidney as regenerative therapies is a possible therapeutic option. However, this is extremely difficult to practically perform with associated risks of cell clumping and kidney damage. The described proximal tubulus model with PTEC monolayers presented on MAB and the shown nephrotoxic responses, it may be possible to explore therapeutic approaches to stimulate PT repair processes. A first step may be to assess whether CD24-positive cells can be observed in our model, and whether these contribute to induced PT damage *in vitro*.

On another pathway, current dialysis principles are based on membranes with filtration function. However, other functions that are provided by PTECs such as hormone secretion are lacking. The use of a standardized source for PTEC within the dialysis process may improve the physiological properties of the machines and thus enhance

patient's quality of life. Humes et al, 1999 developed *in vitro* bioartificial kidney device using PTEC¹⁰⁴. This device actively transported not only nutrients but also hormones. Such devices have been developed for clinical use.

Much research was performed in generating a bioartificial proximal tubule as a source of a functional kidney tissue^{28,105,106}. To engineer a proximal tubule, an adequate number of functional PTEC, an efficient scaffold as well as appropriate 3D culture condition are required. Tubular structures such as blood vessels, urinary bladder, larynx, traches were produced successfully¹⁰⁷, however, at dimensions (>4mm diameter) far exceeding that of proximal tubules (<60µm). Nevertheless, MABB generated PTEC combined with a suitable scaffold and flow conditions supporting self-organization may be used for engineering a functional proximal tubule. The generation of a functional proximal tube also facilitates nephrotoxicity evaluation of compounds, a crucial preclinical step so that medicine can be developed to cure end-stage renal diseases.²⁷.

Individually, mutations of PTEC such as common mutations of SGLT2 causing renal glucouria is also one of clinical importance¹⁰⁸. Specifically, somatic cells from patients with mutations can be reprogramed into hiPSC-lines and the genetic defect corrected be gene editing techniques. Using our protocol, these corrected hiPSC can be differentiated into functional PTEC and may be transplanted into patients for improving function of proximal tubule. The relative regeneration rate of the proximal tubule may facilitate expansion of domination of the normalized cells within the patients PT. This would require transplantation of a relatively low cell number reducing clinical risk. A principle proof of concept for such an approach was provided in patients with epidermulysa bullosa, a severe skin disease¹⁰⁹.

5. Conclusion

We verified our hypothesis that expansion and differentiation of hPSC on Matrigel-coated alginate beads in a fluidic system will facilitate the generation of a scalable number of mature PTEC in a reproducible way.

Reference list

1. Grgic I, Campanholle G, Bijol V, Wang C, Sabbisetti VS, Ichimura T, Humphreys BD, Bonventre J V. Targeted proximal tubule injury triggers interstitial fibrosis and glomerulosclerosis. *Kidney Int.* 2012;82(2):172-183. doi:10.1038/ki.2012.20
2. Weiner ID, Mitch WE, Sands JM. Urea and ammonia metabolism and the control of renal nitrogen excretion. *Clin J Am Soc Nephrol.* 2015;10(8):1444-1458. doi:10.2215/CJN.10311013
3. Baum M, Quigley R. Proximal tubule water transport-lessons from aquaporin knockout mice. *Am J Physiol - Ren Physiol.* 2005;289(6 58-6):1193-1194. doi:10.1152/ajprenal.00283.2005
4. Jorgensen PL. Structure, function and regulation of Na,K-ATPase in the kidney. *Kidney Int.* 1986;29(1):10-20. doi:10.1038/ki.1986.3
5. Malhotra A, Kudyar S, Gupta A, Kudyar R, Malhotra P. Sodium glucose co-transporter inhibitors – A new class of old drugs. *Int J Appl Basic Med Res.* 2015;5(3):161. doi:10.4103/2229-516x.165363
6. Lu YT, Ma XL, Xu YH, Hu J, Wang F, Qin WY, Xiong WY. A Fluorescent Glucose Transport Assay for Screening SGLT2 Inhibitors in Endogenous SGLT2-Expressing HK-2 Cells. *Nat Products Bioprospect.* 2019;9(1):13-21. doi:10.1007/s13659-018-0188-4
7. Ferrell N, Ricci KB, Groszek J, Marmorstein JT, Fissell WH. Albumin handling by renal tubular epithelial cells in a microfluidic bioreactor. *Biotechnol Bioeng.* 2012;109(3):797-803. doi:10.1002/bit.24339
8. Sandoval P, Hagenbuch B, Sciences B. Organic Anion Transporter 1 Drug Transport — Uptake. 2021;1.
9. Faucher Q, Alarcan H, Marquet P, Guellec CB Le. Effects of ischemia-reperfusion on tubular cell membrane transporters and consequences in kidney transplantation. *J Clin Med.* 2020;9(8):1-29. doi:10.3390/jcm9082610
10. Nishijima T, Gatanaga H, Oka S. Tenofovir nephrotoxicity among Asians living with HIV: review of the literature. *Glob Heal Med.* 2019;1(2):88-94. doi:10.35772/ghm.2019.01021
11. Schaub TP, Kartenbeck J, König J, Spring H, Dörsam J, Staehler G, Störkel S, Thon WF, Keppler D. Expression of the MRP2 gene-encoded conjugate export pump in human kidney proximal tubules and in renal cell carcinoma. *J Am Soc*

- Nephrol.* 1999;10(6):1159-1169. doi:10.1681/asn.v1061159
12. Wright SH. Molecular and cellular physiology of organic cation transporter 2. *Am J Physiol - Ren Physiol.* 2019;317(6):F1669-F1679.
doi:10.1152/ajprenal.00422.2019
 13. Ciarimboli G, Lancaster CS, Schlatter E, Franke RM, Sprowl JA, Pavenstädt H, Massmann V, Guckel D, Mathijssen RHJ, Yang W, Pui C-H, Relling M V., Herrmann E, Sparreboom A. Proximal Tubular Secretion of Creatinine by Organic Cation Transporter OCT2 in Cancer Patients. *Clin Cancer Res.* 2012;18(4):1101-1108. doi:10.1158/1078-0432.CCR-11-2503
 14. Pasquier J, Rioult D, Abu-Kaoud N, Marie S, Rafii A, Guerrouahen BS, Le Foll F. P-glycoprotein-activity measurements in multidrug resistant cell lines: Single-cell versus single-well population fluorescence methods. *Biomed Res Int.* 2013;2013. doi:10.1155/2013/676845
 15. Takaori K, Nakamura J, Yamamoto S, Nakata H, Sato Y, Takase M, Nameta M, Yamamoto T, Economides AN, Kohno K, Haga H, Sharma K, Yanagita M. Severity and frequency of proximal tubule injury determines renal prognosis. *J Am Soc Nephrol.* 2016;27(8):2393-2406. doi:10.1681/ASN.2015060647
 16. Liu BC, Tang TT, Lv LL, Lan HY. Renal tubule injury: a driving force toward chronic kidney disease. *Kidney Int.* 2018;93(3):568-579.
doi:10.1016/j.kint.2017.09.033
 17. Chou YH, Huang TM, Chu TS. Novel insights into acute kidney injury—chronic kidney disease continuum and the role of renin—angiotensin system. *J Formos Med Assoc.* 2017;116(9):652-659. doi:10.1016/j.jfma.2017.04.026
 18. Rapa SF, Di Iorio BR, Campiglia P, Heidland A, Marzocco S. Inflammation and oxidative stress in chronic kidney disease—potential therapeutic role of minerals, vitamins and plant-derived metabolites. *Int J Mol Sci.* 2020;21(1).
doi:10.3390/ijms21010263
 19. Yang T, Xu C. Physiology and pathophysiology of the intrarenal renin-angiotensin system: An update. *J Am Soc Nephrol.* 2017;28(4):1040-1049.
doi:10.1681/ASN.2016070734
 20. Huffstater T, Merryman WD, Gewin LS. Wnt/ β -Catenin in Acute Kidney Injury and Progression to Chronic Kidney Disease. *Semin Nephrol.* 2020;40(2):126-137.
doi:10.1016/j.semnephrol.2020.01.004
 21. Bussolati B, Maeshima A, Peti-Peterdi J, Yokoo T, Lasagni L. Renal Stem Cells,

- Tissue Regeneration, and Stem Cell Therapies for Renal Diseases. *Stem Cells Int.* 2015;2015:2-4. doi:10.1155/2015/302792
22. Ryan MJ, Johnson G, Kirk J, Fuerstenberg SM, Zager RA, Torok-Storb B. HK-2: An immortalized proximal tubule epithelial cell line from normal adult human kidney. *Kidney Int.* 1994;45(1):48-57. doi:10.1038/ki.1994.6
 23. American Type Culture Collection. Protocol for RPTEC / TERT1-OCT2 Uptake of 4- (4-(dimethylamino)styryl)-N-methylpyridinium iodide (ASP+) or N,N,N-Trimethyl-2[(7-nitro-1,2,3-benzoxadiazol-4-yl)amino] ethanaminiumiodide(EAM-1). Published online 2017:1-4.
 24. Soo JYC, Jabsen J, Masereeuw R LM. *Advances in Predictive in Vitro Models of Drug-Induced Nephrotoxicity.* Vol 14.; 2018. doi:10.1038/s41581-018-0003-9.Advances
 25. Wieser M, Stadler G, Jennings P, Streubel B, Pfaller W, Ambros P, Riedl C, Katinger H, Grillari J, Grillari-Voglauer R. hTERT alone immortalizes epithelial cells of renal proximal tubules without changing their functional characteristics. *Am J Physiol - Ren Physiol.* 2008;295(5):1365-1375. doi:10.1152/ajprenal.90405.2008
 26. Sánchez-Romero N, Martínez-Gimeno L, Caetano-Pinto P, Saez B, Sánchez-Zalabardo JM, Masereeuw R, Giménez I. A simple method for the isolation and detailed characterization of primary human proximal tubule cells for renal replacement therapy. *Int J Artif Organs.* 2020;43(1):45-57. doi:10.1177/0391398819866458
 27. Faria J, Ahmed S, Gerritsen KGF, Mihaila SM, Masereeuw R. Kidney-based in vitro models for drug-induced toxicity testing. *Arch Toxicol.* 2019;93(12):3397-3418. doi:10.1007/s00204-019-02598-0
 28. Lin NYC, Homan KA, Robinson SS, Kolesky DB, Duarte N, Moisan A, Lewis JA. Renal reabsorption in 3D vascularized proximal tubule models. *Proc Natl Acad Sci U S A.* 2019;116(12):5399-5404. doi:10.1073/pnas.1815208116
 29. Homan KA, Kolesky DB, Skylar-Scott MA, Herrmann J, Obuobi H, Moisan A, Lewis JA. Bioprinting of 3D Convulated Renal Proximal Tubules on Perfusable Chips. *Sci Rep.* 2016;6:1-13. doi:10.1038/srep34845
 30. Vedula EM, Alonso JL, Arnaout MA, Charest JL. A microfluidic renal proximal tubule with active reabsorptive function. *PLoS One.* 2017;12(10):1-15. doi:10.1371/journal.pone.0184330

31. Prange JA, Bieri M, Segerer S, Burger C, Kaech A, Moritz W, Devuyst O. Human proximal tubule cells form functional microtissues. *Pflugers Arch Eur J Physiol*. 2016;468(4):739-750. doi:10.1007/s00424-015-1771-8
32. Faria J, Gerritsen KGF, Nguyen TQ, Mihaila SM, Masereeuw R. Diabetic proximal tubulopathy: Can we mimic the disease for in vitro screening of SGLT inhibitors? *Eur J Pharmacol*. 2021;908(May). doi:10.1016/j.ejphar.2021.174378
33. Harwood SM, Allen DA, Raftery MJ, Yaqoob MM. High glucose initiates calpain-induced necrosis before apoptosis in LLC-PK1 cells. *Kidney Int*. 2007;71(7):655-663. doi:10.1038/sj.ki.5002106
34. Vormann MK, Vriend J, Lanz HL, Gijzen L, van den Heuvel A, Hutter S, Joore J, Trietsch SJ, Stuu C, Nieskens TTG, Peters JGP, Ramp D, Caj M, Russel FGM, Jacobsen B, Roth A, Lu S, Polli JW, Naidoo AA, Vulto P, Masereeuw R, Wilmer MJ, Suter-Dick L. Implementation of a Human Renal Proximal Tubule on a Chip for Nephrotoxicity and Drug Interaction Studies. *J Pharm Sci*. 2021;110(4):1601-1614. doi:10.1016/j.xphs.2021.01.028
35. Turman MA, Bates CM. Susceptibility of human proximal tubular cells to hypoxia: Effect of hypoxic preconditioning and comparison to glomerular cells. *Ren Fail*. 1997;19(1):47-60. doi:10.3109/08860229709026259
36. Jansen J, Schophuizen CMS, Wilmer MJ, Lahham SHM, Mutsaers HAM, Wetzels JFM, Bank RA, Van den Heuvel LP, Hoenderop JG, Masereeuw R. A morphological and functional comparison of proximal tubule cell lines established from human urine and kidney tissue. *Exp Cell Res*. 2014;323(1):87-99. doi:10.1016/j.yexcr.2014.02.011
37. Bao YW, Yuan Y, Chen JH, Lin WQ. Kidney disease models: tools to identify mechanisms and potential therapeutic targets. *Zool Res*. 2018;39(2):72-86. doi:10.24272/j.issn.2095-8137.2017.055
38. Torres R, Velazquez H, Chang JJ, Levene MJ, Moeckel G, Desir G V., Safirstein R. Three-dimensional morphology by multiphoton microscopy with clearing in a model of cisplatin-induced CKD. *J Am Soc Nephrol*. 2016;27(4):1102-1112. doi:10.1681/ASN.2015010079
39. He X, Zhang T, Tolosa M, Goru SK, Chen X, Misra PS, Robinson LA, Yuen DA. A new, easily generated mouse model of diabetic kidney fibrosis. *Sci Rep*. 2019;9(1):1-13. doi:10.1038/s41598-019-49012-4
40. Noshahr ZS, Salmani H, Khajavi Rad A, Sahebkar A. Animal Models of Diabetes-

- Associated Renal Injury. *J Diabetes Res*. 2020;2020. doi:10.1155/2020/9416419
41. Nagao S, Kugita M, Yoshihara D, Yamaguchi T. Animal models for human polycystic kidney disease. *Exp Anim*. 2012;61(5):477-488. doi:10.1538/expanim.61.477
 42. Korstanje R, Caputo CR, Doty RA, Cook SA, Bronson RT, Davisson MT, Miner JH. A mouse Col4a4 mutation causing Alport glomerulosclerosis with abnormal collagen $\alpha3\alpha4\alpha5$ (IV) trimers. *Kidney Int*. 2014;85(6):1461-1468. doi:10.1038/ki.2013.493
 43. Dikalov SI, Nazarewicz RR, Bikineyeva A, Hilenski L, Lassègue B, Griendling KK, Harrison DG, Dikalova AE. Nox2-Induced production of mitochondrial Superoxide in Angiotensin ii-mediated endothelial oxidative stress and hypertension. *Antioxidants Redox Signal*. 2014;20(2):281-294. doi:10.1089/ars.2012.4918
 44. Leelahavanichkul A, Yan Q, Hu X, Eisner C, Huang Y, Chen R, Mizel D, Zhou H, Wright EC, Kopp JB, Schnermann J, Yuen PST, Star RA. Angiotensin II overcomes strain-dependent resistance of rapid CKD progression in a new remnant kidney mouse model. *Kidney Int*. 2010;78(11):1136-1153. doi:10.1038/ki.2010.287
 45. Simons JP, Al-Shawi R, Ellmerich S, Speck I, Aslam S, Hutchinson WL, Mangione PP, Disterer P, Gilbertson JA, Hunt T, Millar DJ, Minogue S, Bodin K, Pepys MB, Hawkins PN. Pathogenetic mechanisms of amyloid A amyloidosis. *Proc Natl Acad Sci U S A*. 2013;110(40):16115-16120. doi:10.1073/pnas.1306621110
 46. Nickerson KM, Cullen JL, Kashgarian M, Shlomchik MJ. Exacerbated Autoimmunity in the Absence of TLR9 in MRL. Fas lpr Mice Depends on Ifnar1. *J Immunol*. 2013;190(8):3889-3894. doi:10.4049/jimmunol.1203525
 47. Cao Q, Wang Y, Zheng D, Sun Y, Wang Y, Lee VWS, Zheng G, Tan TK, Ince J, Alexander SI, Harris DCH. IL-10/TGF- β -modified macrophages induce regulatory T cells and protect against adriamycin nephrosis. *J Am Soc Nephrol*. 2010;21(6):933-942. doi:10.1681/ASN.2009060592
 48. Ganeva V, Unbekandt M, Davies JA. An improved kidney dissociation and re-aggregation culture system results in nephrons arranged organotypically around a single collecting duct system. *Organogenesis*. 2011;7(2):83-87. doi:10.4161/org.7.2.14881
 49. Sebinger DDR, Unbekandt M, Ganeva V V., Ofenbauer A, Werner C, Davies JA.

- A novel, low-volume method for organ culture of embryonic kidneys that allows development of cortico-medullary anatomical organization. *PLoS One*. 2010;5(5):1-10. doi:10.1371/journal.pone.0010550
50. Buzhor E, Harari-Steinberg O, Omer D, Metsuyanin S, Jacob-Hirsch J, Noiman T, Dotan Z, Goldstein RS, Dekel B. Kidney spheroids recapitulate tubular organoids leading to enhanced tubulogenic potency of human kidney-derived cells. *Tissue Eng - Part A*. 2011;17(17-18):2305-2319. doi:10.1089/ten.tea.2010.0595
 51. Morizane R, Bonventre J V. Kidney Organoids: A Translational Journey. *Trends Mol Med*. 2017;23(3):246-263. doi:10.1016/j.molmed.2017.01.001
 52. Chandrasekaran V, Carta G, da Costa Pereira D, Gupta R, Murphy C, Feifel E, Kern G, Lechner J, Cavallo AL, Gupta S, Caiment F, Kleinjans JCS, Gstraunthaler G, Jennings P, Wilmes A. Generation and characterization of iPSC-derived renal proximal tubule-like cells with extended stability. *Sci Rep*. 2021;11(1):1-17. doi:10.1038/s41598-021-89550-4
 53. Mae SI, Shono A, Shiota F, Yasuno T, Kajiwara M, Gotoda-Nishimura N, Arai S, Sato-Otubo A, Toyoda T, Takahashi K, Nakayama N, Cowan CA, Aoi T, Ogawa S, McMahon AP, Yamanaka S, Osafune K. Monitoring and robust induction of nephrogenic intermediate mesoderm from human pluripotent stem cells. *Nat Commun*. 2013;4. doi:10.1038/ncomms2378
 54. Lam AQ, Freedman BS, Morizane R, Lerou PH, Valerius MT, Bonventre J V. Rapid and efficient differentiation of human pluripotent stem cells into intermediate mesoderm that forms tubules expressing kidney proximal tubular markers. *J Am Soc Nephrol*. 2014;25(6):1211-1225. doi:10.1681/ASN.2013080831
 55. Hariharan K, Stachelscheid H, Rossbach B, Oh SJ, Mah N, Schmidt-Ott K, Kurtz A, Reinke P. Parallel generation of easily selectable multiple nephronal cell types from human pluripotent stem cells. *Cell Mol Life Sci*. 2019;76(1):179-192. doi:10.1007/s00018-018-2929-2
 56. Kandasamy K, Chuah JKC, Su R, Huang P, Eng KG, Xiong S, Li Y, Chia CS, Loo LH, Zink D. Prediction of drug-induced nephrotoxicity and injury mechanisms with human induced pluripotent stem cell-derived cells and machine learning methods. *Sci Rep*. 2015;5(June):1-15. doi:10.1038/srep12337
 57. Wilmer MJ, Ng CP, Lanz HL, Vulto P, Suter-Dick L, Masereeuw R. Kidney-on-a-

- Chip Technology for Drug-Induced Nephrotoxicity Screening. *Trends Biotechnol.* 2016;34(2):156-170. doi:10.1016/j.tibtech.2015.11.001
58. Heussner AH, Dietrich DR. Primary porcine proximal tubular cells as an alternative to human primary renal cells in vitro: An initial characterization. *BMC Cell Biol.* 2013;14(1). doi:10.1186/1471-2121-14-55
 59. Lai KN, Leung JCK, Chan LYY, Guo H, Tang SCW. Interaction between proximal tubular epithelial cells and infiltrating monocytes/T cells in the proteinuric state. *Kidney Int.* 2007;71(6):526-538. doi:10.1038/sj.ki.5002091
 60. Vinaiphath A, Charngkaew K, Thongboonkerd V. More complete polarization of renal tubular epithelial cells by artificial urine. *Cell Death Discov.* 2018;4(1). doi:10.1038/s41420-018-0112-z
 61. Nilsson K. Microcarrier cell culture. *Biotechnol Genet Eng Rev.* 1988;6(1):403-439. doi:10.1080/02648725.1988.10647854
 62. Rowley JA, Madlambayan G, Mooney DJ. Alginate hydrogels as synthetic extracellular matrix materials. *Biomaterials.* 1999;20(1):45-53. doi:10.1016/S0142-9612(98)00107-0
 63. EUROPEAN PATENT APPLICATION. European Patent Application. Published online 2011. <http://info.sipcc.net/files/patent/fulltext/EP/200605/EP2099194A1/EP2099194A1.PDF>
 64. Zimmermann H, Zimmermann D, Reuss R, Feilen PJ, Manz B, Katsen A, Weber M, Ihmig FR, Ehrhart F, Geßner P, Behringer M, Steinbach A, Wegner LH, Sukhorukov VL, Vásquez JA, Schneider S, Weber MM, Volke F, Wolf R, Zimmermann U. Towards a medically approved technology for alginate-based microcapsules allowing long-term immunoisolated transplantation. *J Mater Sci Mater Med.* 2005;16(6):491-501. doi:10.1007/s10856-005-0523-2
 65. Lee KY, Mooney DJ. Alginate: Properties and biomedical applications. *Prog Polym Sci.* 2012;37(1):106-126. doi:10.1016/j.progpolymsci.2011.06.003
 66. Gilmozzi V, Gentile G, Riexchnitz DA, Von Troyer M, Lavdas AA, Kerschbamer E, Weichenberger CX, Rosato-Siri MD, Casarosa S, Conti L, Pramstaller PP, Hicks AA, Pichler I, Zanon A. Generation of hiPSC-Derived Functional Dopaminergic Neurons in Alginate-Based 3D Culture. *Front Cell Dev Biol.* 2021;9(August):1-16. doi:10.3389/fcell.2021.708389
 67. Enobakhare B, Bader DI, Lee D. Concentration and M/G ratio influence the

- physiochemical and mechanical properties of alginate constructs for tissue engineering. *J Appl Biomater Biomech*. 2006;4(2):87-96.
doi:10.1177/228080000600400203
68. Smidsrod O BG. Alginate as immobilization matrix for cells. *Tibtech*. 1990;8.
doi:10.1007/s13164-012-0093-4
 69. Dhoot NO, Tobias CA, Fischer I, Wheatley MA. Peptide-modified alginate surfaces as a growth permissive substrate for neurite outgrowth. *J Biomed Mater Res - Part A*. 2004;71(2):191-200. doi:10.1002/jbm.a.30103
 70. Gepp MM, Fischer B, Schulz A, Dobringer J, Gentile L, Vásquez JA, Neubauer JC, Zimmermann H. Bioactive surfaces from seaweed-derived alginates for the cultivation of human stem cells. *J Appl Phycol*. 2017;29(5):2451-2461.
doi:10.1007/s10811-017-1130-6
 71. Borys BS, So T, Colter J, Dang T, Roberts EL, Revay T, Larijani L, Krawetz R, Lewis I, Argiropoulos B, Rancourt DE, Jung S, Hashimura Y, Lee B, Kallos MS. Optimized serial expansion of human induced pluripotent stem cells using low-density inoculation to generate clinically relevant quantities in vertical-wheel bioreactors. *Stem Cells Transl Med*. 2020;9(9):1036-1052. doi:10.1002/sctm.19-0406
 72. Elanzew A, Sommer A, Pusch-Klein A, Brüstle O, Haupt S. A reproducible and versatile system for the dynamic expansion of human pluripotent stem cells in suspension. *Biotechnol J*. 2015;10(10):1589-1599. doi:10.1002/biot.201400757
 73. Fischer B, Meier A, Dehne A, Salhotra A, Anh T, Neumann S, Schmidt K, Meiser I, Neubauer JC. A complete work flow for the differentiation and the dissociation of hiPSC-derived cardiospheres. *Stem Cell Res*. 2018;32(March):65-72.
 74. Humes HD, Mackay SM, Funke AJ and B DA. Tissue engineering of a bioartificial renal tubule assist device: In vitro transport and metabolic characteristics. *Kidney International*. 1999;55(2502-2514).
 75. Ellis JK, Athersuch TJ, Cavill R, Radford R, Slattery C, Jennings P, McMorrow T, Ryan MP, Ebbels TMD, Keun HC. Metabolic response to low-level toxicant exposure in a novel renal tubule epithelial cell system. *Mol Biosyst*. 2011;7(1):247-257. doi:10.1039/c0mb00146e
 76. Radford R, Slattery C, Jennings P, Blaque O, Pfaller W, Gmuender H, van Delft J, Ryan MP, McMorrow T. Carcinogens induce loss of the primary cilium in human renal proximal tubular epithelial cells independently of effects on the cell cycle.

- Am J Physiol - Ren Physiol.* 2012;302(8). doi:10.1152/ajprenal.00427.2011
77. Chang SH, Chiang IN, Chen YH, Young TH. Serum-free culture of rat proximal tubule cells with enhanced function on chitosan. *Acta Biomater.* 2013;9(11):8942-8951. doi:10.1016/j.actbio.2013.06.032
 78. Slyne J, Slattery C, McMorrow T, Ryan MP. New developments concerning the proximal tubule in diabetic nephropathy: In vitro models and mechanisms. *Nephrol Dial Transplant.* 2015;30:iv60-iv67. doi:10.1093/ndt/gfv264
 79. Pal R, Mamidi MK, Das AK, Bhonde R. Diverse effects of dimethyl sulfoxide (DMSO) on the differentiation potential of human embryonic stem cells. *Arch Toxicol.* 2012;86(4):651-661. doi:10.1007/s00204-011-0782-2
 80. Jasmin, Spray DC, De Carvalho ACC, Mendez-Otero R. Chemical induction of cardiac differentiation in P19 embryonal carcinoma stem cells. *Stem Cells Dev.* 2010;19(3):403-411. doi:10.1089/scd.2009.0234
 81. Skerjanc IS. Cardiac and skeletal muscle development in P19 embryonal carcinoma cells. *Trends Cardiovasc Med.* 1999;9(5):139-143. doi:10.1016/S1050-1738(99)00017-1
 82. Van Der Heyden MAG, Van Kempen MJA, Tsuji Y, Rook MB, Jongsma HJ, Opthof T. P19 embryonal carcinoma cells: A suitable model system for cardiac electrophysiological differentiation at the molecular and functional level. *Cardiovasc Res.* 2003;58(2):410-422. doi:10.1016/S0008-6363(03)00247-5
 83. Nadasdy T, Zoltan Laszik, Kenneth E. Buck, Loranine D. Johnson and FGS. Proliferative Activity of Intrinsic Cell Populations in the Normal Human Kidney. 2005;19(1988):3-5.
 84. Ngo TTT, Rossbach B, Sébastien I, Neubauer JC, Kurtz A, Hariharan K. Functional differentiation and scalable production of renal proximal tubular epithelial cells from human pluripotent stem cells in a dynamic culture system. *Cell Prolif.* 2022;55(3):1-14. doi:10.1111/cpr.13190
 85. Clark JM, Hirtenstein MD. Optimizing Culture Conditions for the Production of Animal Cells in Microcarrier Culture. *Ann N Y Acad Sci.* 1981;369(1):33-46. doi:10.1111/j.1749-6632.1981.tb14175.x
 86. Ugwu MC, Pelis R, Esimone CO, Agu RU. Fluorescent organic cations for human OCT2 transporters screening: Uptake in CHO cells stably expressing hOCT2. *ADMET DMPK.* 2017;5(2):135-145. doi:10.5599/admet.5.2.389
 87. Szablewski L. Distribution of glucose transporters in renal diseases. *J Biomed*

- Sci.* 2017;24(1):1-12. doi:10.1186/s12929-017-0371-7
88. Albarrán OG, Ampudia-Blasco FJ. Dapagliflozina, el primer inhibidor SGLT 2 en el tratamiento de la diabetes tipo 2. *Med Clin (Barc)*. 2013;141(SUPPL. 2):36-43. doi:10.1016/S0025-7753(13)70062-9
 89. Truong DM, Kaler G, Khandelwal A, Swaan PW, Nigam SK. Multi-level analysis of organic anion transporters 1, 3, and 6 reveals major differences in structural determinants of antiviral discrimination. *J Biol Chem*. 2008;283(13):8654-8663. doi:10.1074/jbc.M708615200
 90. Lee WK, Reichold M, Edemir B, Ciarimboli G, Warth R, Koepsell H, Thévenod F. Organic cation transporters OCT1, 2, and 3 mediate high-affinity transport of the mutagenic vital dye ethidium in the kidney proximal tubule. *Am J Physiol - Ren Physiol*. 2009;296(6):1504-1513. doi:10.1152/ajprenal.90754.2008
 91. Yasujima T, Ohta K, Inoue K, Yuasa H. Characterization of Human OCT1-Mediated Transport of DAPI as a Fluorescent Probe Substrate. *J Pharm Sci*. 2011;100(9):4006-4012. doi:10.1002/jps.22548
 92. Lawrence ML, Chang CH, Davies JA. Transport of organic anions and cations in murine embryonic kidney development and in serially-reaggregated engineered kidneys. *Sci Rep*. 2015;5:1-8. doi:10.1038/srep09092
 93. Kimura N, Okuda M, Inui KI. Metformin transport by renal basolateral organic cation transporter hOCT2. *Pharm Res*. 2005;22(2):255-259. doi:10.1007/s11095-004-1193-3
 94. Higgins JW, Bedwell DW, Zamek-Gliszczyński MJ. Ablation of both organic cation transporter (oct)1 and oct2 alters metformin pharmacokinetics but has no effect on tissue drug exposure and pharmacodynamics. *Drug Metab Dispos*. 2012;40(6):1170-1177. doi:10.1124/dmd.112.044875
 95. Çetinkaya I, Ciarimboli G, Yalçinkaya G, Mehrens T, Velic A, Hirsch JR, Gorboulev V, Koepsell H, Schlatter E. Regulation of human organic cation transporter hOCT2 by PKA, PI3K, and calmodulin-dependent kinases. *Am J Physiol Physiol*. 2003;284(2):F293-F302. doi:10.1152/ajprenal.00251.2002
 96. Glavinás H, Von Richter O, Vojnits K, Mehn D, Wilhelm I, Nagy T, Janossy J, Krizbai I, Couraud P, Krajcsi P. Calcein assay: A high-throughput method to assess P-gp inhibition. *Xenobiotica*. 2011;41(8):712-719. doi:10.3109/00498254.2011.587033
 97. Pasquier J, Rioult D, Abu-Kaoud N, Marie S, Rafii A, Guerrouahen BS, Le Foll F.

- P-glycoprotein-activity measurements in multidrug resistant cell lines: Single-cell versus single-well population fluorescence methods. *Biomed Res Int.* 2013;2013. doi:10.1155/2013/676845
98. Fransen MFJ, Addario G, Bouten CVC, Halary F, Moroni L, Mota C. Bioprinting of kidney in vitro models: Cells, biomaterials, and manufacturing techniques. *Essays Biochem.* 2021;65(3):587. doi:10.1042/EBC20200158
 99. King SM, Higgins JW, Nino CR, Smith TR, Paffenroth EH, Fairbairn CE, Docuycanan A, Shah VD, Chen AE, Presnell SC, Nguyen DG. 3D proximal tubule tissues recapitulate key aspects of renal physiology to enable nephrotoxicity testing. *Front Physiol.* 2017;8(MAR):1-18. doi:10.3389/fphys.2017.00123
 100. Ullah I, Busch JF, Rabien A, Ergün B, Stamm C, Knosalla C, Hippenstiel S, Reinke P, Kurtz A. Adult Tissue Extracellular Matrix Determines Tissue Specification of Human iPSC-Derived Embryonic Stage Mesodermal Precursor Cells. *Adv Sci.* 2020;7(5). doi:10.1002/advs.201901198
 101. Freedman BS, Lam AQ, Sundsbak JL, Iatrino R, Su X, Koon SJ, Wu M, Daheron L, Harris PC, Zhou J, Bonventre J V. Reduced ciliary polycystin-2 in induced pluripotent stem cells from polycystic kidney disease patients with PKD1 mutations. *J Am Soc Nephrol.* 2013;24(10):1571-1586. doi:10.1681/ASN.2012111089
 102. Chevalier RL. The proximal tubule is the primary target of injury and progression of kidney disease: Role of the glomerulotubular junction. *Am J Physiol - Ren Physiol.* 2016;311(1):F145-F161. doi:10.1152/ajprenal.00164.2016
 103. Smeets B, Boor P, Dijkman H, Sharma S V., Jirak P, Mooren F, Berger K, Bornemann J, Gelman IH, Floege J, Van Der Vlag J, Wetzels JFM, Moeller MJ. Proximal tubular cells contain a phenotypically distinct, scattered cell population involved in tubular regeneration. *J Pathol.* 2013;229(5):645-659. doi:10.1002/path.4125
 104. Ginai M, Elsby R, Hewitt CJ, Surry D, Fenner K, Coopman K. The use of bioreactors as in vitro models in pharmaceutical research. *Drug Discov Today.* 2013;18(19-20):922-935. doi:10.1016/j.drudis.2013.05.016
 105. Ng CP, Zhuang Y, Lin AWH, Teo JCM. A Fibrin-Based Tissue-Engineered Renal Proximal Tubule for Bioartificial Kidney Devices: Development, Characterization and In Vitro Transport Study . *Int J Tissue Eng.* 2013;2013:1-10. doi:10.1155/2013/319476

106. Chiang IN, Huang WC, Huang CY, Pu YS, Young TH. Development of a chitosan-based tissue-engineered renal proximal tubule conduit. *J Biomed Mater Res - Part B Appl Biomater*. 2018;106(1):9-20. doi:10.1002/jbm.b.33808
107. Batchelder CA, Martinez ML, Tarantal AF. Natural scaffolds for renal differentiation of human embryonic stem cells for kidney tissue engineering. *PLoS One*. 2015;10(12):1-18. doi:10.1371/journal.pone.0143849
108. Santer R, Kinner M, Lassen CL, Schneppenheim R, Eggert P, Bald M, Brodehl J, Daschner M, Ehrich JHH, Kemper M, Li Volti S, Neuhaus T, Skovby F, Swift PGF, Schaub J, Klaerke D. Molecular Analysis of the SGLT2 Gene in Patients with Renal Glucosuria. *J Am Soc Nephrol*. 2003;14(11):2873-2882. doi:10.1097/01.ASN.0000092790.89332.D2
109. De Rosa L, Enzo E, Zardi G, Bodemer C, Magnoni C, Schneider H, De Luca M. Hologene 5: A Phase II/III Clinical Trial of Combined Cell and Gene Therapy of Junctional Epidermolysis Bullosa. *Front Genet*. 2021;12(September). doi:10.3389/fgene.2021.705019

Statutory Declaration

“I, [Thi Thanh Thao, Ngo], by personally signing this document in lieu of an oath, hereby affirm that I prepared the submitted dissertation on the topic [Scalable differentiation of human pluripotent stem cells into in two and three - dimensional proximal tubule cells” or “Skalierbare Differenzierung human pluripotenter Stammzellen in zwei- und dreidimensionale proximale Tubuluszellen”, independently and without the support of third parties, and that I used no other sources and aids than those stated.

All parts which are based on the publications or presentations of other authors, either in letter or in spirit, are specified as such in accordance with the citing guidelines. The sections on methodology (in particular regarding practical work, laboratory regulations, statistical processing) and results (in particular regarding figures, charts and tables) are exclusively my responsibility.

My contributions to any publications to this dissertation correspond to those stated in the below joint declaration made together with the supervisor. All publications created within the scope of the dissertation comply with the guidelines of the ICMJE (International Committee of Medical Journal Editors; <http://www.icmje.org>) on authorship. In addition, I declare that I shall comply with the regulations of Charité – Universitätsmedizin Berlin on ensuring good scientific practice.

I declare that I have not yet submitted this dissertation in identical or similar form to another Faculty.

The significance of this statutory declaration and the consequences of a false statutory declaration under criminal law (Sections 156, 161 of the German Criminal Code) are known to me.”

Date

17/10/2022

Signature

Declaration of your own contributions to the publications

Thi Thanh Thao, Ngo contributed the following to the below publication:

Publication: Thao Thi Thanh Ngo, Bella Rossbach, Isabelle Sébastien, Julia C. Neubauer, Andreas Kurtz, Krithika Hariharan, Functional differentiation and scalable production of renal proximal tubular epithelial cells from human pluripotent stem cells in a dynamic culture system, Cell proliferation, January 2022.

My contributions to the publication: “Functional differentiation and scalable production of renal proximal tubular epithelial cells from human pluripotent stem cells in a dynamic culture system” included study conceptualization, design and direct conduct of experiments, data analysis, data interpretation, data presentation, the manuscript writing.

I got the **concept** for culturing cells on Matrigel-coated alginate beads from Prof.Andreas Kurtz and Dr.Julia C. Neubauer. With **direct guidance** of M.Sc.Isabelle Sébastien, and **comments** from Dr.Krithika Hariharan and Prof.Andreas Kurtz, I set up protocol for culture and differentiate hPSC on Matrigel-coated alginate beads in Cero. I self-optimized cell number seeding, cell inoculation step to get maximum cell yields after culture.

I read extensive literature to identify important factors for **formation of an optimized medium** for differentiation PTEC from hPSC-derived renal progenitor cells. Then, I **exerted many screening** experiments to find out good medium with support of Dr.Krithika Hariharan in recognize the best medium relying on **cell morphology and flow cytometry**.

For flow cytometric experiments to analyse targeted marker-positive subsets, I used a standadized **flow cytometric protocol** of Dr.Bella Rossbach and also benefitted from her knowlegde for some data acquisition. I designed negative samples, performed all treatments, fluorescent (antibodies) combinations and stainings, data acquisition. For flow cytometric data analysis, I discussed **gating strategies and graphs presentation** with Dr.Bella Rossbach, Dr.Krithika Hariharan.

Based on finding in literature, I established the setups for **almost functional assays** including glucose assay, albumin assay, organic anion and cation assays. I benefitted from the knowlegde of Dr.Bella Rossbach and Dr.Krithika Hariharan for **cytotoxicity and transport assay** of renal efflux P-gp, respectively. For Transepithelial electrical resistance measurement, I established the protocol to culture PTEC effectively on Transwell inserts, and got help in measuring TEER from Dr.Bella Rossbach.

For getting ultra-structures of PTEC by Transmission Electron Microscopy, I treated samples according to instructions of Dr.Sara Timm and sent samples to Core Facility for Electron Microscopy of Charité for analysis.

With support from Dr.Iris Fischer, M.Sc Enrico Fritsche and Dr.Imran Ullah, I got familiar with devices and sectioning methods, I found out my effective way to section Matrigel-coated alginate beads that preserved cells morphology and beads structure after the dehydration process.

I composed the initial structure of the manuscript, that was optimized and proofread by all co-authors, primarily and mainly by Prof.Andreas Kurtz and Dr.Krithika Hariharan. During review process at Cell Proliferation, I further optimised the manuscript that was proofread by Dr.Bella Rossbach, Prof.Andreas Kurtz and Dr.Krithika Hariharan.

Except figure 1 prepared by Dr.Krithika Hariharan and me, all figures and tables were prepared by me.

Signature, date and stamp of first supervising university professor / lecturer

Signature of doctoral candidate

Excerpt from Journal Summary List


Journal Data Filtered By: Selected JCR Year: 2020 Selected Editions: SCIE,SSCI
 Selected Categories: "CELL BIOLOGY" Selected Category Scheme: WoS
 Gesamtanzahl: 195 Journale

Rank	Full Journal Title	Total Cites	Journal Impact Factor	Eigenfactor Score
1	NATURE REVIEWS MOLECULAR CELL BIOLOGY	58,477	94.444	0.075480
2	NATURE MEDICINE	114,401	53.440	0.184050
3	CELL	320,407	41.582	0.526960
4	CANCER CELL	50,839	31.743	0.081040
5	NATURE CELL BIOLOGY	52,554	28.824	0.070950
6	Cell Metabolism	52,192	27.287	0.091000
7	Journal of Extracellular Vesicles	8,485	25.841	0.011820
8	CELL RESEARCH	24,108	25.617	0.034400
9	Cell Stem Cell	32,147	24.633	0.062780
10	TRENDS IN CELL BIOLOGY	19,007	20.808	0.030120
11	Signal Transduction and Targeted Therapy	3,848	18.187	0.005730
12	MOLECULAR CELL	86,299	17.970	0.161840
13	Science Translational Medicine	45,509	17.956	0.103780
14	Autophagy	25,343	16.016	0.027970
15	CELL DEATH AND DIFFERENTIATION	27,701	15.828	0.028730
16	NATURE STRUCTURAL & MOLECULAR BIOLOGY	32,038	15.369	0.051210
17	Protein & Cell	5,352	14.870	0.009500
18	Annual Review of Cell and Developmental Biology	11,884	13.827	0.011100
19	DEVELOPMENTAL CELL	36,177	12.270	0.058350
20	TRENDS IN MOLECULAR MEDICINE	13,213	11.951	0.014720

Rank	Full Journal Title	Total Citas	Journal Impact Factor	Eigenfactor Score
21	EMBO JOURNAL	76,189	11.598	0.055000
22	MATRIX BIOLOGY	8,972	11.583	0.011010
23	GENES & DEVELOPMENT	61,885	11.361	0.048660
24	PLANT CELL	64,794	11.277	0.036260
25	AGEING RESEARCH REVIEWS	10,264	10.895	0.013510
26	Cell Discovery	3,492	10.849	0.006770
27	CURRENT BIOLOGY	78,289	10.834	0.116100
28	JOURNAL OF CELL BIOLOGY	79,173	10.539	0.057070
29	Cell Systems	5,813	10.304	0.035330
30	Cold Spring Harbor Perspectives in Biology	22,738	10.005	0.030460
31	Wiley Interdisciplinary Reviews-RNA	3,743	9.957	0.008220
32	ONCOGENE	77,576	9.867	0.059180
33	Cell Reports	73,442	9.423	0.254400
34	AGING CELL	13,890	9.304	0.017950
35	CELLULAR AND MOLECULAR LIFE SCIENCES	34,003	9.261	0.033790
36	EMBO REPORTS	19,502	8.807	0.027490
37	Cell Death & Disease	40,835	8.469	0.063770
38	JOURNAL OF BIOMEDICAL SCIENCE	6,621	8.410	0.007330
39	CURRENT OPINION IN CELL BIOLOGY	15,784	8.382	0.019750
40	Science Signaling	15,954	8.192	0.023910
41	Stem Cell Reports	10,762	7.765	0.029290

Rank	Full Journal Title	Total Cites	Journal Impact Factor	Eigenfactor Score
42	SEMINARS IN CELL & DEVELOPMENTAL BIOLOGY	14,105	7.727	0.021440
43	CYTOKINE & GROWTH FACTOR REVIEWS	7,650	7.638	0.005850
44	AMERICAN JOURNAL OF RESPIRATORY CELL AND MOLECULAR BIOLOGY	15,280	6.914	0.015050
45	Stem Cell Research & Therapy	13,356	6.832	0.018900
46	CELL PROLIFERATION	5,130	6.831	0.005130
47	CELL CALCIUM	6,842	6.817	0.006250
48	International Review of Cell and Molecular Biology	3,057	6.813	0.004320
49	CURRENT OPINION IN STRUCTURAL BIOLOGY	12,448	6.809	0.018970
50	CELLULAR ONCOLOGY	2,462	6.730	0.002430
51	CELL BIOLOGY AND TOXICOLOGY	2,298	6.691	0.001370
52	Frontiers In Cell and Developmental Biology	7,731	6.684	0.015420
53	Cells	18,802	6.600	0.026970
54	Oxidative Medicine and Cellular Longevity	27,913	6.543	0.036150
55	Tissue Engineering Part B-Reviews	4,536	6.389	0.003040
56	JOURNAL OF CELLULAR PHYSIOLOGY	39,997	6.384	0.041830
57	MOLECULAR MEDICINE	6,239	6.354	0.004460
58	STEM CELLS	23,967	6.277	0.017860
59	Journal of Molecular Cell Biology	3,144	6.216	0.004700
60	TRAFFIC	7,808	6.215	0.007630
61	MOLECULAR CANCER RESEARCH	11,253	5.852	0.013250

Functional differentiation and scalable production of renal proximal tubular epithelial cells from human pluripotent stem cells in a dynamic culture system

Thao Thi Thanh Ngo¹ | Bella Rossbach^{1,3} | Isabelle Sébastien² | Julia C. Neubauer² | Andreas Kurtz^{1,3} | Krithika Hariharan^{1,2} 

¹BIH Center for Regenerative Therapies, Charité – Universitätsmedizin Berlin, Berlin, Germany

²Project Centre for Stem Cell Process Engineering, Fraunhofer Institute for Biomedical Engineering (IBMT), Würzburg, Germany

³Fraunhofer Institute for Biomedical Engineering (IBMT), Berlin, Germany

Correspondence

Andreas Kurtz and Krithika Hariharan, Charité – Universitätsmedizin Berlin, BIH Center for Regenerative Therapies, Berlin, Fraunhofer Institute for Biomedical Engineering (IBMT), Project Centre for Stem Cell Process Engineering, Würzburg, Germany.
Email: andreas.kurtz@bih-charite.de(A.K.); krithika.hariharan@ibmt.fraunhofer.de(K.H.)

Funding information

Bundesministerium für Bildung und Forschung - BMBF, Grant/Award Number: 01EK1612D; Bundesministerium für Wirtschaft und Technologie, Grant/Award Number: ZF4274303

Abstract

Objective: To provide a standardized protocol for large-scale production of proximal tubular epithelial cells (PTEC) generated from human pluripotent stem cells (hPSC).

Methods: The hPSC were expanded and differentiated into PTEC on matrix-coated alginate beads in an automated levitating fluidic platform bioLevigator. Differentiation efficacy was evaluated by immunofluorescence staining and flow cytometry, ultrastructure visualized by electron microscopy. Active reabsorption by PTEC was investigated by glucose, albumin, organic anions and cations uptake assays. Finally, the response to cisplatin-treatment was assessed to check the potential use of PTEC to model drug-induced nephrotoxicity.

Results: hPSC expansion and PTEC differentiation could be performed directly on matrix-coated alginate beads in suspension bioreactors. Renal precursors arose 4 days post hPSC differentiation and PTEC after 8 days with 80% efficiency, with a 10-fold expansion from hPSC in 24 days. PTEC on beads, exhibited microvilli and clear apico-basal localization of markers. Functionality of PTECs was confirmed by uptake of glucose, albumin, organic anions and cations and expression of KIM-1 after Cisplatin treatment.

Conclusion: We demonstrate the efficient expansion of hPSC, controlled differentiation to renal progenitors and further specification to polarized tubular epithelial cells. This is the first report employing biolevitation and matrix-coated beads in a completely defined medium for the scalable and potentially automatable production of functional human PTEC.

1 | INTRODUCTION

The kidney has a crucial role in blood clearance, homeostasis maintenance, and waste product elimination. Through renal arteries, the blood enters the kidney where it is passively filtered in the glomeruli, followed by selective reabsorption of between 70% and 100% of

the substances in the pre-urine, including water, amino acids, electrolytes, and glucose by proximal tubular epithelial cells (PTEC) via numerous transport systems.¹ PTEC are cuboidal, mononuclear cells with apical-basal polarization and densely microvilli covered brush borders on the apical side, a typical morphological feature distinguishing PTEC and distal tubular cells.² PTEC are also responsible for

This is an open access article under the terms of the Creative Commons Attribution License, which permits use, distribution and reproduction in any medium, provided the original work is properly cited.

© 2022 The Authors. Cell Proliferation published by John Wiley & Sons Ltd.

detoxification and secretion of exogenous compounds such as drugs and xenobiotics into the urine.

Due to high susceptibility to toxic and waste compounds, PTEC are extremely vulnerable, and their injury may result in renal failure or total destruction. There is a high demand of PTEC for tissue modeling, large-scale drug-induced nephrotoxicity screening, and potentially for regenerative therapies. Immortalized and primary PTEC cultivated as 3-dimensional microtissue were reported to dedifferentiated within 10 days.³ Moreover, although exhibiting a variety of functional transporters, primary PTEC are variable depending on donors, and partially dedifferentiate *in vitro* while immortalized PTEC lines show functional changes related to the immortalization procedures.⁴ To improve PTEC-models, several differentiation protocols of human pluripotent stem cells (hPSC) into PTEC have been developed.⁴⁻⁶ The use of human induced pluripotent stem cells (hiPSC) provides an unlimited source of cells that are donor specific and can be genetically modified to present specific kidney disease backgrounds. However, general limitations of these hPSC-derived PTEC are often their immature transporter properties, limited polarization and short lifespan. A lack of technologies for efficient, robust and automatable mass production of high quality PTEC limits their applicability.

Many biomaterials have been developed for expansion, embedding, and differentiation of stem cells.⁷ Alginate hydrogel, for example, offers a variety of advantages such as low cost, environmental friendliness, high biocompatibility, low cytotoxicity, easy purification, functionalization, and adjustable gelation.⁸ Spherical alginate beads after coating with extracellular matrix allow cultivation of cells and expansion of surfaces by bead supplementation.⁹ In addition, the beads are easily applied to fluidic culture systems of diverse designs including stirring, rotating, and agitation bioreactors. These fluidic systems can be adapted to mimic the fluidic environment of the proximal tubule epithelia and may increase polarization, barrier, and transport functions of PTEC.¹⁰ In 2015, Elanzew and colleagues first reported long-term expansion of hPSC as undifferentiated aggregates with low inoculation density using a BioLevigator™, now CERO from OLS.¹¹ In 2017, expansion of human stem cells on Matrigel-coated alginate beads using this system was reported.⁹

We used a biolevitation-based approach allowing scalable cell culture to expand and differentiate hPSC into human PTEC cultivated on Matrigel-coated alginate beads. The biolevitation together with the floating cell-covered beads models a fluidic environment. This system supported the efficient expansion of hPSC and their immediate differentiation to renal progenitors in a single system. This is the first report of using biolevitation of cell-coated alginate beads for scalable and potentially automated production of functional human PTEC.

2 | MATERIALS AND METHOD

2.1 | Cell culture and maintenance in static culture

The hiPSC lines WISCI004-A (referred to as IMR90-4-iPS, derived from female lung fibroblast) from passages 35 to 65, BCRTi005¹² derived from urinary cells at passage 25 to 35, and WAe001-A derived

from male blastocyst were cultured on 6-well plates (Falcon) coated with Geltrex (Thermo Fisher Scientific) in serum-free, defined Essential 8 (E8) medium (STEMCELL Technologies). Cells were maintained in a humidified 5% CO₂ atmosphere at 37°C. 0.5mM ethylenediamine-tetraacetic acid (EDTA Gibco) in calcium/magnesium free phosphate-buffered saline (PBS) was used to passage hPSC as colonies.

2.2 | Bioreactor platform

BioLevigator™, now CERO from Omni Life Science GmbH & Co was designed as a sealed miniaturized incubator, where parameters for cell culture including CO₂ level, temperature, speed of tube rotation, and thus, fluidic stress can be adjusted. It can manage separately four 50ml vessels called Levitubes™, now CEROTubes™ with a maximum working capacity of 50ml each.

2.3 | Preparation, seeding and expansion of hPSC on Matrigel-coated alginate beads

Matrigel-coated alginate beads or Matrigel-coated beads were supplied by Fraunhofer Institute for Biomedical Engineering (IBMT), Project Centre for Stem Cell Process Engineering, Würzburg, Germany. Growth factor-reduced Matrigel was used to cover alginate beads. Matrigel-coated beads were stored at 4°C until use. Before hPSC seeding, Matrigel-coated beads were rinsed twice with E8 medium. Around 40cm² Matrigel-coated beads were used for each 50 ml CEROTubes™. Confluent hPSC were harvested using 0.5mM EDTA and reseeded on Matrigel-coated beads at a density of 2.6×10^6 cells in a final volume of 4ml E8 medium for each tube. On the next day, E8 was filled up to 10ml and changed every day. 4 days after seeding, 90% of Matrigel-coated beads were covered by cells. Observation of beads and cells on beads was performed with phase contrast microscopy (Nikon Eclipse Ts2).

2.4 | PTEC differentiation and expansion

Confluent hPSC on Matrigel-coated beads were differentiated into renal progenitors following the protocol developed by Hariharan et al.⁶ Specifically, hPSC were induced into intermediate mesoderm during the first 4 days in STEMdiff™ APEL2™ Medium (Stemcell Technologies) with 5% Protein free hybridoma medium (PFHMII) in presence of 10ng/ml Activin A (Peprotech), 1μM Retinoic Acid (Sigma-Aldrich), and 30ng/ml recombinant human bone morphogenetic protein 4 (BMP4) (Peprotech). This step was followed by further 4 days in the same basal medium supplemented with 150ng/ml Glial derived neurotrophic factor (GDNF) (Peprotech) (Figure 1(A)).

To induce differentiation and expansion of PTEC, an optimized low glucose, serum-free medium, called PTEC medium was replaced on day 8 (d8). Basal medium composition of PTEC medium included a mixture of low glucose Gibco™ DMEM (11054) and Ham's F-12K (21127022, Thermo Fisher) in a 1:1 ratio, then this mixture was

mixed to Defined Keratinocyte-serum-free medium (KSFM) (10785-012[®], Gibco) in a 1:1 ratio. This basal medium was supplemented with Insulin-Transferrin-Selenium (ITS) (Gibco), 10ng/ml Epidermal growth factor (EGF), 1 μ M Hydrocortisone and 0.5% Dimethyl sulfoxide (DMSO). Cells were maintained in this medium until day 20 (d20) (Figure 1(A)). PTEC medium was changed every other day. The differentiation was monitored by marker expression analysis on day 4 (d4) and day 8 (d8) for renal progenitors, and on days 10 (d10), 12 (d12), 14 (d14), 16 (d16), 20 (d20) for PTEC.

In static culture of hPSCs, the differentiation protocol for renal progenitors and PTEC was performed with identical media and timelines with the exception that Geltrex was used for coating instead of Matrigel. For matrix comparison, renal progenitor cells were harvested on day 8 using Accutase cell dissociation reagent (Gibco), re-plated on Laminin521 (LN521) (BioLamina) and differentiated into PTEC.

2.5 | Immunofluorescence staining

Cultured cells on 96-well plates were washed with PBS, fixed with Cytifix (BD Biosciences) for 10 minutes at room temperature (RT). Afterward, cells were washed twice with PBS, blocked with 10% secondary antibody host serum for 30 minutes at RT and further incubated with primary antibodies overnight at 4°C. Primary antibodies were diluted in BD Perm/Wash[™] with dilution factor 1:100 or following the manufacturer's instructions. After washing twice with BD Perm/Wash[™], labeled secondary antibodies were applied to the cells in 1:1000 dilution for 1h at RT in the dark. Finally, the cells were stained with fluorescent dye 4', 6-diamidino-2-phenylindole (DAPI; Sigma-Aldrich, D-8417) to label nuclei. Negative controls omitted either primary or both primary and secondary antibodies. The primary antibodies using in this study were Aquaporin 1 (AQP1) (Proteintech), Sodium-Potassium ATPase (Na⁺/K⁺-ATPase) (Abcam), Sodium-Glucose cotransporter-2 (SGLT2) (Abcam), Megalin/LRP2 (Abcam), E-Cadherin (BD Biosciences), and Kidney injury molecular-1 (KIM-1) (Thermo Fisher). Secondary antibodies were Donkey anti-Mouse IgG (H + L) Secondary Antibody, Alexa Fluor 488; Donkey anti-Mouse IgG (H + L) Secondary Antibody, Alexa Fluor 647; Donkey anti-Rabbit IgG (H + L) Secondary Antibody, Alexa Fluor 488; Donkey anti-Rabbit IgG (H + L) Secondary Antibody, Alexa Fluor 647 (all from Thermo Fisher). Biotinylated Lotus Tetragonolobus Lectin (LTL) (Vector Laboratories), Texas Red[™]-X Phalloidin (Thermo Fisher) were used to detect Fucose on microvilli and actin filaments, respectively, of PTEC. The Operetta high content imager and Columbus image analysis server (both PerkinElmer, Waltham, MA, US) were used for imaging and analyzing.

2.6 | Paraffin embedding and sectioning

Matrigel-coated beads covered with cells were harvested, fixed, washed and encapsulated in 4% low melting agarose. Half an hour after gelation, agarose blocks containing beads were dehydrated and subsequently embedded into paraffin. The samples were sectioned

at 4 μ m thickness using a microtome (Leica RM2255). After removing the paraffin by Xylene (Sigma-Aldrich), the sections were heated in Target Retrieval solution (Dako) at 96°C in a water bath for 30 minutes for antigen retrieval and stained with antibodies.

2.7 | Flow Cytometry

Adherent cells were dissociated to a single-cell suspension using Trypsin/EDTA 0.5% (Thermo Fisher) and discriminated alive cells and dead cells using LIVE/DEAD[™] Fixable Dead Cell Stain Kit (Thermo Fisher) for 30 min at 4°C. For labeling of intracellular antigen, cells were permeabilized using Phosflow Perm Buffer II (BD Biosciences) for 15 minutes at RT, incubated with primary antibodies for 30 minutes, and further for another 30 minutes with secondary antibodies. The dilution factor for primary antibodies was 1:100 or according to the manufacturer's instructions, and for secondary antibody it was 1:1000. Labeled cells were measured using MACSQuant Analyzer (Miltenyi Biotec), and data was analyzed with FlowJo software. All samples were performed in duplicates and all experiments were repeated 3 times. Antibodies used were SIX Homebox 2 (SIX2) (H00010736-M01, Abnova), Receptor tyrosine kinase (RET) (53164, LSBio), Jagged 1 (JAG1) (ab77771, Abcam), Wilms' tumor protein 1 (WT1) (sc192, SCBT), AQP1 (20333-1-AP, Proteintech), Na⁺/K⁺-ATPase (ab76020, Abcam), Megalin/LRP2 (ab76969, Abcam), SGLT2 (ab58298, Abcam), LTL (FL-1321, Vector Laboratories), organic cation transporter 2 (OCT2) (ab242317, Abcam), organic anion transporter 1 (OAT1) (LS-B10034, LSBio), organic anion transporter 3 (OAT3) (ab247055, Abcam), AF647 Anti P-Glycoprotein (P-gp) (ab253265, Abcam), multi-drug resistance protein 2 (MRP2) (MA1-26535, Thermo Fisher).

2.8 | Transmission electron microscopy

Matrigel-coated beads covered with cells were harvested, rinsed with PBS and fixed with 2.5% glutaraldehyde (Serva, Heidelberg, Germany) in 0.1 M sodium cacodylate buffer (Serva, Heidelberg, Germany) for 30 min at RT and stored at 4°C. The samples were postfixated with 1% osmium tetroxide (Electron Microscopy Sciences, Hatfield, USA) and 0.8% potassium ferrocyanide II (Roth, Karlsruhe, Germany) in 0.1 M cacodylate buffer for 1.5 h and embedded in agarose overnight. After cutting the agarose in smaller blocks, the samples were dehydrated in a graded ethanol series and transferred to Epon resin (Roth, Karlsruhe, Germany). Finally, ultrathin sections of the samples (70nm) were stained with uranyl acetate, and lead citrate. The examination was carried out with a Zeiss EM 906 electron microscope at 80kV acceleration voltage (Carl Zeiss, Oberkochen, Germany).

2.9 | Glucose assay

Glucose uptake of cells on Matrigel-coated beads was measured through cellular uptake of 2-NBDG (2-(N-(7-Nitrobenz-2-oxa-1,3-diazol-4-yl) Amino)-2-Deoxyglucose) (Thermo Fisher). Matrigel-coated

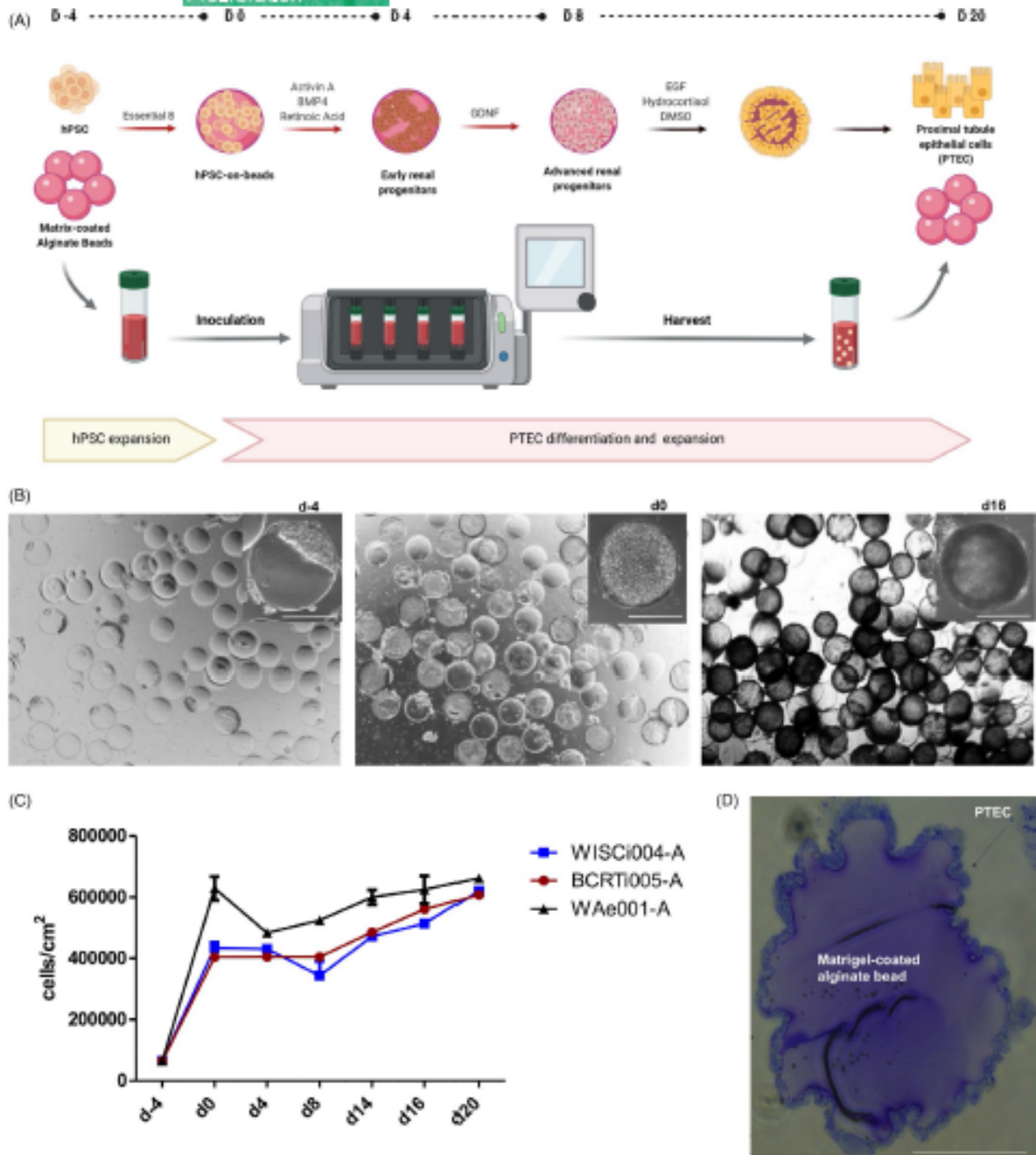


FIGURE 1 Expansion and differentiation of hPSC into PTEC on Matrigel-coated alginate beads by biolevitation. (A) Schematic illustration of hPSC expansion and PTEC differentiation on Matrigel-coated alginate beads by biolevitation. The protocol includes two definite steps: (i) Expansion of hPSC in Essential 8 medium for 4 days from d4 to d0; (ii) Differentiation and Expansion of PTEC from d0 to d20. This step includes: (1) differentiation of hPSC into renal progenitors for 8 days and (2) generation, expansion and maintenance of PTEC; (B) Phase contrast pictures of cells on Matrigel-coated alginate beads on d4, d0, d16. One representative bead for each time point was taken with scale bar = 500 μ m; (C) Growth rate of cells on 40 cm² of Matrigel-coated alginate beads from seeding (d-4) until d20 for the hiPSC lines (WISCi004-A, BCRTi005-A) and the embryonic stem cell (ESC) line WAe001-A, respectively (n = 3); (D) Toluidine blue stained histological section of a Matrigel-coated alginate bead at d16 with a PTEC monolayer on the bead surface. Scale bar = 100 μ m

beads for assay were washed twice with DMEM without glucose, incubated with 400 μ M 2-NBDG for 30 minutes in presence or absence of 1 μ M Dapagliflozin inhibitor. Beads were washed twice with DMEM without glucose before cells were harvested from beads using Trypsin/EDTA. Uptake of 2-NBDG was measured using MACSQuant Analyzer (Miltenyi Biotec) and data analyzed with FlowJo software.

2.10 | Albumin assay

Cellular endocytosis of albumin was investigated through application of different concentrations of FITC-Albumin (Abcam) to cells on Matrigel-coated beads. Matrigel-coated beads for the assay were incubated with serum-free medium with/without 50 μ g/ml, 100 μ g/ml, 500 μ g/ml, 1mg/ml FITC-Albumin for 2 hours at 37°C. For immunofluorescence staining, cells were fixed using BD Cytotfix, embedded into paraffin, sectioned and analyzed by Operetta high content imager and Columbus image analysis server (both PerkinElmer, Waltham, MA, US). For FACS analysis, cells were harvested from Matrigel-coated beads using Trypsin/EDTA and albumin uptake was assessed using MACSQuant Analyzer and data analyzed with FlowJo software.

2.11 | Organic anion uptake assay

To investigate organic anion transport by the basolateral organic anion transporters OAT1 and OAT3, an assay was performed using the fluorescent anion 6-Carboxyfluorescein (6-CF) (Thermo Fisher), a tracer dye, as described by Lawrence et al.¹³ Briefly, d16 cells on Matrigel-coated beads were incubated with 50 μ M 6-CF for 40 minutes in presence or absence of 2.5mM Probenecid inhibitor (Sigma-Aldrich). Beads were washed twice with PBS before cells were harvested from beads using Trypsin/EDTA. Uptake of 6-CF was measured using MACSQuant Analyzer (Miltenyi Biotec) and data analyzed with FlowJo software.

2.12 | Organic cation uptake assays

Organic cation uptake by PTEC was investigated using the fluorescent cationic molecule DAPI, transported into live PTEC through the organic cation transporter 2 (OCT2) as described by Lawrence et al.¹³ Shortly, uptake of 1 μ M DAPI for 90 minutes by OCT2 was evaluated in presence or absence of Metformin and Cimetidine inhibitors (Abcam). Additionally, the activity of renal OCT2 influx protein was checked through the exposure to 5 μ M fluorescent OCT substrate 4-Di-2-ASP (Sigma-Aldrich) for 15 minutes in presence or absence of 15mM OCT inhibitor Tetrapentylammonium chloride (TPA) (Santa Cruz) as demonstrated by Jansen et al.¹⁴

The uptake of these fluorescent substrates was measured using MACSQuant Analyzer (Miltenyi Biotec) and data analyzed with FlowJo software.

2.13 | Transport assay of renal efflux P-Glycoprotein

ABC transporter permeability (P)-glycoprotein (ABCB1; MDR1/P-gp) of d16 cells on Matrigel-coated beads was evaluated using Calcein accumulation.¹³ Thus, cells were incubated with 100nM Calcein, AM, cell-permeable dye (Thermo Fisher) for 15 minutes in presence or absence of 40 μ M P-gp inhibitor PSC-833 (MedChemExpress). Calcein retention was measured using MACSQuant Analyzer (Miltenyi Biotec) and data analyzed with FlowJo software.

2.14 | Cytotoxicity assay

PTEC were harvested from the beads at d14 using TrypLE™ Express (Gibco) and reseeded at a concentration of 50,000 cells/well into Geltrex-coated 96 wells. After incubation at 37°C for 2 days, PTEC medium was replaced. Confluent monolayers of cells were treated with various concentrations of Cisplatin (Sigma) from 50 μ M to 400 μ M for 6 hours in triplicates. Nephrotoxicity of Cisplatin was measured by MTT assay (Sigma-Aldrich). After 6 hours of Cisplatin treatment, medium was changed to fresh medium, supplemented with 0.5mg/ml MTT labeling reagent yellow tetrazole and incubated in the dark for further 4 hours. NAD(P)H-dependent cellular oxidoreductase enzymes of living cells were capable of reducing tetrazolium dye MTT to its purple insoluble formazan. Insoluble formazan was dissolved by incubating cells with solubilization solution overnight. The absorbance or optical density (OD) was measured at 570nm and 650nm using a microplate reader (Spectra max 384). Cisplatin untreated cells were used as negative controls.

Cell viability was calculated by formula:

$$\frac{OD(570) - OD(650) \text{ of treated sample}}{OD(570) - OD(650) \text{ of untreated sample}} \times 100$$

2.15 | Transepithelial electrical resistance

Transepithelial electrical resistance (TEER) of matured PTEC monolayers on Transwell inserts (cellQART) was measured using an EVOM3 Ohmmeter. TEER was measured according to manufacturer's instruction. D14 cells were harvested from Matrigel-coated beads and reseeded on 24-Transwell insert with a density of 50,000 cells per insert. 2 days after cell seeding, epithelial resistance was measured daily. To obtain TEER value (Ω cm²), blank resistance (insert with media only) was subtracted from the measured resistance and afterward multiplied by the surface area.

2.16 | Statistical analysis

Cell culture on Matrigel-coated beads were performed in duplicates and further cell characterization and functionality tests were repeated 3 times ($n = 3$). Statistical analysis was performed by GraphPad Prism 5 (GraphPad Software, La Jolla, US). Statistical significance was calculated by two-way ANOVA.

3 | RESULTS

3.1 | Matrix-coated alginate beads offer an adjustable surface for hPSC expansion and renal differentiation in a dynamic culture system

The differentiation protocol (Figure 1(A)) was applied to three different hPSC-lines, the fibroblast derived hPSC-line WISCI004-A, the urinary cell derived hPSC-line BCRTi005-A, and the human embryonic stem cell (ESC)-line WAe001-A. Cells attached to >90% of the beads with optimized inoculation density and culture medium volume (Figure 1(B)). 4 days after seeding hPSC, fold expansion was 6.2 (BCRTi005-A), 6.7 (WISCI004-A), and 9.7 (WAe001-A), respectively (Table 1, Figure 1(C)).

Attachment and expansion of hPSC in 4 days was immediately followed by successive differentiation into mesoderm, renal progenitors and PTEC (Figure 1(A)).⁸ After an initial increase in cell numbers during expansion of hPSC (d0), a steady number of renal progenitor cells was maintained until d8 (Table 1, Figure 1(C)). After subsequent differentiation and expansion of PTEC (Figure 1(A)), the cell numbers further increased until d20 (Table 1). More specific, when a starter culture of 2.6×10^5 hPSCs were cultured on 40cm² of beads, around $24\text{--}26 \times 10^5$ PTEC were obtained on d20. In comparison, in parallel static culture on Matrigel-coated 6-well plates, 4 to 5 times fewer renal progenitor cells were obtained at d8 ($<1 \times 10^5$ cells/cm²), and at d20 ($<1.4 \times 10^5$ cells/cm²) for all cell lines, when the starting cell numbers were same as in the fluidic culture. Toluidine blue stained histological section of a Matrigel-coated alginate bead at d16 showed a PTEC monolayer on the bead surface (Figure 1(D)).

In summary, starting with hPSC, the average number of cells increased reproducibly 9.2 and 10.2 times using hiPSC lines and the ESC line, respectively, after expansion and differentiation into PTEC (Figure 1(C)).

3.2 | Differentiation of hPSC to PTEC on matrix-coated alginate beads recapitulates the developmental stages of nephrogenesis

hPSC treatment with Activin A, Retinoic Acid and BMP4 increased SIX2 expression, a key transcription factor for metanephric mesenchyme.¹⁴ About 80% of BCRTi005-A-derived cells and 68% of WISCI004-A and WAe001-A cells showed SIX2 expression on d4 (Figure 2(A)). These percentages decreased with further specification in the renal lineage, to 50% on d8 for all three pluripotent cell lines. Around 60% of the cells expressed RET, an indicator of ureteric bud formation,¹⁵ in all three cell lines on d4 (Figure 2(A)). Occurrence of a RET positive population already on d4, before inducing ureteric bud by GDNF, could be explained by SIX2+ cells producing GDNF locally for ureteric bud formation and growth.¹⁴ The nephron progenitors emerging by d4 progressed to the renal vesicle stage as visualized by the appearance of WT1 and JAG1 by d8 (Figure 2(B)). The three hPSC lines showed a higher population of JAG1 than WT1. The Notch ligand JAG1 is typically expressed in renal vesicle cells closest to the ureteric bud tip as well as in the prospective proximal tubular cells.¹⁶ Its consistent appearance at d8 indicates initiation of PTEC differentiation. The successive appearance of metanephric mesenchyme, ureteric bud and renal vesicle cells during the induced differentiation process is consistent with renal development and the results obtained in static culture in previous work⁸ (Figure S1).

3.3 | hPSC-derived renal progenitors give rise to polarized PTEC layers on matrix-coated alginate beads

PTEC medium was used to further differentiate renal progenitors starting on d8 into PTEC. Differentiation efficiency was assessed on d10, d12, d14, d16 and d20. Cells started to express PTEC markers like AQP1, Megalin/LRP2, and SGLT2 as early as d12. On d16, above 80% of cells derived from the hiPSC and around 50% of the ESC-derived cells expressed PTEC-specific markers AQP1, Na⁺/K⁺-ATPase, as well as protein transporters including Megalin/LRP2 and SGLT2 (Figure 3(A)). Around 40–60% d16 cells also expressed other transporter proteins required for transepithelial movement of organic ions, such as OCT2, OAT1, OAT3 on the basolateral side; P-gp and MRP2 on the apical side (Figure S2). For hiPSC-derived PTEC, expression of these markers was stable until d20 while

TABLE 1 Cell yields during hPSC differentiation on Matrigel-coated beads in the bioreactor

	Day -4	Day 0	Day 4	Day 8	Day 20
	hPSC	hPSC	metanephric mesenchyme	renal vesicle progenitors	PTEC
Cell lines	cells/cm ²	cells/cm ²	cells/cm ²	cells/cm ²	cells/cm ²
BCRTi005-A	6.5×10^4	4×10^5	4.1×10^5	4.3×10^5	6×10^5
WISCI004-A	6.5×10^4	4.4×10^5	4.3×10^5	3.8×10^5	6×10^5
WAe001-A	6.5×10^4	6.3×10^5	4.9×10^5	5.4×10^5	6.6×10^5

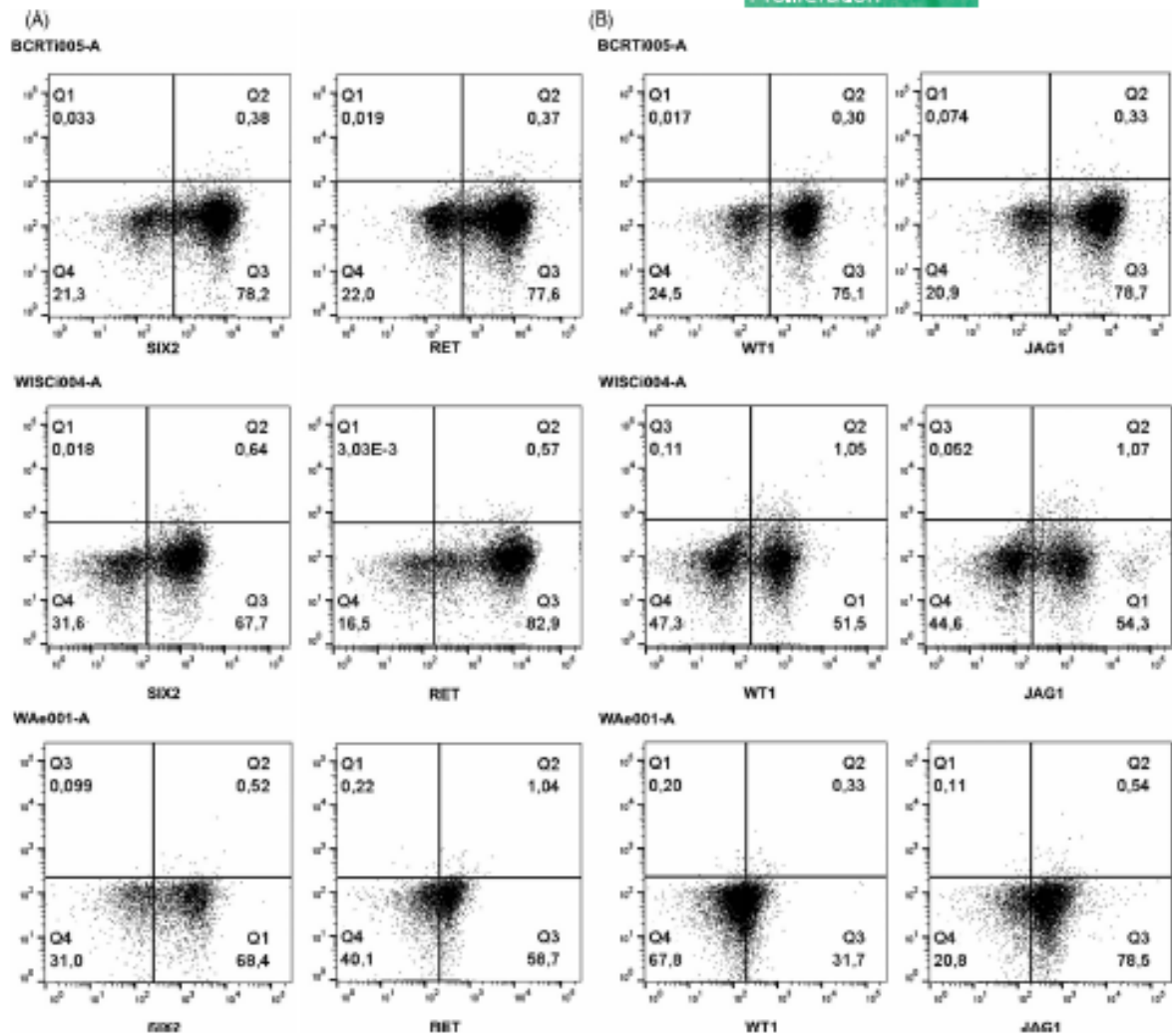


FIGURE 2 Efficiency of renal progenitor cell induction. Flow cytometry analysis of d4 and d8 cells generated from hPSC lines BCRT005-A, WISC004-A and WAe001-A showed a high percentage of (A) SIX2 and RET positive cells on d4; (B) WT1 and JAG1 positive cells on d8

the ESC-derived PTEC showed decreasing expression over time. Lotus lectin (LTL) that binds to Fucose on microvilli of PTEC and is an indicator for mature PTEC²⁷ was also abundant (around 70%) on d16 (Figure 3(B)). Moreover, Phalloidin allowed visualization of actin bundles, suggesting the presence of microvilli²⁸ on the hPSC-derived PTEC, confirmed by immunofluorescence analysis on d16 (Figure 3(C)). In contrast, in static culture with the same medium and the same protocol, around 60% of the cells expressed AQP1 and 55% were positive for LTL on d16 (Figure S3(A)). When cultivated on Laminin 521 during static culture, PTEC expressed LTL (66%) and AQP1 (82%) (Figure S3(B)), which was localized on the membrane but not homogeneously in the culture; however, they showed a cuboidal morphology (Figure S3(C)) typical of tubular epithelial cells in the proximal tubule. The expression data obtained by flow cytometry were confirmed by immunofluorescence microscopy of cells on

Matrigel beads (Figure 3(D), Figure S4). In addition, the basement membrane was explored by analyzing Laminin localization in combination with the typical apical membrane localized cotransporter SGLT2. Both proteins showed the expected apico-basal localization in hPSC-derived PTEC (Figure 4(A)).

To check further polarity and ultra-structures of PTEC, cells were visualized on d16 by transmission electron microscopy (TEM) (Figure 3(E)). Polarization was confirmed with the basement side resting on beads and the apical side with numerous microvilli. Large numbers of mitochondria were visible, a physiologically relevant feature of kidney proximal tubules. PTEC also contained many large lysosomes of different stages. Proximal tubular lysosomes are responsible for catabolizing proteins such as albumin after uptake from the glomerular filtrate and are present at high numbers in the cytoplasm.²⁹ Tight junctions were well-developed between PTEC.

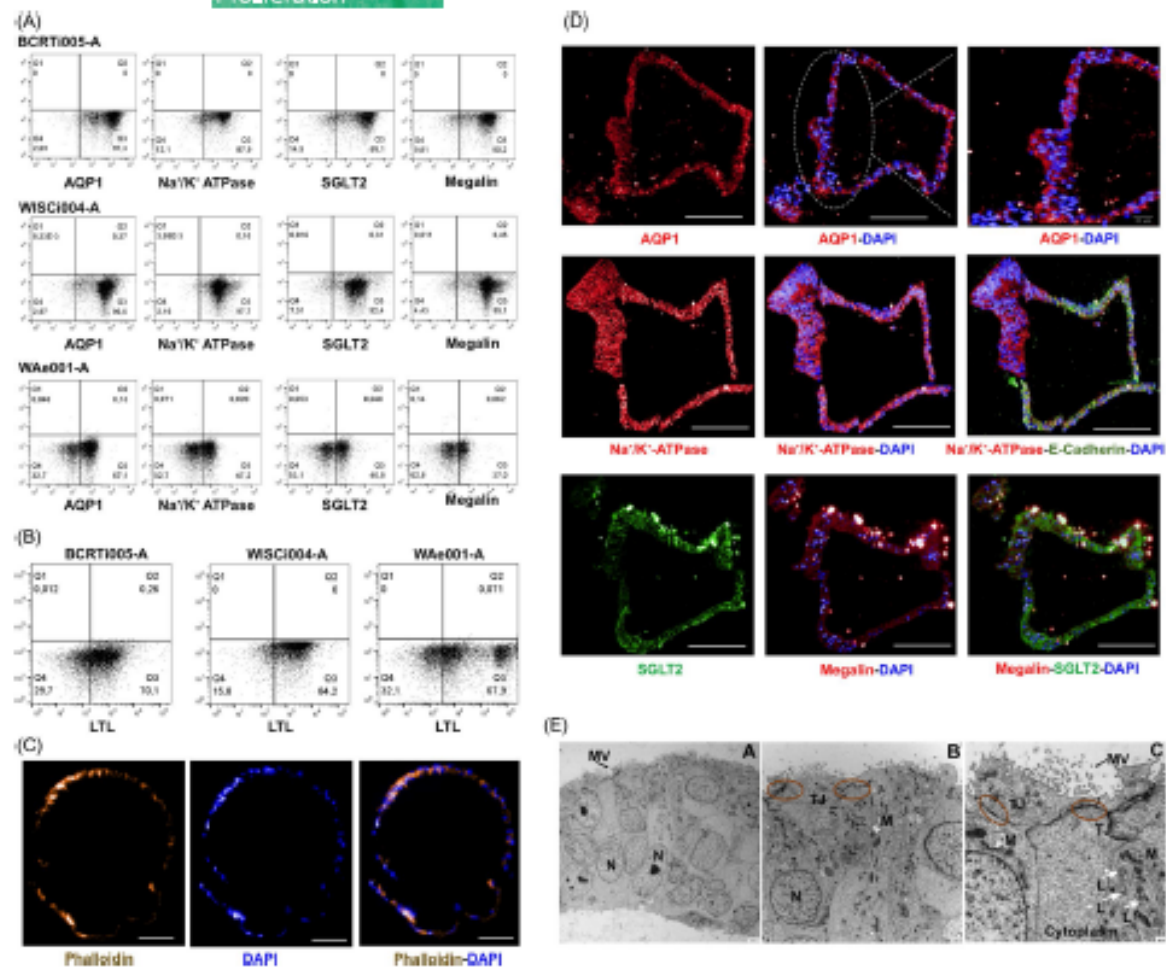


FIGURE 3 Assessment of hPSC-derived PTEC. hPSC were seeded, expanded and differentiated in suspension on Matrigel-coated alginate beads for scalable automated manufacture of PTEC (A) Flow cytometry analysis of cells on d16 post-differentiation induction for AQP1, Na⁺/K⁺-ATPase, SGLT2, Megalin/LRP2. Starting cells were the hiPSC lines BCRT1005-A, WISC1004-A and the ESC-line WAe001-A, respectively; (B) Flow cytometry analysis of d16 cells showing LTL and (C) Fluorescence microscopy for Phalloidin (yellow); DAPI (blue) shows nuclei. Scale bar = 50 μm; (D) Immunofluorescence analysis of d20 cells showed expression of AQP1, Na⁺/K⁺-ATPase, Megalin/LRP2 (all in red); SGLT2, E-Cadherin (CDH1) (green). Scale bar = 100 μm; (E) Transmission electron microscope images of d16 cells showed apical-basal polarization (A). Basal side oriented toward Matrigel beads. Microvilli on apical side (MV). (A-C) Tight junction (TJ); nuclei (N), mitochondria (M) and lysosomes (L)

3.4 | hPSC-derived PTEC are capable of active reabsorption

Selective uptake of glucose and albumin from glomerular filtrate is a main function of PTEC in the kidney. The uptake capacity of substances was investigated on d16 post-differentiation induction. In PTEC, SGLT2 is responsible for 90% of the glucose-reabsorption from the glomerular filtrate *in vivo*. This transporter is expressed on the apical side of PTEC (Figure 4(A)). d16 cells were incubated with 400 μM 2-Deoxy-2-[7-nitro-2,1,3-benzoxadiazol-4-yl]-amino]-D-glucose (2-NBDG) for 30 minutes in presence or absence of 1 μM Dapagliflozin, a selective inhibitor of SGLT2. 2-NBDG was taken

up by 50% of cells (Figure 4(B)). In the presence of Dapagliflozin, 2-NBDG uptake decreased by 50% (Figure 4(B)).

Receptor-mediated albumin endocytosis by PTEC is carried out by Megalin/LRP2. Albumin uptake of d16 cells were maximum, by 20% - 40% of PTEC when cells were incubated with 1 mg/ml FITC-Albumin for 2 hours (Figure 4(C)). Fluorescence microscopy analysis showed expression of Megalin/LRP2 and endocytosis of FITC-Albumin (Figure 4(D)).

The ability of d16 cells on Matrigel-coated beads to take up organic cations was investigated using the fluorescent cationic molecule DAPI, which can be transported into live PTEC through the basolateral organic cation transporter 2 (OCT2).²³ Around 45%

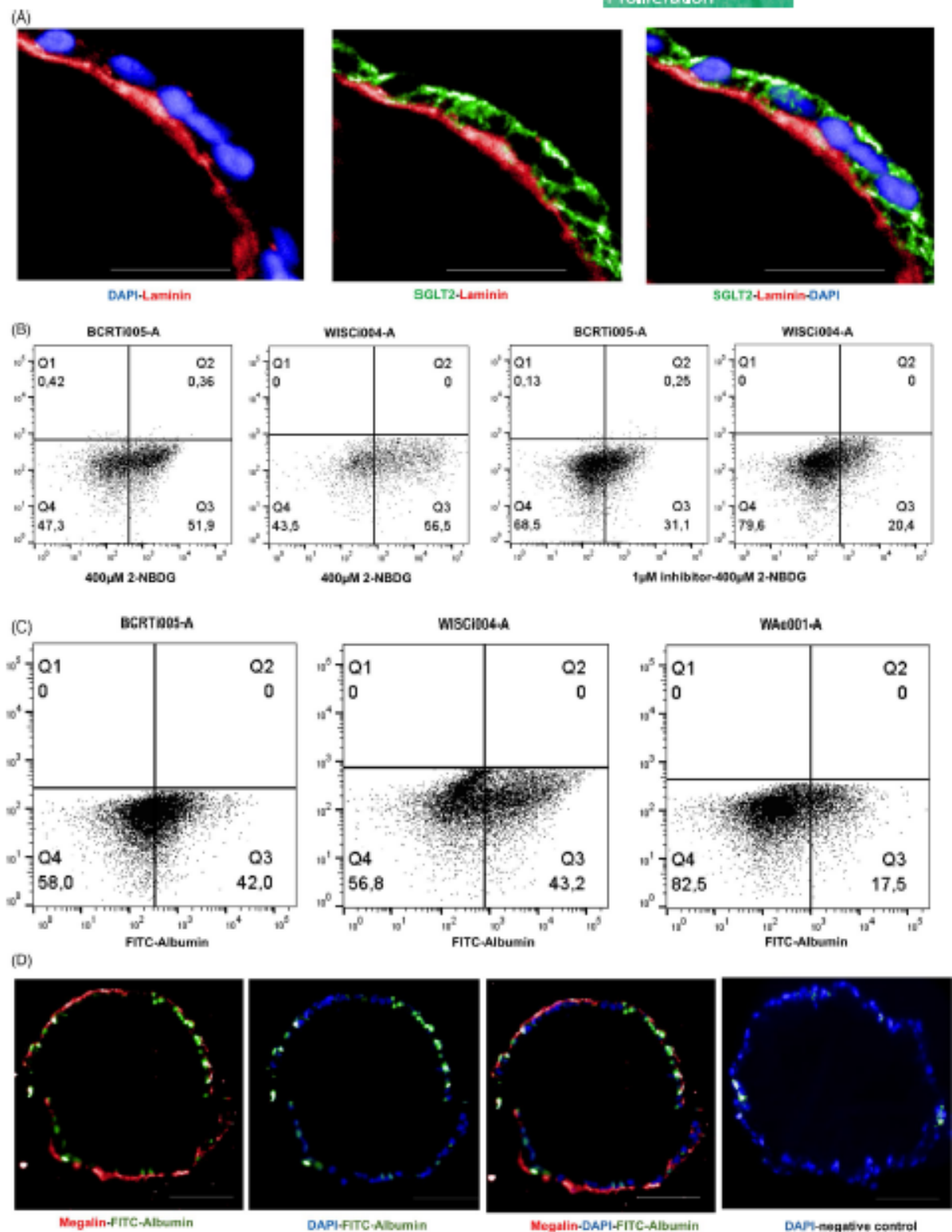


FIGURE 4 Functional analysis of hPSC-derived PTEC (a-b) SGLT2 localization and Glucose uptake of d16 PTEC. (A) Immunofluorescence staining for SGLT2 (green), Laminin (red); Scale bar = 20 μm; (B) Flow cytometry analysis of 400 μM 2-NBDG uptake in absence or presence of 1 μM Dapagliflozin of d16 PTEC; (C) Flow cytometry analysis for 1 mg/ml FITC-Albumin-endoctyosis of d16 PTEC; (D) Immunofluorescence staining for Megalin/LRP2 and FITC-Albumin of d16 PTEC; Scale bar = 50 μm

of d16 cells were able to uptake the fluorescent OCT substrate 4-Di-2-ASP and about 26% showed DAPI transport. In the presence of OCT2 inhibitors, uptake of both substrates decreased appreciably (Figure S5(A,B)). The fluorescent anion 6-Carboxyfluorescein (6-CF), a tracer dye, was used to investigate organic anion transport by the basolateral organic anion transporters OAT1 and OAT3.²³ Activity of OAT1/OAT3 was determined as probenecid-sensitive fluorescein uptake since only around 8% of the inhibitor-treated cells took up 6-CF as opposed to untreated cells, where up to 50% cells were capable of 6-CF uptake (Figure S5(C)). PTEC were incubated with Calcein AM and an increase in fluorescence intensity was seen due to the cell-permeant nature of the dye. To investigate if the efflux of the dye was mediated by P-gp, cells were treated with the inhibitor PSC-833. The fluorescence intensity of Calcein AM was unchanged indicating that the P-gp (Figure S5(D)), though expressed on d16 cells, was not fully functional.

3.5 | Modeling drug-induced nephrotoxicity in hPSC-derived PTEC

PTEC were harvested from Matrigel-coated beads on d14, post-differentiation and reseeded on Geltrex-coated 96-well plates. The cells maintained expression of AQP1, SGLT2, Megalin/LRP2 on d2, 4 and 8 post-seeding (Figure 5(A)) and formed a tight epithelial monolayer on transwell inserts within the first 2 days of seeding (Figure S6). At d22, a week of culture on the transwell insert later, the transepithelial resistance of PTEC stabilized at 90 Ω cm², which is very similar to the TEER values historically demonstrated by Whittin et al. for HK-2 cells (100 Ω cm²).²⁰ 2 days after reseeding on Geltrex-coated 96-well plates, cells were treated with Cisplatin for 6 hours showing a concentration dependent reduction in viability (Figure 5(B)). For all three cell lines used, PTEC started showing cytotoxic effect of Cisplatin at 50 μ M and a complete deterioration in cell viability at 400 μ M (Figure 5(C)). Sensitivity with Cisplatin of PTEC induced from WAe001-A and BCRTi005-A was quite similar and higher than of PTEC induced from WISCI004-A. 50% reduction of cell viability in WISCI004-A, WAe001-A, and BCRTi005-A-derived PTEC was at 300 μ M, 200 μ M, and 100 μ M, respectively. KIM-1 was detected by immunofluorescence staining on samples treated with Cisplatin for 6 hours (Figure 5(C)).

4 | DISCUSSION

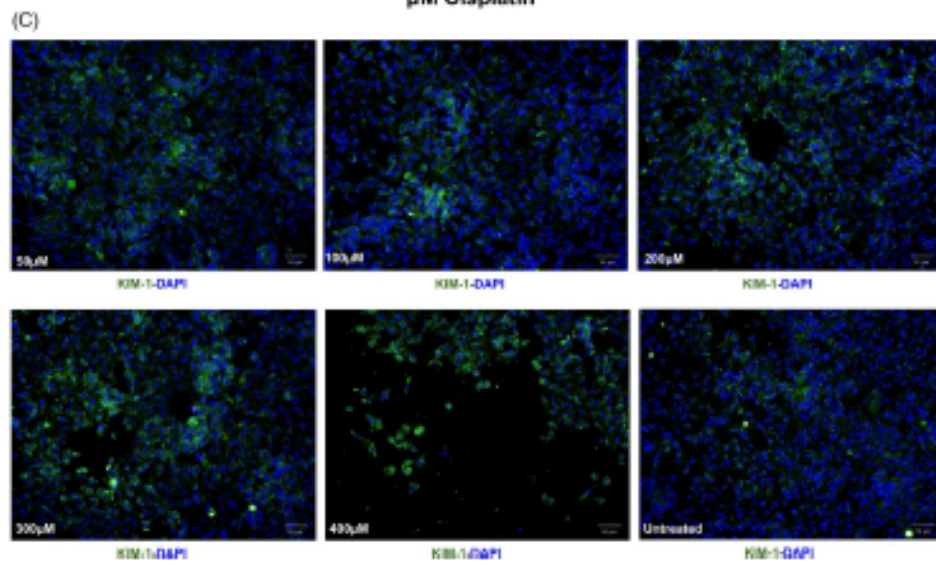
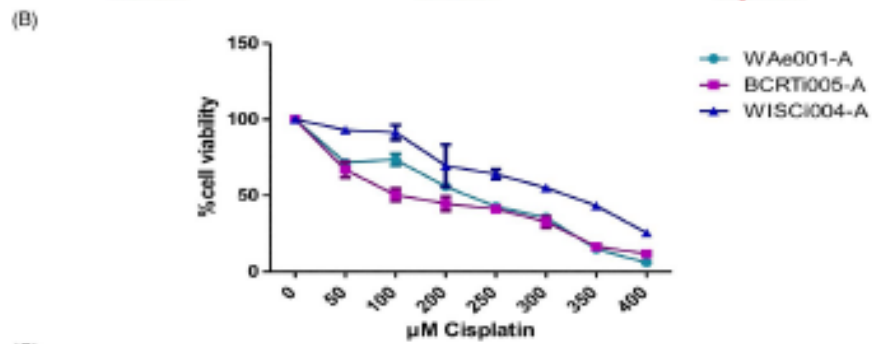
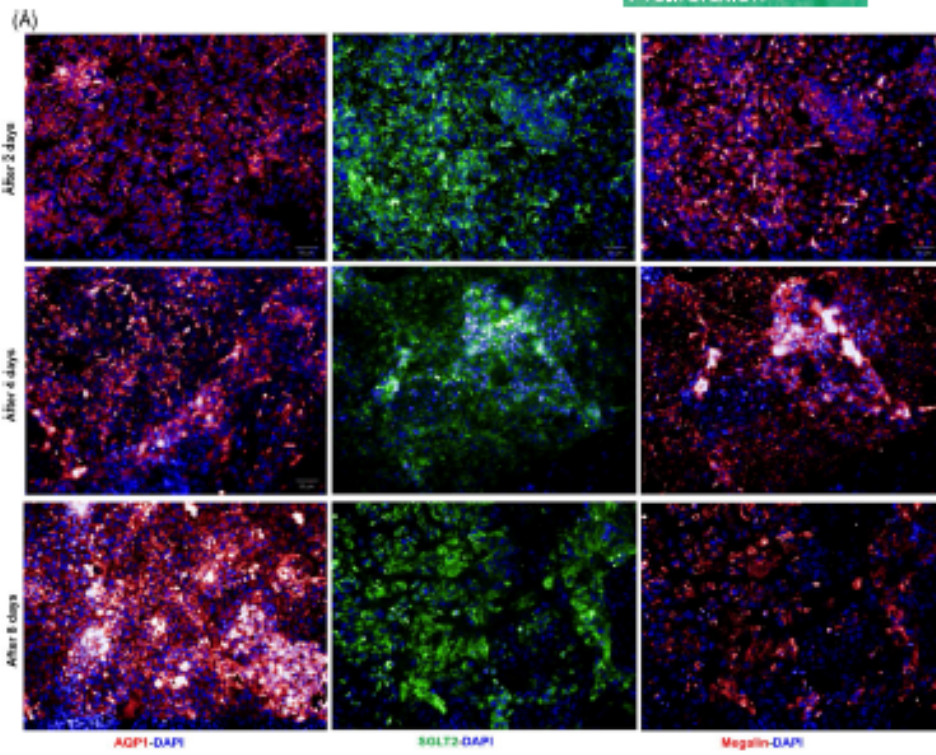
To establish an effective, economical, simple and reproducible protocol for expansion and differentiation of hPSC-derived PTEC, a

platform was developed using a levitating fluidic bioreactor together with an adjustable surface for cell adhesion, proliferation and directed differentiation based on alginate beads coated with Matrigel. The system allows expansion and differentiation without further cell processing in a single culture system. Cell yield and differentiation efficacy were compared with conventional cultivation in static culture on Matrigel-coated polystyrene.⁶ Both, expansion rates and yield of PTEC was 2 times higher for hiPSC lines and 2.2 times for WAe001-A hPSC-lines, when expanded on alginate beads in the CERO bioreactor compared to static culture in the same medium and timeline. Although reproducible for the three selected hPSC-lines, there was variability detectable between hiPSC lines and hESC line in terms of expansion and differentiation efficacy. This variability certainly did not affect functional differentiation, but it indicates the need for cell-line specific optimization of cultivation conditions.

Biolevitation has been used previously to expand hPSC on Matrigel-coated alginate beads.²¹ However, this method has never been utilized to obtain renal cells. Renal cells were previously differentiated and expanded in rotating-wall vessels,²² in wave bioreactors²³ or in specialized bioreactors.²⁴ An advantage of biolevitation and cell cultivation on floating beads is the continuous and adjustable flow exposure of the surface-covering cells. Additionally it has been shown in many systems that flow promotes functional differentiation, *in vivo* cell behavior as well as it mimics the cellular environment by providing mechanical stimulation.^{6,25-28} Thus, we believe that biolevitation in combination with alginate beads benefit differentiation of pluripotent stem cells into PTEC regarding both quality and quantity.

Despite the wide variety of applications of alginate hydrogel in cell encapsulation, cell transplantation, and tissue engineering, efficacy of using alginate hydrogel as three dimensional cell culture substrates have been only investigated for a few cell types such as mouse skeletal myoblasts,³⁰ human and rat bone marrow stromal fibroblastic cells³¹ and hPSC.⁹ The high porosity of the biopolymer network in alginate hydrogels helps to establish a continuous exchange of nutrients, gases, waste products and signaling molecules with cells grown on the hydrogel. Indeed, our results show that the formed PTEC monolayers polarize on the alginate bead with the vascular side forming a basal membrane and their apical microvilli exposed to the fluidic side. The functionality of such a polarized epithelium has also been demonstrated by the uptake of substrates by solute transporters, indicating a high-level suitability for nephrotoxicity applications. Existing proximal tubule models rely on immortalized human proximal tubule cell lines like HK-2, RPTEC-hTERT and ciPTEC-hTERT. The HK-2 cells do not show the presence of organic ion transporters, whereas RPTEC and ciPTEC lines express them but require an additional lentiviral transduction of each transporter to be utilized for drug toxicity testing.³²

FIGURE 5 Cisplatin-induced cytotoxicity on harvested hPSC-derived PTEC. (A) Immunofluorescence showed expression of AQP1, Megalin/LRP2 (both in red), and SGLT2 (green) in PTEC harvested from Matrigel beads on d14 and cultured on 96-well plates after 2 days, 4 days and 8 days in 2D culture. Scale bar = 50 μ m; (B) MTT assay showed concentration – dependent effects on cell viability after 6 hours of treatment of PTEC derived from WAe001-A, BCRTi005-A, and WISCI004-A; (C) Immunofluorescence showed expression of KIM-1 on BCRTi005-A-derived PTEC treated with Cisplatin for 6 hours. Scale bar = 50 μ m



Alginate can be easily modified in terms of stiffness and its surface chemically modified, to allow protein coating.^{33,34} The utility of extracellular matrix (ECM)-functionalized alginate hydrogel beads could be modified by selecting purpose-specific matrices. ECM compositions including type IV collagen, entactin, heparan sulfate proteoglycan, and laminin differentially decorate the basement membrane of all segments along the nephron. For instance, laminin concentration in proximal tubules is 50% higher compared to the distal tubule.³⁵ We chose Matrigel as a protein surface on alginate beads as this growth factor-reduced ECM contains abundant animal glycoproteins (laminin, type IV collagen, heparan) and factors that mimic the basement membrane and help to support epithelial growth.³⁶ For animal-free cultivation, laminin or other matrix proteins may be used. Indeed, on 2D culture, when we used LNS21 instead of Matrigel, differentiation efficacy increased slightly from 70% to 80% AQP1, 55% to 66% LTL positive cells by forming a typical cuboidal epithelial layer of PTEC on d16 (Figure S2(B), Figure S2(C)). Further optimization of alginate surface coating, for example with human kidney derived-ECM or ECM-components specific to the target nephron structure may enhance speed and efficacy of renal cell differentiation and maturation.³⁷

Differentiation media to obtain PTEC from hPSC offer additional possibilities to modify and optimize the environment of the cells. We developed a simplified culture medium based on a medium used for growing rat PTEC on chitosan³⁸ with significant variations. Specifically, we verified a basal medium with defined low glucose in normoglycemia ranges^{39,40} and eliminated the xeno-component, bovine pituitary extract and cholera toxin. In addition, hydrocortisone that sensitizes cells to EGF and increases proliferation was reduced to 1 μ M as PTEC are usually low-proliferating cells *in vivo*. Thus, we designed a medium that is serum-free and xeno-free with minimal factors, offering a high controllability of the PTEC medium. Although the commercially produced REGM was used in previous studies to successfully generate renal vesicles and PTEC from hPSC,⁶ its disadvantage is the undisclosed growth factor concentration and the presence of serum with potential for batch variation and unsuitability for clinical application of the cell products. We observed continuous proliferation of PTEC after d16, when differentiation was completed. This is non-physiological as epithelial cells of the proximal tubule under normal conditions do not proliferate. Not providing growth stimulation after a PTEC monolayer has formed may further improve physiological maturation.⁴¹

The successful large-scale production of renal cells on matrix-coated alginate beads by biolevitation offers an effective and low-cost production of high quality PTEC derived from hPSC for multiple applications where there is a high demand, such as bioprinting, therapeutic application or as cellular components for tissue engineering. The monolayer coverage of the alginate beads with polarized PTEC and tight junctions furthermore may provide a system for high throughput screening of PTEC function where each bead mimics a tubular element with a basal tubular surface and an outer urinary surface. Additionally, even when harvested from the beads, these cells are capable of forming a tight epithelium within two days and

express functional solute transporters, making them superior to existing immortalized cell lines.

In conclusion, we have successfully developed a platform technology for differentiation and expansion of hPSC-derived PTEC in a serum-free xeno-free medium without the need for passaging, in a single cultivation unit, providing high cell numbers in a reproducible manner for multiple applications.

FUNDING STATEMENT

This work was supported by grants from the Federal Ministry of Education and Research (Bundesministerium für Bildung und Forschung - BMBF): miro-iPSC Profiler - 01EK1612D, Bundesministerium für Wirtschaft und Technologie - TIME ZF4274303, Charité 3R| Replace - Reduce - Refine and the Vietnam International Education Development (VIED).

ACKNOWLEDGMENTS

We thank Dr. Ina Meiser at Fraunhofer IBMT for providing Matrigel-coated alginate beads. We thank Dr. Iris Fischer, Mr. Enrico Fritsche (M. Sc.), Dr. Imran Ullah for support in acquisition the data. We thank the Core Facility for Electron Microscopy of Charité for support in acquisition and analysis of the data. We thank Stem Cell Core Facility of Charité for support in using equipments and medium to facilitate the project. The illustration in graphical abstract and Figure 1 was created with BioRender.com. This work was supported by BIH Center for Regenerative Therapies and Fraunhofer Project Centre, Würzburg. The authors have no conflict of interest.

AUTHOR CONTRIBUTION

Thao Ngo involved in methodology, investigation, formal analysis, visualization, writing original draft preparation. Bella Rossbach involved in methodology, investigation, formal analysis, visualization, validation, writing original draft preparation. Isabelle Sébastien involved in conceptualization, methodology, investigation. Julia C. Neubauer involved in conceptualization, methodology, resources. Andreas Kurtz involved in conceptualization, resources, supervision, funding acquisition. Krithika Hariharan involved in conceptualization, methodology, formal analysis, visualization, writing original draft preparation, supervision, project administration. All authors contributed to writing and review and editing of this manuscript.

DATA AVAILABILITY STATEMENT

The data that support the findings of this study, are available from the corresponding author upon reasonable request.

ORCID

Krithika Hariharan  <https://orcid.org/0000-0001-6172-9602>

REFERENCES

1. Malhotra A, Kudyar S, Gupta A, Kudyar R, Malhotra P. Sodium glucose co-transporter inhibitors - A new class of old drugs. *Int J Appl Basic Med Res.* 2015;5(3):161. doi:10.4103/2229-516x.165363

2. Du Z, Duan Y, Yan Q, Weinbaum S, Weinstein AM, Wang T. Flow-activated proximal tubule function underlies glomerulotubular balance. *Physiol Behav.* 2016;176(1):139-148.
3. Prange JA, Bieri M, Segerer S, et al. Human proximal tubule cells form functional microtissues. *Pflügers Arch Eur J Physiol.* 2016;468(4):739-750. doi:10.1007/s00424-015-1771-8
4. Narayanan K, Schumacher KM, Taznim F, et al. Human embryonic stem cells differentiate into functional renal proximal tubular-like cells. *Kidney Int.* 2013;83(4):593-603. doi:10.1038/ki.2012.442
5. Lam AQ, Freedman BS, Morizane R, Lerou PH, Valerius MT, Bonventre JV. Rapid and efficient differentiation of human pluripotent stem cells into intermediate mesoderm that forms tubules expressing kidney proximal tubular markers. *J Am Soc Nephrol.* 2014;25(6):1211-1225. doi:10.1681/ASN.2013080831
6. Hariharan K, Stachelscheid H, Rossbach B, et al. Parallel generation of easily selectable multiple nephron cell types from human pluripotent stem cells. *Cell Mol Life Sci.* 2019;76(1):179-192. doi:10.1007/s00018-018-2929-2
7. Seale NM, Varghese S. Biomaterials for pluripotent stem cell engineering: From fate determination to vascularization. *Physiol Behav.* 2017;176(3):139-148. doi:10.1039/C5TB02658J.Biomaterials
8. Lee KY, Mooney DJ. Alginate: Properties and biomedical applications. *Prog Polym Sci.* 2012;37(1):106-126. doi:10.1016/j.progpolymsci.2011.06.003
9. Gepp MM, Fischer B, Schulz A, et al. Bioactive surfaces from seaweed-derived alginates for the cultivation of human stem cells. *J Appl Physiol.* 2017;29(5):2451-2461. doi:10.1007/s10811-017-1130-6
10. Sakolich CM, Mahler GJ. A novel microfluidic device to model the human proximal tubule and glomerulus. *RSC Adv.* 2017;7(8):4216-4225. doi:10.1039/c6ra25641d
11. Elanzew A, Sommer A, Pusch-Klein A, Brüstle O, Haupt S. A reproducible and versatile system for the dynamic expansion of human pluripotent stem cells in suspension. *Biotechnol J.* 2015;10(10):1589-1599. doi:10.1002/biot.201400757
12. Rossbach B, Hildebrand L, El-Ahmad L, Stachelscheid H, Reinke P, Kurtz A. Generation of a human induced pluripotent stem cell line from urinary cells of a healthy donor using integration free Sendai virus technology. *Stem Cell Res.* 2017;21:167-170. doi:10.1016/j.scr.2016.09.002
13. Jansen J, Schophuizen CMS, Wilmer MJ, et al. A morphological and functional comparison of proximal tubule cell lines established from human urine and kidney tissue. *Exp Cell Res.* 2014;323(1):87-99. doi:10.1016/j.yexcr.2014.02.011
14. Self M, Lagutin OV, Bowling B, et al. Six2 is required for suppression of nephrogenesis and progenitor renewal in the developing kidney. *EMBO J.* 2006;25(21):5214-5228. doi:10.1038/sj.emboj.7601381
15. Costantini F, Shakya R. GDNF/Ret signaling and the development of the kidney. *BioEssays.* 2006;28(2):117-127. doi:10.1002/bies.20357
16. Cheng HT, Kim M, Valerius MT, et al. Notch2 (but not Notch1) is required for proximal fate acquisition in the mammalian nephron. *Bone.* 2011;23(1):1-7. doi:10.1242/dev.02773.Notch2
17. Galarraga CI, Grantham JJ, Forbes MS, Maser RL, Wallace DP, Chevalier RL. Tubular obstruction leads to progressive proximal tubular injury and atubular glomeruli in polycystic kidney disease. *Am J Pathol.* 2014;184(7):1957-1966. doi:10.1016/j.ajpath.2014.03.007
18. Kumaran GK, Hanukoglu I. Identification and classification of epithelial cells in nephron segments by actin cytoskeleton patterns. *FEBS J.* 2020;287(6):1176-1194. doi:10.1111/febs.15088
19. Andersen KJ, Haga HJ, Dobrota M. Lysosomes of the renal cortex: Heterogeneity and role in protein handling. *Kidney Int.* 1987;31(4):886-897. doi:10.1038/ki.1987.82
20. Whitin JC, Bhamre S, Tham DM, Cohen HJ. Extracellular glutathione peroxidase is secreted basolaterally by human renal proximal tubule cells. *Am J Physiol Renal Physiol.* 2002;283(1):20-28. doi:10.1152/ajprenal.00014.2001
21. Chen WC, Lin HH, Tang MJ. Regulation of proximal tubular cell differentiation and proliferation in primary culture by matrix stiffness and ECM components. *Am J Physiol Renal Physiol.* 2014;307(6):F695-F707. doi:10.1152/ajprenal.00684.2013
22. Hammond TG, Hammond JM. Optimized suspension culture: The rotating-wall vessel. *Am J Physiol Renal Physiol.* 2001;281(1):50-1;12-25. doi:10.1152/ajprenal.2001.281.1.f12
23. Lohr V, Genzel Y, Behrendt I, Scharfenberg K, Reichl U. A new MDCK suspension line cultivated in a fully defined medium in stirred-tank and wave bioreactor. *Vaccine.* 2010;28(38):6256-6264. doi:10.1016/j.vaccine.2010.07.004
24. Mollet BB, Bogaerts IL, van Almen GC, Dankers PYW. A bioartificial environment for kidney epithelial cells based on a supramolecular polymer basement membrane mimic and an organotypical culture system. *J Tissue Eng Regen Med.* 2017;11(6):1820-1834. doi:10.1002/term.2080
25. Jang KJ, Suh KY. A multi-layer microfluidic device for efficient culture and analysis of renal tubular cells. *Lab Chip.* 2010;10(1):36-42. doi:10.1039/b907515a
26. Ferrell N, Ricci KB, Groszek J, Marmorstein JT, Fissell WH. Albumin handling by renal tubular epithelial cells in a microfluidic bioreactor. *Bone.* 2011;23(1):1-7. doi:10.1002/bit.24339.Albumin
27. Jang KJ, Cho HS, Kang DH, Bae WG, Kwon TH, Suh KY. Fluid-shear-stress-induced translocation of aquaporin-2 and reorganization of actin cytoskeleton in renal tubular epithelial cells. *Integr Biol.* 2011;3(2):134-141. doi:10.1039/c0ib00018c
28. Raghavan V, Rbaibi Y, Pastor-Soler NM, Carattino MD, Erratum WOA. Shear stress-dependent regulation of apical endocytosis in renal proximal tubule cells mediated by primary cilia (Proceedings of the National Academy of Sciences of the United States of America). *Proc Natl Acad Sci U S A.* (2014);111:8506-8511. 10.1073/pnas.1602041113
29. Sciancalepore AG, Sallustio F, Girardo S, et al. A bioartificial renal tubule device embedding human renal stem/progenitor cells. *PLoS One.* 2014;9(1): doi:10.1371/journal.pone.0087496
30. Rowley JA, Madambayan G, Mooney DJ. Alginate hydrogels as synthetic extracellular matrix materials. *Biomaterials.* 1999;20(1):45-53. doi:10.1016/S0142-9612(98)00107-0
31. Lawson MA, Barralet JE, Wang L, Shelton RM, Triffitt JT. Adhesion and growth of bone marrow stromal cells on modified alginate hydrogels. *Tissue Eng.* 2004;10(9-10):1480-1491. doi:10.1089/ten.2004.10.1480
32. Faria J, Ahmed S, Gerritsen KGF, Mihaila SM, Masereeuw R. Kidney-based in vitro models for drug-induced toxicity testing. *Arch Toxicol.* 2019;93(12):3397-3418. doi:10.1007/s00204-019-02598-0
33. Machida-Sano I, Matsuda Y, Namiki H. In vitro adhesion of human dermal fibroblasts on iron cross-linked alginate films. *Biomed Mater.* 2009;4(2): doi:10.1088/1748-6041/4/2/025008
34. Machida-Sano I, Hirakawa M, Matsumoto H, et al. Surface characteristics determining the cell compatibility of ionically cross-linked alginate gels. *Biomed Mater.* 2014;9(2): doi:10.1088/1748-6041/9/2/025007
35. Desjardins M, Bendayan M. Heterogeneous Distribution of Type IV Collagen, Entactin, Heparan Sulfate Proteoglycan, and Laminin Among Renal Basement Membranes as Demonstrated by Quantitative Immunocytochemistry. *J Histochem Cytochem.* 1989;37(6):885-897.
36. Vuoristo S, Toivonen S, Weltner J, et al. A Novel Feeder-Free Culture System for Human Pluripotent Stem Cell Culture and Induced Pluripotent Stem Cell Derivation. *PLoS One.* 2013;8(10):1-14. doi:10.1371/journal.pone.0076205
37. Ullah I, Busch JF, Rabien A, et al. Adult Tissue Extracellular Matrix Determines Tissue Specification of Human iPSC-Derived

- Embryonic Stage Mesodermal Precursor Cells. *Adv Sci.* 2020;7(5): doi:10.1002/advs.201901198
38. Chiang IN, Huang WC, Huang CY, Pu YS, Young TH. Development of a chitosan-based tissue-engineered renal proximal tubule conduit. *J Biomed Mater Res - Part B Appl Biomater.* 2018;106(1):9-20. doi:10.1002/jbm.b.33808
 39. Morais C, Westhuyzen J, Pat B, Gobe G, Healy H. High ambient glucose is effect neutral on cell death and proliferation in human proximal tubular epithelial cells. *Am J Physiol Renal Physiol.* 2005;289(2):401-409. doi:10.1152/ajprenal.00408.2004
 40. Radford R, Slattery C, Jennings P, et al. Carcinogens induce loss of the primary cilium in human renal proximal tubular epithelial cells independently of effects on the cell cycle. *Am J Physiol - Ren Physiol.* 2012;302(8): doi:10.1152/ajprenal.00427.2011
 41. Nadasdy T, Laszik Z, Buck KE, Johnson LD, Silva FG. Johnson and FGS. Proliferative Activity of Intrinsic Cell Populations in the Normal Human Kidney. 1988;2005(19):3-5.

SUPPORTING INFORMATION

Additional supporting information may be found in the online version of the article at the publisher's website.

How to cite this article: Ngo TTT, Rossbach B, Sébastien I, Neubauer JC, Kurtz A, Hariharan K. Functional differentiation and scalable production of renal proximal tubular epithelial cells from human pluripotent stem cells in a dynamic culture system. *Cell Prolif.* 2022;55:e13190. doi:10.1111/cpr.13190

Curriculum vitae

"For data protection reasons, my curriculum vitae will not be published in the electronic version of my work."

Publication list

Ngo TTT, Rossbach B, Sébastien I, Neubauer JC, Kurtz A, Hariharan K. Functional differentiation and scalable production of renal proximal tubular epithelial cells from human pluripotent stem cells in a dynamic culture system. *Cell Proliferation*. Impact factor 2021/2022: 6.8

Acknowledgements

I am deeply grateful to my supervisors, Prof.Reinke Petra and Prof.Andreas Kurtz for allowing me to work in Stem Cell laboratory despite of my limitations about laboratorous skills at the beginning, for giving me opportunity to work with new and attractive scientific objects, for giving me a working atmosphere without any pressure. Prof.Andreas Kurtz always provided me good comments, timely orientations for my experiments, encouraged me when the experiement results were not like expected, and be patient and tolerant for my mistakes. I express sincerely grateful to my two mentors, Dr.Krithika Hariharan and Dr.Bella Rossbach for teaching me laboratorous skills, for many discussions that contributed greatly to my good results, for being dedicated with my publication, for involving me to challenge projects so that I had good chance to learn more.

I am especially thankful to Dr.Julia C. Neubauer, M.Sc.Isabelle Sébastien and Dr. Ina Meiser at Fraunhofer Institute for Biomedical Technology for providing materials, devices to support for my study, for contribution to my publication. In addition, I thank all my colleagues from A.G Kurtz group and Stem Cell Core Facility of Charité, especially Dr.Iris Fischer, for helping me to get familiar with devices or whenever needed as well as for sharing experiences. I thank Dr. Dang Van Duc in [German Rheumatism Research Centre](#) for finding my professor for me, for giving me first guidances about life in Germany.

I highly thank my family and friends, especially thank my father, my husband, my daughter and my sister. My father encouraged me to get scholarship for oversea study, strengthened my mind to overcome difficulties in my life. My husband and daughter were always active and healthy then I could focus on my study. My sister took care well herself, my mother and my niece so that I were not worry about them.

